ILLINOIS

UNIVERSITY OF ILLINOIS AT URBANA-CHAMPAIGN

-

PRODUCTION NOTE

University of Illinois at
Urbana-Champaign Library
Large-scale Digitization Project, 2007.

STUDIES OF SLAB AND BEAM HIGHWAY BRIDGES: PART III

Small-Scale Tests of Shear Connectors and Composite T-Beams

C. P. Siess

I. M. Viest

N. M. Newmark

Price: One Dollar

UNIVERSITY OF ILLINOIS BULLETIN

UNIVERSITY OF ILLINOIS ENGINEERING EXPERIMENT STATION

STUDIES OF SLAB AND BEAM HIGHWAY BRIDGES: PART III

Small-Scale Tests of Shear Connectors
and Composite T-Beams

CHESTER P. SIESS
*Research Associate Professor of
Civil Engineering*

IVAN M. VIEST
*Research Assistant Professor of
Theoretical and Applied
Mechanics*

NATHAN M. NEWMARK
*Research Professor of Structural
Engineering*

ABSTRACT

Three types of tests of shear connectors for composite concrete and steel I-beam bridges are reported in this bulletin: (1) tests of push-out specimens, (2) static tests of composite T-beams, and (3) tests of composite T-beams in fatigue. All specimens tested were approximately one-quarter scale models. The push-out specimens were made with various types of rigid and flexible connectors; the T-beams were made with channel shear connectors only.

The purpose of the push-out tests was primarily the selection of the particular types of connector most deserving of additional study. The static and fatigue tests of T-beams were planned primarily to study the action of composite beams with channel connectors. The fatigue tests also provided data regarding the strength characteristics of channel shear connectors.

Most of the findings from these tests are only qualitative. The principal findings are three: (1) The shear connector selected for more detailed studies was of the rolled steel channel type. (2) The behavior of the channel connector is similar to that of a dowel embedded in elastic medium. A large part of the load transmitted by this connector is concentrated on the channel flange welded to the top flange of the I-beam and only the remaining smaller part is carried by the connector web. (3) A shear connection made from several channel connectors, if properly designed, insures a practically complete interaction between the concrete slab and the steel beam of the composite T-beam.

The tests are presented in detail in this bulletin. Wherever practicable, comparisons are made with theoretical calculations; a theory for composite beams with incomplete interaction presented in the Appendix was used for this purpose.

3

This page is intentionally blank.

CONTENTS

CONTENTS (Concl.)

FIGURES

FIGURES (Concl.)

TABLES

I. INTRODUCTION

1. Object of Tests

It has been shown by both tests and analysis that composite construction for I-beam bridges leads to a stiffer and stronger structure and in many cases to a cheaper one.[1] This type of construction is provided by tying the concrete deck slab to the steel I-beams by shear connectors which serve to prevent movement between the slab and the beam and which are capable of transmitting shear between the two elements. In such case the slab serves a dual purpose: it acts not only as a concrete deck but also as an added top flange of the composite beam. The resulting structure may be pictured as consisting of a concrete deck slab supported by composite steel and concrete T-beams.

Composite I-beam bridges of both right and skew spans have been investigated by means of tests on scale models, reported in previous bulletins,[2] which demonstrated the feasibility, reliability, and advantages of composite construction. However, little attention was given to the shear connectors themselves or to the fundamental behavior of the composite T-beams. The tests reported in the present bulletin were intended to provide information on these subjects.

Since the questions to be investigated were broad in scope these tests were planned primarily as an exploratory series. Consequently small-scale models were used so that a large number of specimens incorporating many variables could economically be tested. Two principal types of specimens were employed: (1) push-out specimens in which pairs of shear connectors were subjected to shearing forces, and (2) T-beam specimens consisting of a steel I-beam and a mortar slab tied together with shear connectors.

A number of different types of shear connectors have been proposed and used in I-beam bridges, but few attempts have been made to determine experimentally which of the types now in use, or available for use, is the most efficient in performance of its particular function. This question was studied by means of tests on several different types of shear connectors in

---

[1] C. P. Siess, "Composite Construction for I-beam Bridges," Transactions ASCE, Vol. 114, 1949, pp. 1023–1045.

[2] N. M. Newmark, C. P. Siess, R. R. Penman, "Studies of Slab and Beam Highway Bridges, Part I: Tests of Simple-Span Right I-beam Bridges," Univ. of Ill. Eng. Exp. Sta. Bul. 363, 1946; and N. M. Newmark, C. P. Siess, W. M. Peckham, "Studies of Slab and Beam Highway Bridges, Part II: Tests of Simple-Span Skew I-beam Bridges," Univ. of Ill. Eng. Exp. Sta. Bul. 375, 1948.

push-out specimens. Push-out specimens were also used to study the effect of several variables, including mortar strength, shape of the specimen, and bond conditions, on the behavior of channel shear connectors.

The composite action of an I-beam bridge is significantly influenced by the amount of slip which can take place between the concrete slab and the steel I-beam. If the slab is free to slip along the top flange of the I-beam, no interaction between the two elements exists. If, on the other hand, the connection effectively prevents slip, perfect interaction is accomplished. In practical cases, however, some amount of slip is always present and the interaction is thus incomplete. The studies of the degree of interaction accomplished with shear connectors of the channel type was the object of the second part of the tests made on T-beam specimens. Another important object of these tests was to compare the characteristics of channel shear connectors as determined from tests of push-out specimens and tests of T-beams.

An I-beam bridge and the shear connectors in it are subject to repeated loading due to highway traffic. Furthermore, in bridges built without shoring, the shear connectors are stressed only due to live loads and the connectors near midspan undergo a complete reversal of stress for each passage of a vehicle. The effect of repeated loading may be important and was therefore investigated for a number of T-beams utilizing channel shear connectors. These tests also provided a basis for studies of maximum stresses in the webs of channel connectors.

2. Scope of Bulletin

Three types of tests are reported: (1) tests of push-out specimens, (2) static tests of composite T-beams, and (3) tests of composite T-beams in fatigue. All specimens were approximately one-quarter scale models. The push-out tests described in Chapter III included several types of flexible and rigid shear connectors—channels, bent and straight plates, angles, and tees. The static and repeated-load tests of T-beams, described in Chapters IV and V, were limited to channel shear connectors. The tests were made in the period 1942–1948.

Sixty-four push-out specimens were tested with static loading. The variables studied include the type of connector, the width and thickness of connector, the mortar strength, and the condition of bond between the slab and the beam or the connector. Only slip between the mortar slab and the steel I-beam was measured in these tests.

Three composite T-beams were tested statically with a single concentrated load. The mortar strength and the strength of the shear connection were the only variables included in these tests. Slip between the mortar slab and the steel beam, slab and beam strains, and beam deflection were measured at various locations along the beam.

Eighty-five composite T-beams were tested in fatigue. The mortar strength, the thickness of the web and flange of the shear connectors were the principal variables. Slip and deflection were measured during the fatigue test. Slip, deflection, and strain were measured in static tests both before and after the repeated load test.

A theory for composite beams with incomplete interaction is presented in detail in the Appendix. Although no comparisons of the theory with the test results are made in the Appendix, some theoretical studies of the effects of an incomplete shear connection are presented.

3. Acknowledgments

The tests described in this bulletin were made as a part of an investigation of slab and beam highway bridges conducted at the Talbot Laboratory by the Engineering Experiment Station of the University of Illinois in cooperation with the Illinois Division of Highways and the Bureau of Public Roads of the U. S. Department of Commerce.

The program of the investigation was guided by an Advisory Committee having the following personnel.

Representing the Bureau of Public Roads:

E. F. Kelley, Chief, Physical Research Branch

Raymond Archibald, Chairman, Bridge Committee, American Association of State Highway Officials

E. L. Erickson, Chief, Bridge Branch

Representing the Illinois Division of Highways:

G. F. Burch, Bridge Engineer

W. J. Mackay, Engineer of Railroad Crossings

L. E. Philbrook, Assistant Bridge Engineer

Representing the University of Illinois:

F. E. Richart, Research Professor of Engineering Materials

N. M. Newmark, Research Professor of Structural Engineering

C. P. Siess, Research Associate Professor of Civil Engineering

General direction of the investigation was provided by Professors Richart and Newmark. All work in connection with this bulletin was under the immediate direction of Professor Siess, who also conducted and interpreted the tests of the push-out specimens, the static tests of the T-beams, and a part of the repeated-load tests of T-beams. Parts of the repeated-load tests were conducted also by W. E. Johnson, former Special Research Associate in Theoretical and Applied Mechanics, and Messrs. R. F. Mosher R. A. Bennitt, Jr., and J. H. Appleton, then graduate students in Civil Engineering.

The information from various sources was correlated and the bulletin prepared by I. M. Viest with the assistance of C. P. Siess.

The theory of composite beams with incomplete interaction, presented in the Appendix, was developed by Professor Newmark, who also took active part in planning the tests and gave continuous guidance during their conduct.

4. Definitions

A *composite T-beam* is a beam composed of a concrete slab and an I-beam interconnected in such a manner that they act as a unit.

Composite action is the interaction between the slab and beam which results from the transfer of shear between these two elements.

Complete composite action exists when the amount of shear transferred is equal to the shear computed for the beam and slab considered as a homogeneous member.

If less than this amount of shear is transferred, *partial composite action* is said to exist.

The case of *no interaction* is that for which the slab and the beam act independently and no horizontal force is transferred between the two elements.

A *shear connector* is a device for the transfer of horizontal shear from one element of the composite T-beam to the other.

A *rigid shear connector* is a connector in which the bending stress is insignificant.

A *flexible connector* is one which carries at least a part of the load by bending.

A *shear connection* connects the slab and the beam of a composite T-beam in such a way that it transfers the horizontal shear from one element of the T-beam to the other. It consists of a number of individual shear connectors.

II. DESCRIPTION OF TEST SPECIMENS AND APPARATUS

A. PUSH-OUT TESTS

5. Description of Specimens

The push-out specimens were approximately one-quarter scale models. The form of the specimens is shown in Fig. 1. Each specimen consisted of a short steel I-beam and two mortar slabs, one attached to each flange of the beam. One shear connector was welded to each flange and was embedded in the slab. In this type of specimen both the slabs and the beam are in compression, the load being transmitted from the beam to the slabs through the shear connectors. The loading of the shear connectors corresponds, with some limitations, to that of similar connectors in a composite I-beam.

The beams used were 3-in. I-beams of either 6.5 lb per ft or 5.7 lb per ft. They differed only in the thickness of the web and the width of the flange. These differences did not affect the results of the tests. All slabs were $1\frac{3}{4}$ in. thick and 6 in. wide except specimen C1d, which was 9 in. wide. The slabs were made from sand-cement mortar.

The types of shear connectors used are shown in Fig. 2, and photographs of typical connectors after welding to the beam are shown in Fig. 3. The shear connectors consisted of channels, plates bent to a leaning Z-shape, straight plates, angles, and tees. The width of the connector and the thickness of the metal varied, but the height of all connectors was 1 in. except for the Z-plates, which were $1\frac{1}{8}$ in. high. It can be seen from Figs. 2 and 3 that the channel connectors C1–C6, the bent-plate connectors B1–B5, and the straight plate connectors P1–P3 are flexible. The remaining types—C7, A1, A2, and T1—represent rigid connectors.

In most specimens no treatment other than a thorough cleaning was given to the surface of the beam flanges and to the shear connectors. Thus an initial natural bond existed between the steel and mortar at the beginning of the tests. For typical connectors of some types, however, the natural bond was destroyed between the mortar slabs and the beam flanges, and between the mortar slabs and the shear connectors.

6. Materials

The sand-cement mortar used in the slabs consisted of Universal brand standard Portland cement, and an artificially graded mixture of Wabash
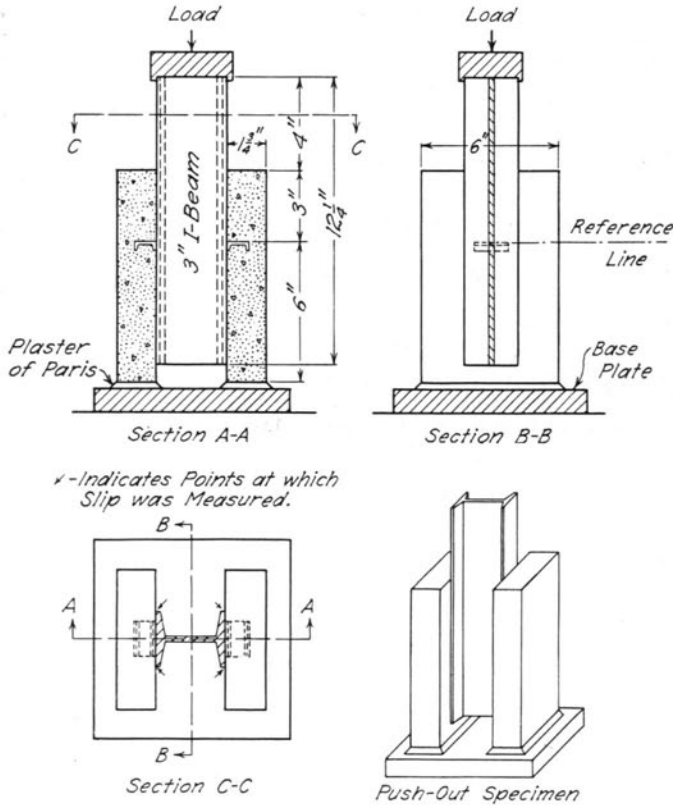
Fig. 1. Details of Push-out Specimens

River torpedo sand and fine Lake Michigan beach sand. The sand mixture was similar in all respects to that used in the I-beam bridges described in Bulletin 363.

The slabs of all specimens except C1aL and C1aM were made from mixes having proportions of cement to sand of 1:3.5 and a water-cement ratio of 0.60, both by weight. The proportions for specimens C1aL and C1aM were 1:6.5 and 1:4.22 respectively, and the water-cement ratios were 1.00 and 0.70 respectively. The mortar was of a rather stiff consistency. Four 2-in. by 4-in. control cylinders made from each batch were tested to determine the compressive strength of the mortar used in each slab. The results of these tests are given in Table 1.

The channels used for shear connectors were standard hot-rolled bar channels. Tensile tests on two coupons taken from the webs of the channels showed a yield point stress of 42,500 psi and an ultimate stress of 60,600

psi. No tension tests were made of the material in the angles and tees, but they also were hot-rolled sections and their values should not differ appreciably from those found for the channels. All bent and straight plate connectors, except B4, were made from hot-rolled mild steel strips. The tensile properties obtained from three test coupons made from strips of various widths and thicknesses were fairly uniform. The average yield point stress was 37,200 psi and the average ultimate stress was 50,300 psi. The thin bent plate, B4, was made from a piece of sheet metal for which no tensile properties have been determined. All the "B"-type connectors were bent cold except B5, which was bent hot.

Specimen	W, in.	T, in.	Weight of One Connector, lb.
C 1	1.50	0.125	0.086
C 2	2.31	0.125	0.133
C 3	0.75	0.125	0.043
C 4	1.50	0.098	0.078
C 5	1.50	0.125	0.070
C 6	1.50	0.097	0.060
C 7	As Shown		0.058
B 1	0.50	0.135	0.046
B 2	1.00	0.125	0.086
B 3	1.50	0.130	0.131
B 4	1.00	0.050	0.036
B 5	1.00	0.190	0.125
P 1	1.50	0.097	0.041
P 2	1.50	0.130	0.055
P 3	1.50	0.158	0.067
A 1	As Shown		0.066
A 2	As Shown		0.066
T 1	As Shown		0.049
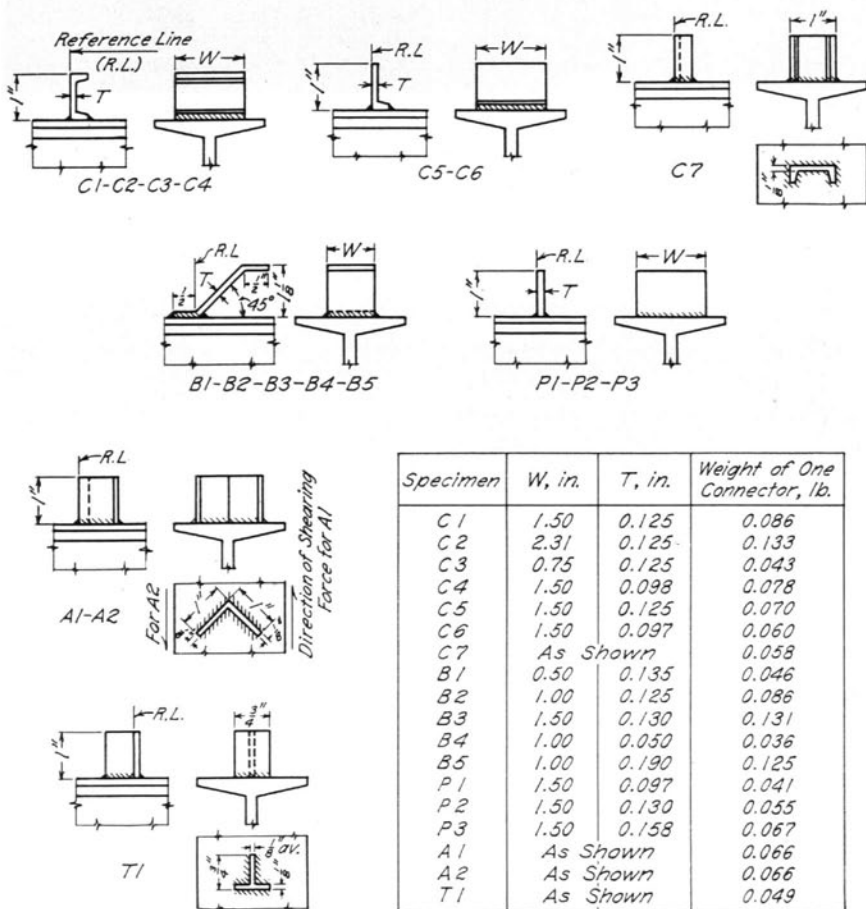
Fig. 2. Details of Various Types of Shear Connectors
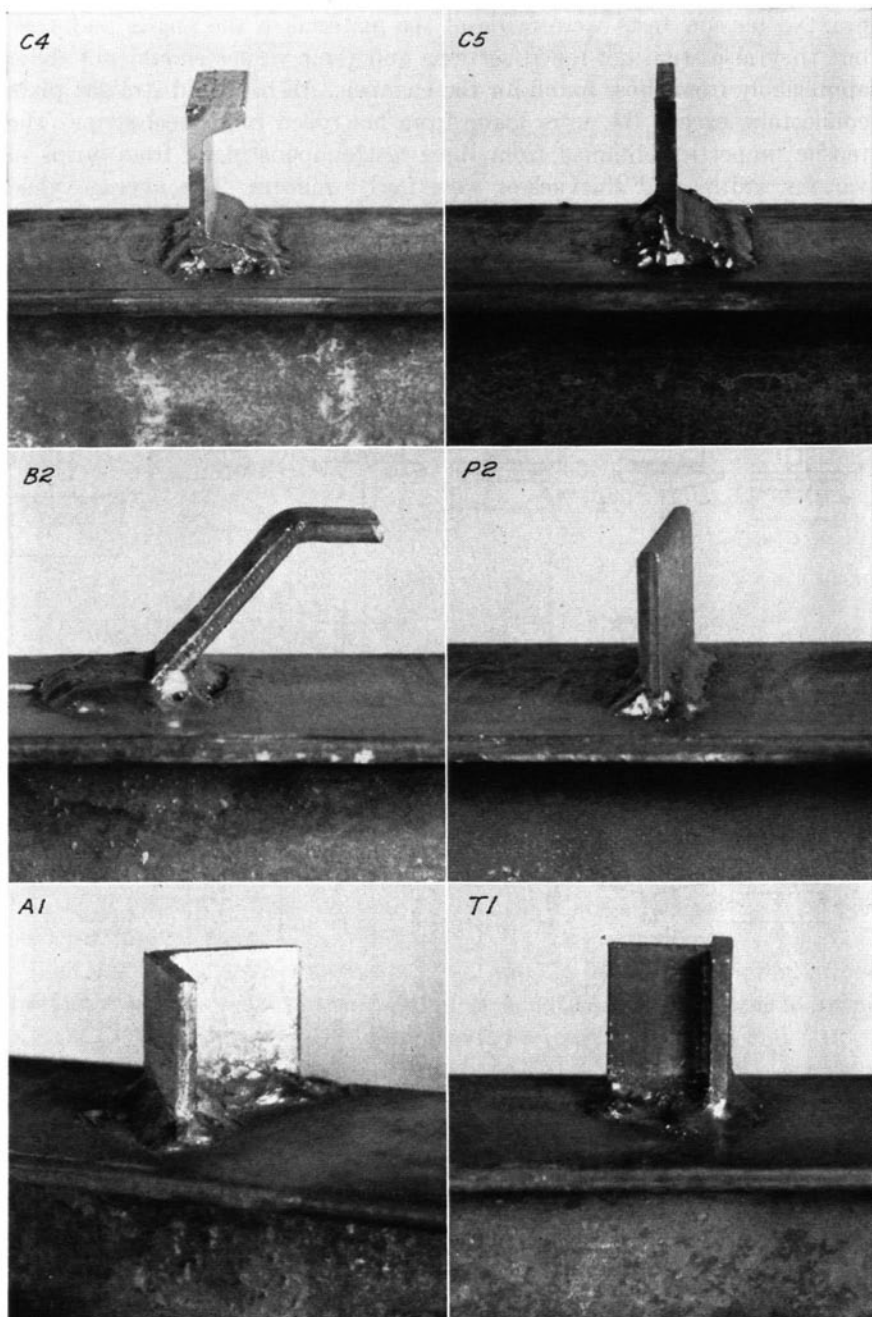
Fig. 3. Typical Shear Connectors

7. Manufacture of Specimens

The first step in the manufacture of the specimens was welding the shear connectors to the beams. The location of the shear connectors along the length of the beam is indicated by the reference line on Fig. 1 for the beam and on Fig. 2 for the shear connectors. All welds were continuous fillet

Table 1
Cylinder Compressive Strength of Mortar for Push-out Specimens

All values are averages of four 2-in. × 4-in. cylinders made from the same batch. "First" slab was tested at the age of 28 days, "second" at the age of 27 days; both slabs received 7 days of moist curing. Proportions of cement to sand were in all mixes 1:3.5 by weight and the water-cement ratio was 0.60 by weight except where otherwise noted.

Specimen	Mortar Strength in psi for		
	"First" Slab	"Second" Slab	Average for Both Slabs
C1a*	4740	5350	5050
C1aL†	1330	1480	1410
C1aM‡	4600	3380	3990
C1aH	5460	5610	5540
C1b	5820	5450	5640
C1bp	4980	4880	4930
C1c	5450	5570	5510
C1cp	4980	4880	4930
C1d	5220	5240	5230
C1x	4980	4880	4930
C2a	5220	5240	5230
C3a	5460	4720	5090
C4a	5020	5700	5360
C5a	5700	5170	5440
C5b	5170	3880	4530
C5c	3880	5190	4540
C6a	4300	5060	4680
C7a	5060	5000	5030
B1a	5000	5300	5150
B2a	5300	4920	5110
B2b	4920	4460	4690
B2c	4020	4960	4490
B3a	4960	5090	5030
B4a	5090	4440	4770
B5a	4440	3920	4180
P1a	3920	3010	3470
P2a	3680	5030	4360
P3a	5030	5250	5140
A1a	5250	5760	5510
A2a	5760	5250	5510
T1a	5250	4650	4950

* Averages of twelve cylinders.
† Mix 1:6.50, $w/c = 1.00$.
‡ Mix 1:4.22, $w/c = 0.70$.

welds as shown on Fig. 2. Arc welding with a $\frac{1}{8}$-in. semi-shielded Fleetweld No. 11 electrode was used throughout.

Before casting the slabs, the surfaces of the beams and the shear connectors were brushed with a wire brush and cleaned with a piece of waste soaked in gasoline. For specimens having natural bond between the steel and the mortar, this was the only preparation. Where the bond to the beam was to be destroyed, the surface of the beam flange, in contact with the mortar, was covered with a rather liberal layer of cup grease. Where the bond to the shear connector was to be destroyed, two methods were used. In some cases all exposed surfaces of the connector and the weld metal were greased and care was taken to apply only a very thin film of grease to the connector. The other method was to polish the shear connector with an abrasive wheel and with emery cloth until a reasonably smooth surface was secured.

In casting the slabs, it was recognized that the orientation of the beam and connector at the time of casting would probably have some effect on the resistance of the connector to slip. Since in an actual structure the concrete would be cast on the top of the beam, it was deemed advisable to follow a similar procedure in these tests. This was accomplished by first casting the slab on one side of the beam, the so-called first slab, and allowing it to set overnight. On the following day the forms were stripped, the beam was turned over, and the slab on the other side, the second slab, was cast.

The mortar was mixed in a Lancaster mixer with a capacity of approximately 2 cu ft. Four slabs were made from each mix—two of them as first and two as second slabs. A few batches from which only two slabs were cast were mixed by hand.

The mortar was worked into the forms and around the shear connectors with the aid of a small steel trowel. Special care was taken to prevent the formation of voids around the connector. Two to three hours after the slabs had been cast they were struck off flush with the forms. No other finishing of the slab was done.

On the day following that on which the second slab was cast, the forms were stripped and the specimen placed in the moist room, where it remained for 7 days. It was then removed, and curing was completed in the air of the laboratory. All specimens were tested 28 days after the first slab was cast.

Duplicate specimens were cast at the same time. This procedure was altered in four cases. It was desirable to have the companion specimens of types C1bp and C1cp made from different batches, and for the slabs of

9-in. width on C1d only one set of forms was available; therefore the duplicate specimens could not be cast on the same day.

Four 2-in. by 4-in. control cylinders were made from each batch of mortar. They were cured and tested together with the corresponding slabs. Thus two of the four cylinders from each batch were tested at the age of 28 days and two at the age of 27 days. The one-day difference in curing, however, caused no marked variations in strengths. Because the two slabs on the same specimen were cast from two different batches the strengths of the two slabs varied to some extent, as shown in Table 1.

8. Loading Apparatus and Instruments

The general set-up for testing is shown in Fig. 4. The load was applied by means of a screw jack of 50-ton capacity, and was measured by an elastic ring dynamometer placed between the jack and the specimen. The specimen was loaded through a ball bearing resting on a steel bearing block which in turn rested on the end of the I-beam. At the lower end the slabs were bedded in plaster of paris on a machined steel base plate. The reactions for jacking were obtained by placing the entire assembly in a Riehle screw-type testing machine of 200,000-lb capacity.

Two dynamometers, one of 50,000-lb capacity and one of 20,000-lb capacity (shown in Fig. 4) were used. Each of the dynamometers was capable of measuring load with a sensitivity of 10 to 20 lb and an accuracy of the same order of magnitude.

One of the specimens, C5b2, was tested in a Riehle screw power testing machine of 30,000-lb capacity. This test was made in an attempt to eliminate a possible source of eccentricity in loading by using a spherical loading head which was fixed against rotation after a small load had been applied to the specimen. The results obtained by this procedure were about the same as those obtained by the usual more simple procedure; hence no more tests were made in this manner.

The only measurements made were for slip between the I-beam and the slabs. The slip was measured at the outside edges of the beam at the level of the back of the connectors. This level is shown as the reference line on Figs. 1 and 2. A view of the slip-measuring device on one side of the beam is shown in Fig. 5. The dials, two on each side of the beam web, were rigidly attached to the I-beam with set screws. A small cantilever extension arm was attached to the dial stem; this arm rested on a small bracket made of sheet metal which was cemented to the slab at the level of the reference line. The bracket was cemented into place with Duco household cement at least one day prior to testing.

<div align="center">B. T-beam Tests</div>

9. Description of Specimens

The T-beams designed for static and fatigue tests of shear connectors are shown in Fig. 6. They correspond to a section consisting of one I-beam and one panel of the slab from the quarter-scale model I-beam bridges of 5-ft span described in Bulletin 363. The size and spacing of the connectors
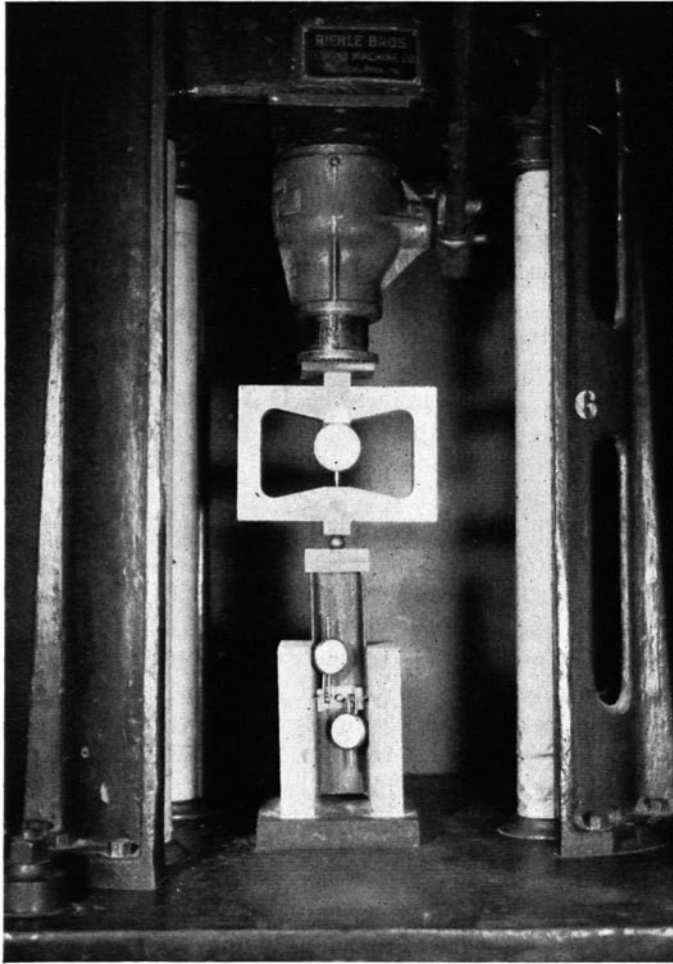
Fig. 4. Arrangement for Testing Push-out Specimens
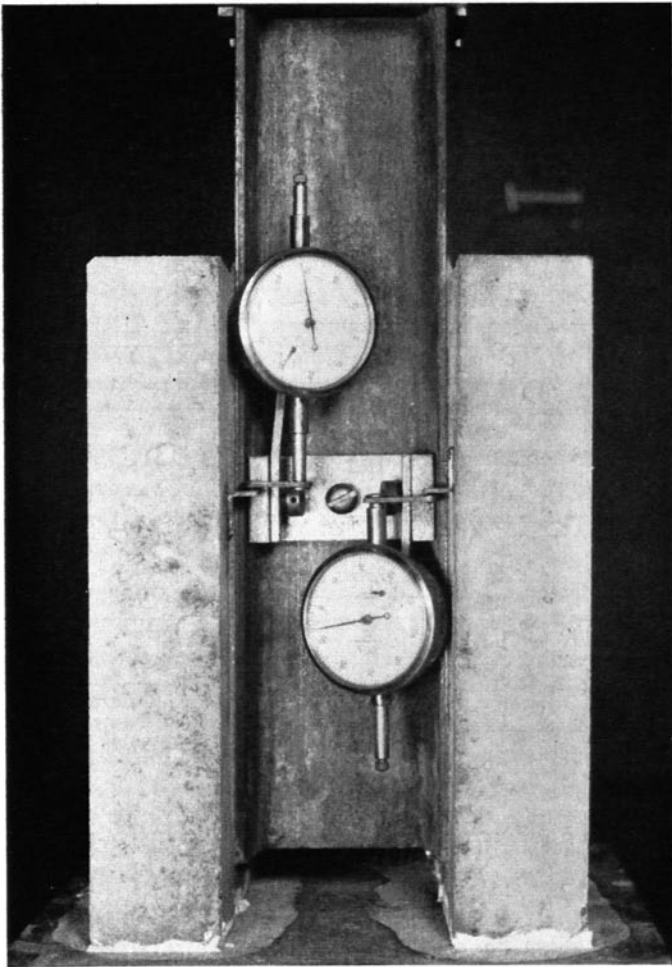
Fig. 5. Slip Measuring Apparatus

differed from those used in the model bridges, however, and only a nominal amount of reinforcing steel was used. The slab was tied to the beams by means of a number of channel shear connectors welded to the top flange of the I-beam.

The steel beams used in the static and fatigue tests were 3-in. I-beams of 6.5 lb per ft and 5.7 lb per ft, respectively. The slabs, made from sand-cement mortar of varying quality, were 18 in. wide and approximately $1\frac{3}{4}$ in. thick. The beams for the static tests were reinforced with $\frac{1}{8}$-in. square

Fig. 6. Details of T-beam Specimens

transverse bars only. The beams for the tests in fatigue were reinforced with either $\frac{1}{8}$-in. square transverse and longitudinal bars or with a 4-in. by 4-in. No. 8 gauge (0.1620 in.) welded wire fabric.

The beams were of four types as shown in Fig. 6. Types A and B were tested by static loading; types C and D were subjected to repeated loads. In addition to the variations already mentioned, the T-beams differed in the orientation, spacing, and size of shear connectors. In the beams of types A, B, and C the shear connectors were oriented symmetrically about the centerline; in the beams of type D all shear connectors faced the same way. In the beams of type A the spacing of the shear connectors varied from $3\frac{3}{4}$ in. at midspan to 2 in. at the support, as shown in Fig. 6; the other beams had shear connectors spaced at a constant distance of 4 in.

All shear connectors were cut from 1-in. channels. One flange of the channel connector was welded to the beam flange by continuous fillet welds

both at the back of the channel web and at the front edge of the channel flange. All connectors were $1\frac{1}{2}$ in. long except those in the beam of type B where 1-in. long channels were used. The width of the flange of the channels was generally $\frac{3}{8}$ in. The connectors in the beam of type B and in six specimens of type C were made from channels having a flange width of $\frac{1}{2}$ in. As this variation was not anticipated, these six specimens of type C are not reported in this bulletin. The thickness of the channel web was either $\frac{1}{16}$ in. or $\frac{1}{8}$ in. Three different thicknesses of the channel flange welded to the beam were investigated: 0.06 in., 0.12 in., and 0.20 in.[1] The radius of the fillet between the flanges and the web of shear connectors was approximately 0.019 in. for all channels. All shear connectors in one specimen were of the same size.

To prevent bond between the steel beam and the mortar slab, the top flange of the I-beam was greased in all specimens of types C and D. No attempt was made to prevent natural bond in the beams subject to static tests (Types A and B).

10. Materials

All slabs were made of a sand-cement mortar consisting of standard Portland cement and an artificially graded mixture of Wabash River torpedo sand and fine Lake Michigan beach sand. The gradation of the sand used was the same as for the push-out specimens.

The properties of the mixes and the corresponding strengths and moduli of elasticity as found from the tests of 2-in. by 4-in. control cylinders are listed in Table 2. Usually 15 control cylinders were made with each specimen. Three were tested moist at the age of 7 days, four were tested at the beginning of the tests, usually 28 days after casting the slab, and the remaining eight cylinders were tested at the conclusion of the tests. Modulus of elasticity was measured at the age of 28 days and at the conclusion of the tests. Seven day tests were not made for beams T1, T2, and T3.

The physical properties of the steel of the I-beams were obtained from tension test coupons cut from the flanges. They are given in Table 3. The properties of the steel in the channel shear connectors were determined from coupons cut from the channel webs and are given in Table 4.

11. Manufacture of Specimens

All shear connectors were made from channels having nominal dimensions of $1 \times \frac{3}{8} \times \frac{1}{8}$ in. When it was desired to vary the web and flange thicknesses, the channels were machined to the specified dimensions, as illustrated in Fig. 7. When only a smaller web thickness was required the web

---

[1] The flange thickness was measured at the theoretical junction of the flange with the web.

Table 2
Properties of Mortar for T-Beams

Specimen	Water-Cement Ratio by Weight	Proportion of Cement to Sand by Weight	7-Day Strength,* psi	Cylinder Strength				Average Strength,† psi	Initial Modulus of Elasticity Ec, 10⁶ psi	$n = \dfrac{E_s}{E_c}$
				At Beginning of Tests		At Conclusion of Tests				
				Age, Days	Strength, psi	Age, Days	Strength, psi			
T1	0.60	1:3.5	.....	28	4250	72	5100	4810	4.09	7.3
T2	1.00	1:6.5	.....	28	1800	110	1820	1820‡	2.85‡	10.5
T3	0.60	1:3.5	.....	28	4870	42	4250	4420	3.44	8.7
R1A	0.63	1:4.4	.....	21	3470	30	4420	4000	3.16	9.5
R2A	0.71	1:5.2	2080	28	4020	31	4150	4100	3.06	9.8
R3A	0.71	1:5.2	1880	28	3380	30	3400	3400	3.58	8.4
R4A	0.71	1:5.2	1780	28	3500	31	3760	3600	3.82	7.9
R5A	0.67	1:4.8	1720	27	3285	29	3335	3320	3.11	9.7
R6A	0.67	1:4.8	2520	29	3850	34	4140	4000	3.82	7.9
R7A	0.67	1:4.8	1830	28	3870	36	3970	3940	3.34	9.0
R1B	1.00	1:7.6	848	28	1900	28	1900	1900	3.50	8.6
R2B	0.91	1:6.9	1600	28	2760	29	3050	2950	3.19¶	9.4
R3B	1.00	1:7.6	910	31	1920	44	1980	1950	2.69	11.2
R4B	0.91	1:6.9	1070	28	2070	42	2400	2200	2.50	12.0
R5B	1.00	1:7.6	728	28	1910	28	1910	1910	2.88	10.4
R6B	0.91	1:6.9	1380	27	2240	36	2320	2280	2.71	11.1
R7B	1.00	1:7.6	930	28	1750	36	1850	1800	2.92	10.3
R1C	0.67	1:4.8	1900	27	3570	29	3610	3600	3.09	9.7
R2C	0.71	1:5.2	1530	29	2820	31	2880	2860	3.22	9.3
R3C	0.67	1:4.8	1740	30	3970	39	4580	4230	3.22	9.3
R4C	0.67	1:4.8	2390	28	4420	31	4230	4320	4.06	7.4
R5C	0.71	1:5.2	1980	30	3690	42	4000	3800	3.97	7.5
R1D	0.91	1:6.9	955	27	2060	29	2010	2030	2.34	12.8
R2D	0.91	1:6.9	950	28	1810	31	2020	1950	2.22	13.5
R3D	0.91	1:6.9	1300	29	2240	36	2310	2280	2.95	10.2
R4D	0.91	1:6.9	1200	32	2920	33	2540	2670	3.08¶	9.8
R5D	1.00	1:7.6	712	29	1820	35	1800	1810	3.32	9.0
R6D	1.00	1:7.6	882	28	1770	31	1770	1770	3.08	9.7

M1L	1.10	1:8.5	809	28	1680	29	1770	1720	2.57	11.7
M2L	1.10	1:8.5	963	28	1410	35	1410	1410	2.29	13.1
M3L	1.10	1:8.5	....	28	1190	36	1350	1270	2.01	14.9
M4L	1.10	1:8.5	995	28	1570	34	1830	1660	2.53	11.8
M5L	1.10	1:8.5	790	29	1270	34	1500	1390	2.35	12.8
M6L	1.10	1:8.5	1070	28	1900	35	1980	1940	2.72	11.0
M7L	1.10	1:8.5	498	28	1010	35	1130	1070	2.04	14.8
M8L	1.10	1:8.5	678	28	1500	35	1040	1270	2.25	13.4
M1M	0.49	1:3.2	2360	29	3530	35	3290	3410	3.08	9.8
M2M	0.82	1:6.1	1790	27	2560	29	2690	2620	3.17	9.5
M3M	0.82	1:6.1	1590	28	2530	30	2390	2440	2.98	10.1
M4M	0.82	1:6.1	1690	27	2590	29	2880	2730	3.13	9.6
M5M	0.82	1:6.1	1730	:	....	34	3110	3110	3.55	8.5
M6M	0.82	1:6.1	2010	28	3060	31	3240	3150	3.40	8.8
M7M	0.82	1:6.1	1850	28	2690	35	3000	2840	3.13	9.6
M1H	0.49	1:3.2	4370	29	5300	31	5120	5240	3.55	8.5
M2H	0.49	1:3.2	4500	28	6100	35	5510	5810	4.02	7.5
M3H	0.49	1:3.2	4580	28	5350	30	6360	5350	4.28	7.0
M4H	0.49	1:3.2	4490	27	6100	36	6500	6200	4.46	6.7
M5H	0.49	1:3.2	4170	27	6110	35	6820	6550	3.89	7.7
F1A	0.71	1:5.2	2750	27	4460	29	4550	4510	3.17	9.5
F2A	0.71	1:5.2	2620	28	3570	35	3600	3580	3.32	9.0
F3A	0.71	1:5.2	2230	29	3740	31	3830	3780	3.48	8.6
F4A	0.71	1:5.2	1900	29	3160	38	3640	3400	3.24	9.3
F5A	0.71	1:5.2	2440	31	3770	37	3550	3660	3.94	7.6
F6A	0.71	1:5.2	2670	31	4080	38	4090	4090	3.49	8.6
F7A	0.71	1:5.2	2450	28	3990	35	4030	4010	3.43	8.8
F8A	0.82	1:6.1	1000	29	2150	36	2290	2220	2.90	10.4
F1B	0.71	1:5.2	2440	28	4020	35	3650	3840	3.44	8.7
F2B	0.71	1:5.2	2180	29	4020	35	3830	3920	3.51	8.6
F3B	0.71	1:5.2	2280	28	4030	35	3820	3920	3.56	8.4
F4B	0.71	1:5.2	2220	28	3530	35	3520	3530	3.32	9.0
F5B	0.71	1:5.2	2220	28	3560	37	3430	3500	3.38	8.9
F6B	0.71	1:5.2	2110	28	3630	37	3480	3550	3.83	7.8
F7B	0.71	1:5.2	2000	28	3440	36	3330	3380	3.62	8.3

Table 2—Concluded

Specimen	Water-Cement Ratio by Weight	Proportion of Cement to Sand by Weight	7-day Strength,* psi	Cylinder Strength				Average Strength,† psi	Initial Modulus of Elasticity E_c, 10^6 psi	$n = \frac{E_s}{E_c}$
				At Beginning of Tests		At Conclusion of Tests				
				Age, Days	Strength, psi	Age, Days	Strength, psi			
F1C	0.71	1:5.2	2330	28	3230	30	3460	3300	3.07	9.8
F2C	0.71	1:5.2	1730	28	3270	35	3510	3390	3.46	9.1
F3C	0.71	1:5.2	2280	30	3000	35	2910	2960	3.22	9.3
F4C	0.71	1:5.2	1730	28	3200	32	3230	3220	2.60	11.5
F5C	0.71	1:5.2	2060	28	3460	35	2970	3220	3.74	8.0
F1L	....	1:3.5	2320	31	2180	36	2250	2220	2.85¶	10.5
F2L	....	1:3.3	2420	27	2520	27	2650	2580	3.04¶	9.9
F3L	....	1:3.5	2920	31	2750	38	2230	2650	3.07¶	9.8
F1H	0.49	1:3.2	3320	28	5280	34	4810	5050	3.80	7.9
F2H	0.49	1:3.3	3530	28	5060	35	5400	5230	3.88	7.7
E1	0.82	1:6.1	1290	31	2260	36	2810	2700	2.25	13.4
E2	0.82	1:6.1	....	31	1440	43	2260	1850	2.63¶	11.4
E3	0.82	1:6.1	....	31	1820	42	1850	1830	2.62¶	11.4
E4	0.82	1:6.1	....	27	1856	55	2090	1970	2.71¶	11.1
E5	0.82	1:6.1	960	28	2040	148	2430	2230	2.86¶	10.5
G	0.67	1:4.8	....	..	....	....	....	2460	2.75	10.9

Note: All cylinders cured 7 days under wet burlap.

* Tested moist.

† 7-day test not included.

‡ Averages of tests at 28, 62, and 110 days; at 62 days $f_c' = 1820$ psi, $E_c = 2.89 \times 10^4$ psi.

¶ Computed from formula $E_c = \dfrac{E_s}{6 + \dfrac{10{,}000}{f_c}}$.

Table 3
Physical Properties of Steel in Beams
All coupons were about $\frac{1}{2} \times \frac{1}{4}$ in. in cross-section

Specimen	Size and Weight of the Beam	Number of Test Coupons	Yield Point, psi	Ultimate Strength, psi	Percent Elongation in 2 in.
T*	3 in.-I 6.5 lb	3	37 400	65 300	36
R1A-R4A, R6A, R1B, R3B, R5B-R7B, R2C, R4C-R5C, R5D-R6D	3 in.-I 5.7 lb	4	39 100	62 900	36
R5A, R7A, R2B, R4B, R1C, R3C, R1D-R4D, M, F, E, G	3 in.-I 5.7 lb	4	41 100	66 900	33

* Data from Bulletin 363.

Table 4
Physical Properties of Steel in Channel Shear Connectors
All coupons were about 0.8×0.125 in. in cross-section

Specimen	Number of Test Coupons	Yield Point, psi	Ultimate Strength, psi	Percent Elongation in 2 in.
T*	2	42 500	60 600	..
R†	8	40 200	57 200	39
R7A, R4B, R3C, R2D, R4D	2	54 700	88 650	25
R2B	2	41 250	63 100	30
M, F, E	18	42 450	64 200	35

* Data from push-out tests, Section 6.
† Except specimens listed separately.

was milled down on the back of the channel as shown in Fig. 7a. If it was desired to reduce the flange thickness in addition to that of the web, the nominal size channel was milled on both the inside and outside faces as shown in Figs. 7b and c. When this was done, care was taken to reproduce the original radius of the fillet between the web and the flange as closely as possible.

The first step in manufacture of the T-beam specimens was to weld shear connectors to the top flange of the steel I-beam. Arc welding with $\frac{1}{8}$-in. semi-shielded Fleetweld No. 11 electrode was used in the beams for the static tests (Types A and B). In the remaining specimens a $\frac{3}{32}$-in. electrode was used and thus a smaller weld was achieved.

Forms for the slab were assembled around the I-beam with the floor of the forms flush with the top flange of the beam and the reinforcing steel was placed in the forms. The wood forms used at first were later replaced by steel forms. While the mortar was being cast and during the moist curing period, the I-beam was supported at the ends and at the center. A view of the forms and reinforcing steel for beam T2 is shown in Fig. 8.

Since in the static tests it was desired to have an initial natural bond between the mortar slab and both the steel beam and the connectors, the
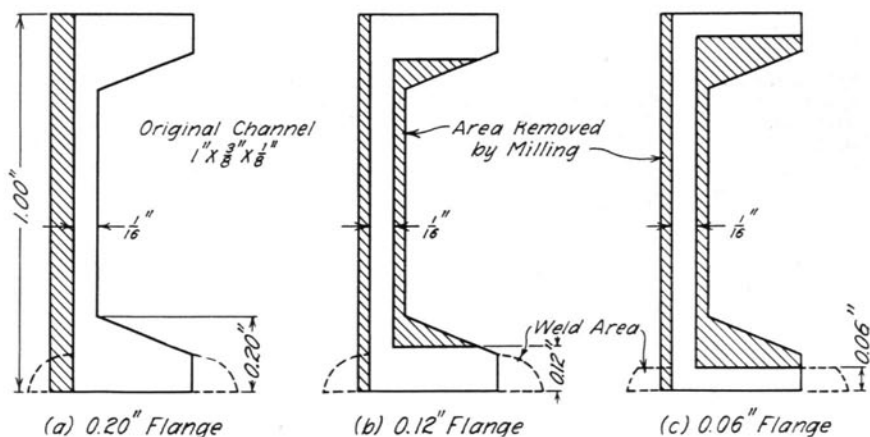

Fig. 7. Milling of Channels

steel surfaces in contact with the slab on specimens T1, T2, and T3 were thoroughly cleaned before the slab was cast. On the other hand, the surface of the upper beam flange of the specimens tested in fatigue was covered with a layer of cup grease to prevent natural bond.

The mortar was mixed in a Lancaster mixer with a capacity of 2 cu ft. In beams T1, T2, and T3 the mix was placed in the forms with the aid of a trowel only; in the other specimens placing was accomplished with the aid of a vibratory screed. After three or four hours, the mortar was struck off flush with the top of the forms, and two or three hours after that the surface was trowelled smooth with a steel trowel. The slab was allowed to cure moist in the forms under wet burlap for 7 days, after which the forms were removed and the slab was given two coats of white traffic lacquer as soon as its surface was dry enough to take the paint. The slab was painted to prevent it from drying out and to prevent the occurrence of shrinkage stresses, curling, and distortion which would accompany such drying. Several 2-in. by 4-in. control cylinders were made with each slab. These cylinders were cured and painted in the same manner as the slab.

Soon after stripping the forms, end bearing blocks were bolted to each end of the beam and the beam was lifted into place on the supports, where it was allowed to cure an additional 21 days before testing was begun.

Before testing, it was necessary to prepare the gage lines on which strains were to be measured. On the beams, this required only that the strain gage holes be drilled, but for the gage lines on the slab it was necessary to set steel plugs in holes in the mortar and to drill the strain gage holes in these plugs. The gage plugs consisted of pieces of $\frac{1}{4}$-in. diameter steel rod set in the holes with a high strength gypsum plaster. On the bottom of the slab, the plugs projected about $\frac{3}{16}$ in. below the bottom of the slab to the level
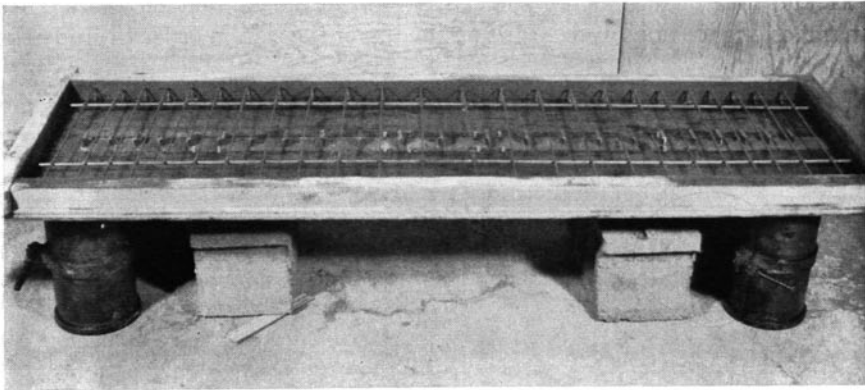
Fig. 8. Forms for Beam T2 Before Casting Slab

of the underside of the top flange of the I-beam. This was done so that the gage lines on the bottom of the slab and those on the upper flange of the I-beam would be at the same level. On top of the slab the plugs were set flush with the surface.

Although the thickness of the slab for all specimens was intended to be 1.75 in., the thickness for beam T3 was actually 1.67 in. This difference was taken into account in all theoretical calculations. Later, when the steel forms replaced the wooden ones used for the manufacture of beams T1, T2 and T3, all slabs had the desired thickness.

12. Loading Apparatus and Instruments

Static Tests. During the tests the beams were supported on railroad rails resting on the top of concrete piers which in turn were supported on the steel beams of a self-contained loading frame. Load was applied to the specimens by means of a screw jack with a capacity of 25 tons, which had for its reaction this same loading frame. In all the tests the load was

applied to the T-beam through a steel disk $3\frac{3}{4}$ in. in diameter centered directly over the I-beam. To insure uniform distribution of the load a $\frac{1}{2}$-in. thick pad of sponge rubber was placed between the steel disk and the slab. The loads were measured by an elastic ring dynamometer placed between the jack and the loading disk. Dynamometers of both 10,000-lb and 20,000-lb capacities were used in these tests. A view of the arrangement for testing beam T2 is shown in Fig. 9. The arrangements for beams T1 and T3 were similar in all respects.

Strains were measured on 2-in. gage lines at several points on the cross-section of the T-beams, at each of a number of locations along the length of the beam as shown in Fig. 10. There were three such locations on beam T1 and four on beams T2 and T3. It will be noted that on beam T3 a number of gage lines were added on the top of the slab in order to study the
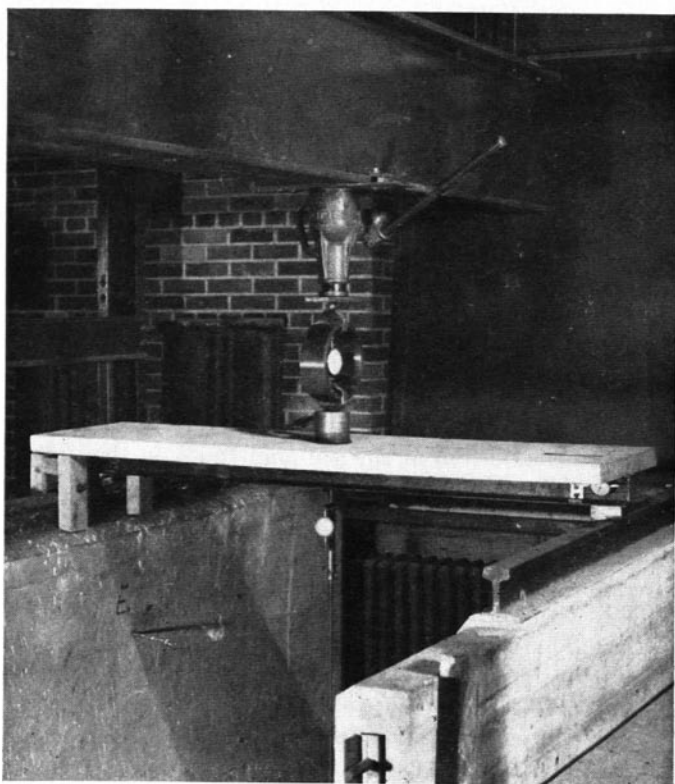

Fig. 9. Arrangement for Static Tests of T-beams

distribution of strain across the width of the slab. All strains were measured with a 2-in. gage length Berry strain gage. This instrument was equipped with a 0.001-in. dial indicator and had a mechanical multiplication of 5.80.

Slip between the slab and the I-beam was measured on both sides of the beam at all sections at which strains were measured except at midspan of beam T1 as shown in Fig. 10. The slip measurements were made with the Berry strain gage, using four gage holes at each location—two on the steel beam and two on the mortar slab. In addition to measuring slab and beam strains, the changes in the distance between one hole located on the slab and another located on the beam 2 in. away were measured in both diagonal directions. The difference between the changes in length of these slip gage lines, extending from beam to slab, and the changes in length of the corresponding strain gage lines, which were wholly on the beam or wholly on the slab, was assumed to be equal to the slip. From a given set of measurements it was possible to compute the slip at each end of the gage
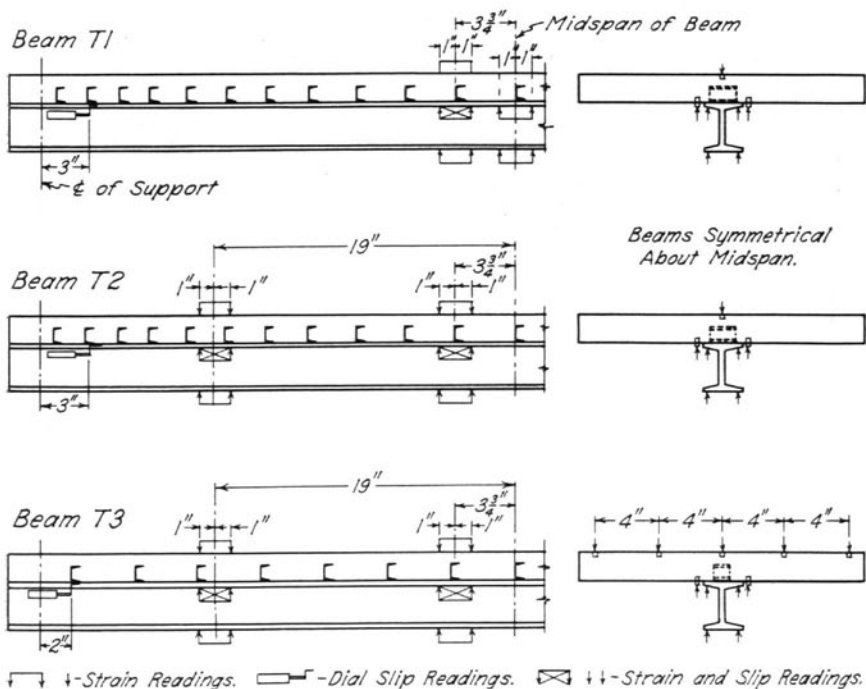

Fig. 10. Location of Gage Lines on Beams T1, T2, and T3

lines by two different calculations. This was done for the gage lines on each side of the beam at each location and the average of all values was taken as the slip at that location.

Slip was also measured on each side of the beam near each end as shown on Fig. 10. For this purpose a 0.001-in. dial indicator was attached to the I-beam in such a manner that its spindle would bear against a small bracket attached to the slab with Duco cement. The point of attachment of the dial to the I-beam was directly opposite the point of attachment of the bracket to the slab so that slip only would be measured.
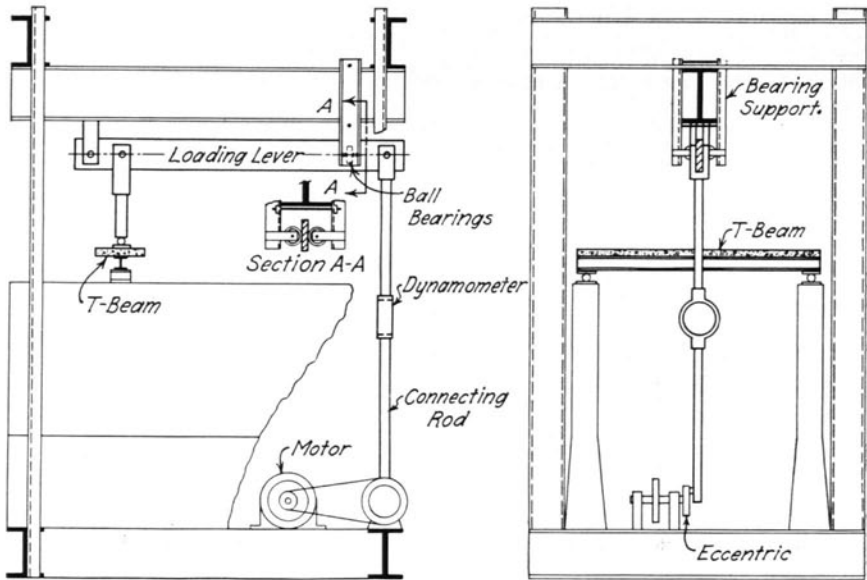
Fig. 11. Repeated-Load Testing Machine

Deflections of the beam at midspan were measured in most of these tests by a deflectometer utilizing a 0.001-in. dial indicator. All deflections were measured with respect to the floor of the laboratory. Since the piers supporting the beams did not bear directly on the floor but were carried on the steel loading frame, a small error was introduced due to the movement of the piers relative to the floor. The magnitude of this movement was determined by test, and account was taken of it in all comparisons of measured and computed deflections.

The control cylinders were tested in a 60,000-lb capacity Southwark-Emery hydraulic testing machine. The modulus of elasticity was measured with the aid of a compressometer of 2-in. gage length equipped with a 0.0001-in. dial indicator.

Gage Lines Symmetrical About Midspan
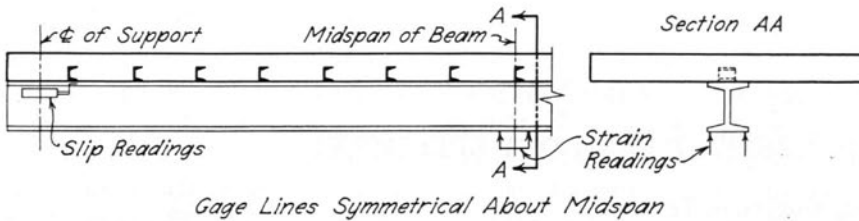
Fig. 12. Location of Gage Lines on Beams Tested in Fatigue

Fatigue Tests. The loading frame and concrete piers used in static tests were used also for repeated-load tests. The railroad rails were replaced by flat steel plates resting on the top of the concrete piers and bedded on neat cement mortar. The beam was supported at each end on steel rollers which in turn were supported on the bearing plates. Load was applied at midspan of the T-beam by a lever of approximately 10:1 ratio actuated by a connecting rod attached to a variable-throw eccentric. The load was applied through a ball bearing to a steel disk $3\frac{3}{4}$ in. in diameter which was centered directly over the I-beam and set in a layer of plaster of paris. The load was measured by a 2000-lb capacity elastic-ring dynamometer inserted in the connecting rod. The loading frame served as a reaction to the loading lever. The speed of operation was 190 cycles per min. The natural frequency of the T-beams was about 5000 cycles per min. The whole testing machine, including the concrete piers, the loading frame, and the loading apparatus, is shown schematically in Fig. 11.

The measurements made during the repeated-load tests included slip between the slab and the I-beam at the ends of the beam and deflections at midspan. The location of the dials for the repeated-load tests, and the strain gage lines for the initial and final static tests, are shown in Fig. 12. The measuring instruments were the same as those for the static tests.

III. TESTS OF PUSH-OUT SPECIMENS

13. Outline of Tests

The tests of push-out specimens were made primarily for the purpose of investigating the basic properties and behavior of various types of shear connectors suitable for use in composite I-beam bridges. Sixty-four push-out specimens were tested in three series. The principal variables were the type and dimensions of the shear connectors, the type of bond between the steel and mortar parts of the specimens, and the mortar strength. Each series was designed to study primarily one of these variables. The tests of push-out specimens were made in 1942–1943.

Table 5
Outline of Push-out Specimens

| Specimen | Shear Connectors | | | | Treatment to Destroy Bond on Surface of* | |
	Type	Width, in.	Thickness, in.	Height, in.	Connector	Beam
	Series I					
C1a†	Channel	1.50	0.125	1	None	None
C1d‡	Channel	1.50	0.125	1	None	None
C2a	Channel	2.31	0.125	1	None	None
C3a	Channel	0.75	0.125	1	None	None
C4a	Channel	1.50	0.098	1	None	None
C5a	Channel, Top Flange Cut Off	1.50	0.125	1	None	None
C6a	Channel, Top Flange Cut Off	1.50	0.097	1	None	None
C7a	Channel on end	1.00	0.125	1	None	None
B1a	Bent Z-Plate	0.50	0.135	$1\frac{1}{8}$	None	None
B2a	Bent Z-Plate	1.00	0.125	$1\frac{1}{8}$	None	None
B3a	Bent Z-Plate	1.50	0.130	$1\frac{1}{8}$	None	None
B4a	Bent Z-Plate	1.00	0.050	$1\frac{1}{8}$	None	None
B5a	Bent Z-Plate	1.00	0.190	$1\frac{1}{8}$	None	None
P1a	Straight Plate	1.50	0.097	1	None	None
P2a	Straight Plate	1.50	0.130	1	None	None
P3a	Straight Plate	1.50	0.158	1	None	None
A1a	Angle on End	1.41	0.125	1	None	None
A2a	Angle on End	1.41	0.125	1	None	None
T1a	Tee on end	0.75	0.125	1	None	None

Series I included 19 types of specimens; there were usually two companion specimens of each type. The main purpose of this series was to compare the effectiveness of the various types of shear connectors. The shear connectors and their dimensions are listed in Table 5 and illustrated in Fig. 2. All slabs of this group were made from mortar of the same proportions and the variations in the resultant mortar strengths were small. In all specimens of Series I the bond on the surfaces of the shear connectors and beams was natural.

The changes in the load-slip characteristics of a connector due to variable bond conditions were studied in Series II. Nine types of specimens of this series, with two companion specimens of each type, together with three types of specimens of the first series (C1a, C5a and B2a), furnished data on the effect of destroying bond between the slab and beam, and on the effect of destroying bond between the slab and the shear connector. The variations of the bond conditions in Series II are listed in Table 5. The

Table 5—Concluded

Specimen	Shear Connectors				Treatment to Destroy Bond on Surface of*	
	Type	Width, in.	Thickness, in.	Height, in.	Connector	Beam
			Series II			
C1b	Channel	1.50	0.125	1	Greased	None
C1c	Channel	1.50	0.125	1	Greased	Greased
C1bp	Channel	1.50	0.125	1	Polished	None
C1cp	Channel	1.50	0.125	1	Polished	Greased
C1x	Channel	1.50	0.125	1	None	Greased
C5b	Channel, Top Flange Cut Off	1.50	0.125	1	Greased	None
C5c	Channel, Top Flange Cut Off	1.50	0.125	1	Greased	Greased
B2b	Bent Z-Plate	1.00	0.125	$1\frac{1}{2}$	Greased	None
B2c	Bent Z-Plate	1.00	0.125	$1\frac{1}{2}$	Greased	Greased
			Series III			
C1aL	Channel	1.50	0.125	1	None	None
C1aM	Channel	1.50	0.125	1	None	None
C1aH	Channel	1.50	0.125	1	None	None

Two companion specimens were made of each type except C1a. In case the companion specimens need to be distinguished, an arabic numeral is added at the end of the specimen number; for example, A1a1 is the first of the two companion specimens A1a1 and A1a2.

All slabs were 6 in. wide except on C1d.

* When no treatment was given to the surface of the connector or beam there was an initial bond between the concrete slab and steel beam or shear connector.

† Four companion specimens.

‡ 9-in. wide slabs.

shear connectors of this series were channels, types C1 and C5, and bent plates, type B2. The mortar was of the same proportions as for the first series.

The three types of specimens in Series III were designed with mortars having strengths ranging from 1500 to 5500 psi. The strengths of the mortars for specimens C1aL, C1aM, and C1aH are given in Table 1. No other variables were involved. All shear connectors of Series III were channels of type C1.

14. Description of Test Procedure

The arrangement of the testing and measuring apparatus used in the push-out tests was described in Section 8. The load was applied through a dynamometer, and slip between the slabs and the beam was measured by four dial indicators. For convenience in recording, all load increments were computed in terms of divisions on the dial of the dynamometer. For the 20,000-lb dynamometer, 1 division was equal to 86 lb, whereas for the 50,000-lb dynamometer, 1 division was equal to 113 lb. At the beginning of the test, load was applied in increments of one division on the dynamometer dial. After a small amount of slip had been recorded, the load increment was increased to 5 divisions and load was applied at this rate until the maximum load was reached. Each of the four slip-measuring dials was read to the nearest 0.0001 in. for each increment of load.

This procedure was modified in the case of specimens Cla4 and ClaHl in order to determine that part of the slip which was recoverable on release of load. For these specimens load was applied in increments as before, but after each increment load was released entirely before applying the next. This procedure was followed until failure was imminent, at which time load was applied continuously in 5-division increments until the specimen failed.

15. Manner of Presentation of Test Data

All the quantitative data obtained in the push-out tests are presented in Figs. 13–26, chiefly in the form of load-slip curves. For each curve in these figures, the values of slip plotted were obtained by first averaging the slips measured by the four dials on the same specimen and then averaging the slips thus obtained for each of the duplicate specimens. In general, load-slip curves for duplicate specimens were in very good agreement. The agreement was better for low values of slip than for large slips. No significant differences in the load-slip curves of duplicate specimens were noted; therefore only the average of the data for the two specimens is presented.

The ordinates of the load-slip curves are equal to one-half the actual loads on the specimens, since there were two connectors on each specimen.

The inaccuracies in this procedure, due to an uneven distribution of the load between the shear connectors were partly compensated for by averaging the slip readings; in any case, the slip readings seemed to indicate a fairly even distribution of load. Another possible source of inaccuracy in the above procedure was introduced by friction between the slab and beam at the contact surfaces. It is believed that the error due to this cause was negligible.

Except for certain specimens, the point at which the load-slip curve is stopped does not indicate the slip at the ultimate load or at failure. In general, the slip at maximum load was greater than that shown at the end of the curve; for several specimens the slip at failure was as much as 0.5 in.

The value of the ultimate load is indicated on the figures by a bar graph to the right of the load-slip curves. The full height of the bar indicates the average of the ultimate loads for duplicate specimens which were in fairly close agreement in most cases. The difference between the duplicate specimens averaged about 7 percent, and in only two instances did it exceed 15 percent.

Although several comparisons are made on the basis of the ultimate loads, it is recognized that the significance of the ultimate load is questionable because of the large slips accompanying failure. The magnitude of slip in a composite beam depends on the type and size of shear connectors, on their spacing, and on several other factors. The tests of T-beam specimens, reported in another part of this bulletin, indicate, however, that in beams with shear connectors comparable to those investigated in the small-size push-out tests a slip of 0.01 in. is almost an upper limit and is representative of an advanced stage of deterioration of the shear connection. With this in mind and on the basis of the shape of the load-slip curves, it was decided to make comparisons of various connectors at an average slip of 0.0025 in. This load is represented by the height of the black portion of the bar graph.

The tests of the first two small-scale T-beams and the tests of the scale-model composite I-beam bridges[1] built with comparable shear connectors indicated that slips at working loads can be expected to be of the order of few ten thousandths of an inch. Therefore, several comparisons were made at an average slip of 0.0002 in. Only a few of these comparisons are presented in the following paragraphs, as the reliability of the measurements of such small slips is questionable.

To obtain a graphical representation of the effects of several variables on the load-carrying capacity of various connectors, Fig. 17, 19, and 22

---

[1] Bulletin 363.

were plotted. In all these figures curves are plotted for three different conditions: (1) at a slip of 0.0002 in., (2) at a slip of 0.0025 in., and (3) at the ultimate load.

16. Comparison of Connectors of Various Types

In general the shear connectors for concrete and steel composite T-beams may be divided into three groups: (1) rigid connectors, (2) flexible connectors, and (3) reinforcing bar connectors. Only the first two types were investigated in these tests. The flexible connectors were represented by the following shapes: regular rolled steel channel, channel with the outstanding flange cut off, plate bent in Z-shape, and straight plate (Fig. 2). The load-slip curves for these types are shown in Fig. 13. The rigid connectors were of three types: channel, angle, and tee sections welded to the beam in such a way that they offered the greatest resistance to bending. Load-slip curves for the various rigid connectors are compared in Fig. 14. Comparisons of various types of flexible and rigid connectors are given in Fig. 15.

All four types of flexible connectors are compared in Fig. 13a. The connectors chosen for this figure were all 1.5 in. wide and 1 in. high, and the thickness of their flexible webs was $\frac{1}{8}$ in. The average strength of the mortar varied from 4360 to 5440 psi. It will be shown later that this variation of mortar strength has very little effect on the load-slip characteristics of a shear connector. Thus the only important difference between specimens C1a, C5a, B3a, and P2a was the shape of the connectors. The load-slip curves for the channel specimens C1a and C5a are practically identical. The absence of the outstanding flange embedded in the mortar of the slab seemed to have no effect on the load-slip characteristics. The corresponding curves for specimens B3a and P2a are lower than those for channel connectors but no difference between the bent plate and straight plate connectors is evident. The bar diagrams at the right side of the figure indicate that the same is true at 0.0025-in. slip and at the ultimate load. The bar diagrams suggest that the straight plate is even somewhat better than the bent one. Since the condition at the free end of the connector seemed to have little influence on the load-slip characteristics and since the flexible parts of all four types of connectors were the same, any difference between the channel type and the plate type connectors must have been caused by the conditions at the end welded to the beam. This portion of the connector, represented in the channel and bent plate types by the flange and in the straight plate type by the weld, is considerably stiffer than the web and therefore is called the stiff portion of the connector. The maximum thickness of the flange of the channel—that is, the height of the stiff portion

of the channel connectors—was about 0.20 in. The corresponding height for the bent plate connectors was about 0.125 in., and for the straight plate (height of welds) also 0.125 in. Furthermore, it seems reasonable to assume that because the stiff portion of the channel type was stiffer than that of the plate connectors the end rotations of the webs were smaller for the channel connectors than for the plate connectors. The differences in both the height and the relative stiffness of the stiff portions indicate that larger slips should be expected for plate connectors, which was the case.
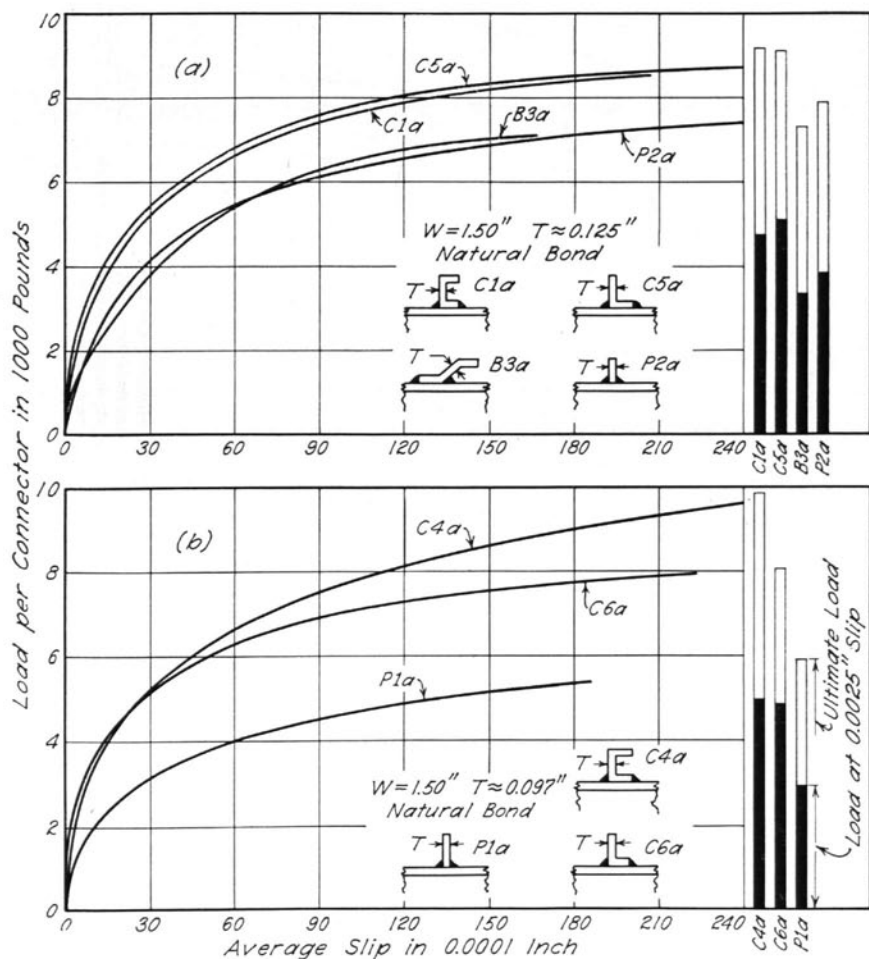

Fig. 13. Load-Slip Curves for Flexible Connectors

The curves shown in Fig. 13b are for specimens 1.5 in. wide, approximately 0.097 in. thick, and of mortar strength varying from 3470 to 5360 psi. Three different types of connectors are included—the regular channel connectors (C4a), the channel connector without the outstanding flange (C6a), and the straight plate connectors (P1a). The superiority of the channel connectors is obvious. The relatively lower slip for channel shear con-
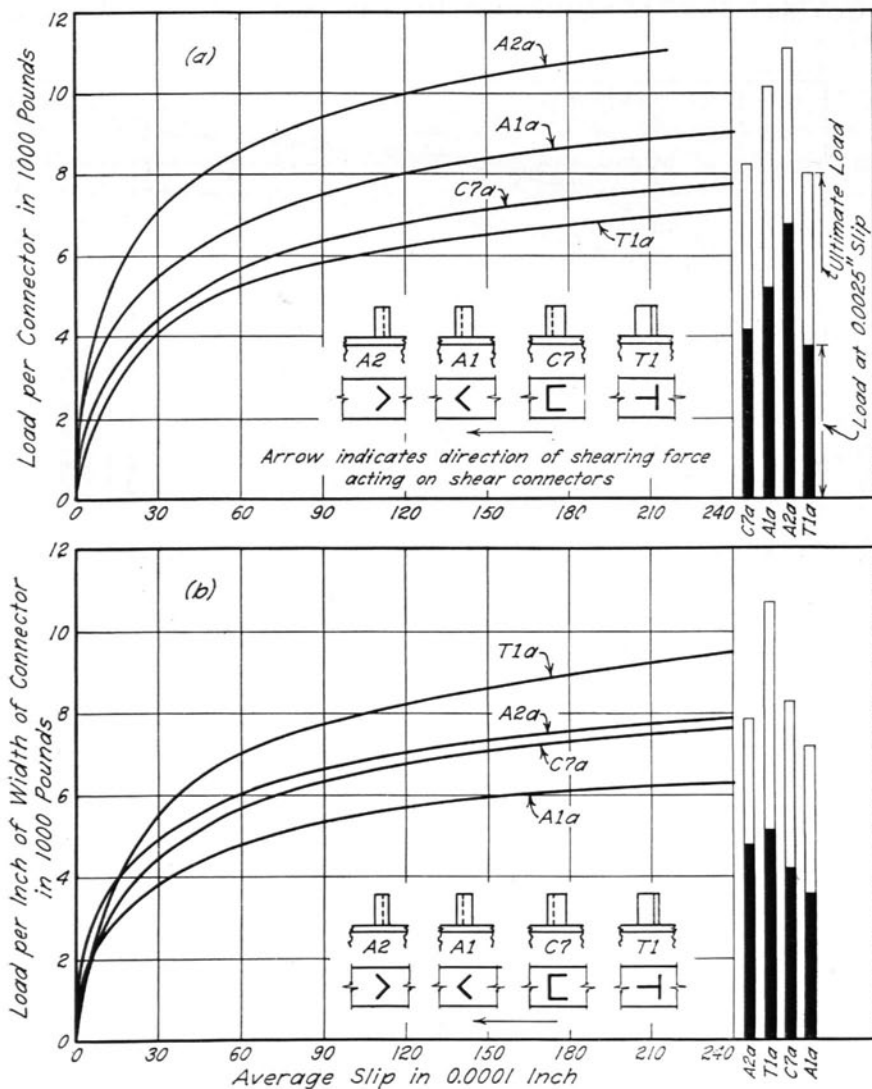

Fig. 14. Load-Slip Curves for Rigid Connectors

nectors must undoubtedly have been caused by the presence of the flange welded to the beam, even though the low mortar strength of specimen P1a accounts for part of the difference. The differences between the curves for specimens C4a and C6a may be explained by a separation of the slabs and the beam at high loads. The separation could take place freely in specimen C6a but was prevented in specimen C4a by the existence of the outstanding flange. This explanation is supported by the bar diagrams, which show practically equal loads at a slip of 0.0025 in. and a difference of 8 percent in the ultimate loads. But it must be remembered that the difference is relatively small and that a similar phenomenon was not observed in the load-slip characteristics of specimens C1a and C5a (Fig. 13a).

The load-slip characteristics for the tee, channel, and angle rigid type shear connectors are plotted in Fig. 14a. These test results, however, cannot be taken as a measure of the relative effectiveness of the individual connectors, since neither the bearing area nor the weight of the various types of connectors was equal. Thus reduction to an equal weight or bearing area must be made first. The latter is done in Fig. 14b, where the load was reduced to a unit width, 1 in., of the connector. The best connector seems to be the tee type; the least desirable, the angle with the apex on the unloaded side. The stiff channel connector and the angle connector with the apex on the loaded side showed about the same load-slip characteristics. The differences between the load-slip characteristics are more pronounced at high loads and at ultimate loads than at a slip of 0.0025 in. The differences between the two angles were probably caused by spreading of the flanges in specimen A1a. It is believed that this type of connector might be strengthened by the use of a welded cross bar tying together the two flanges of the angle.

Comparisons of rigid and flexible types of connectors are shown in Fig. 15. In each of the three parts of this figure the load-slip curves of one rigid and one flexible connector are compared. The pairs were so selected that the two connectors were always of the same width and of the same web thickness. The heights and mortar strengths of all connectors are comparable.

In Fig. 15a the load-slip characteristics for the flexible channel connector C1a and the rigid angle connector A1a are compared. There is only negligible difference between the two curves, but it should be noted that specimen A1a was the weakest type of rigid connector while the channel was the best of the flexible types tested. It may also be noted from Fig. 2 that the weight of the channel connector was about 30 percent greater than that of the angle. This comparison may be misleading, however, as the relative weights for the small-size connectors may differ from those for the prototypes.
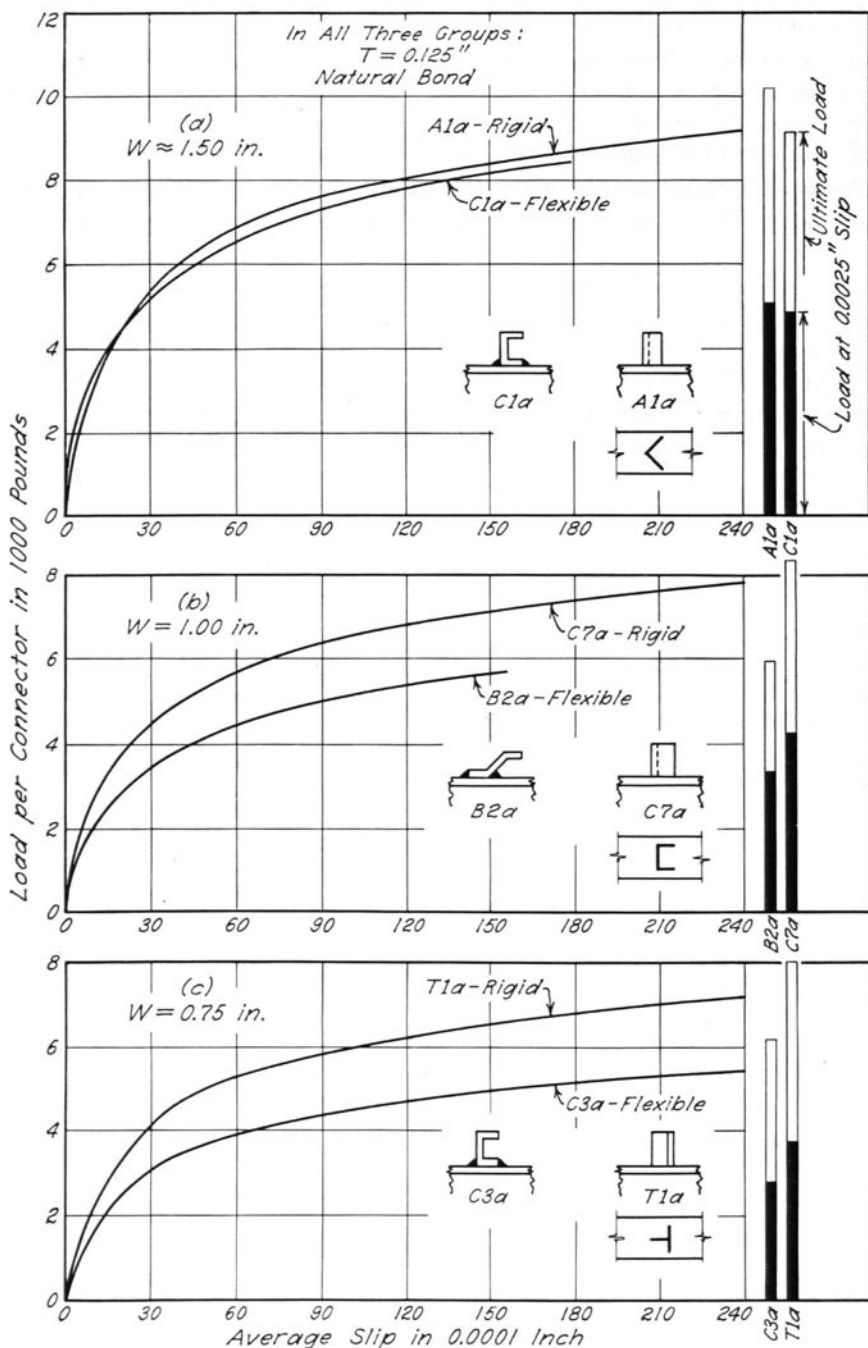
Fig. 15. Comparison of Flexible and Rigid Connectors

A somewhat larger difference between flexible and rigid connectors can be observed in Fig. 15b, in which the test data for specimens B2a and C7a are shown. The load-slip characteristics of the bent plate connector are inferior to those of the rigid type of channel connector. A similar comparison for specimens T1a, with rigid tee connectors, and C3a, with flexible channel connectors, is shown in Fig. 15c.

Although the load-slip characteristics indicate some superiority of the rigid types of connectors over the flexible types, the differences in slip of these two types are nevertheless very small when compared with the differences in their rigidities. The moment of inertia of a rigid connector is many times larger than the moment of inertia of the web of a flexible connector. Only the stiffness of the stiff flange of some of the flexible connectors is comparable to the stiffness of the rigid connectors. It seems likely that the relatively small differences in load-slip characteristics for the rigid and flexible types can be explained by the hypothesis that only a small part of the total load on a flexible connector is resisted by flexure of the web while the major part is transmitted through the stiff flange in direct bearing.

All comparisons of the flexible and rigid types of connectors made thus far have been based on their load-slip characteristics. It must be pointed out, however, that other factors which are not considered here may be more in favor of the flexible channel type. Such factors are the requirement of a positive anchorage of the slab to the beam, the maximum spacing, the ease of manufacture, and others.

17. Effects of Physical Properties of Specimens

It has been shown in the previous section that the load-slip characteristics of a connector are different for rigid and flexible types. It seems reasonable to assume that whereas the load-slip characteristics of a rigid connector will depend mainly on the total load-bearing area of the connector, the same characteristics of a flexible connector are influenced more noticeably by the relative dimensions of its various portions. This section deals with some of the variables which might be important from the standpoint of the behavior of a flexible connector. The effect of the thickness of the flexible web, of the width of the connector, and of the presence or absence of the outstanding flange was investigated. The height of the stiff portion, which seemed to enter as an important factor, was not considered as an independent variable in these tests.

Other factors which must influence the behavior of a shear connector include the properties of the mortar slab in which it is embedded. The strength of the mortar, the embedment of the connector, whether located in a fillet or in the main body of the slab, and the dimensions of the slab may all be of some importance. However, only the effect of the mortar strength and of the width of the slab was investigated in these tests.
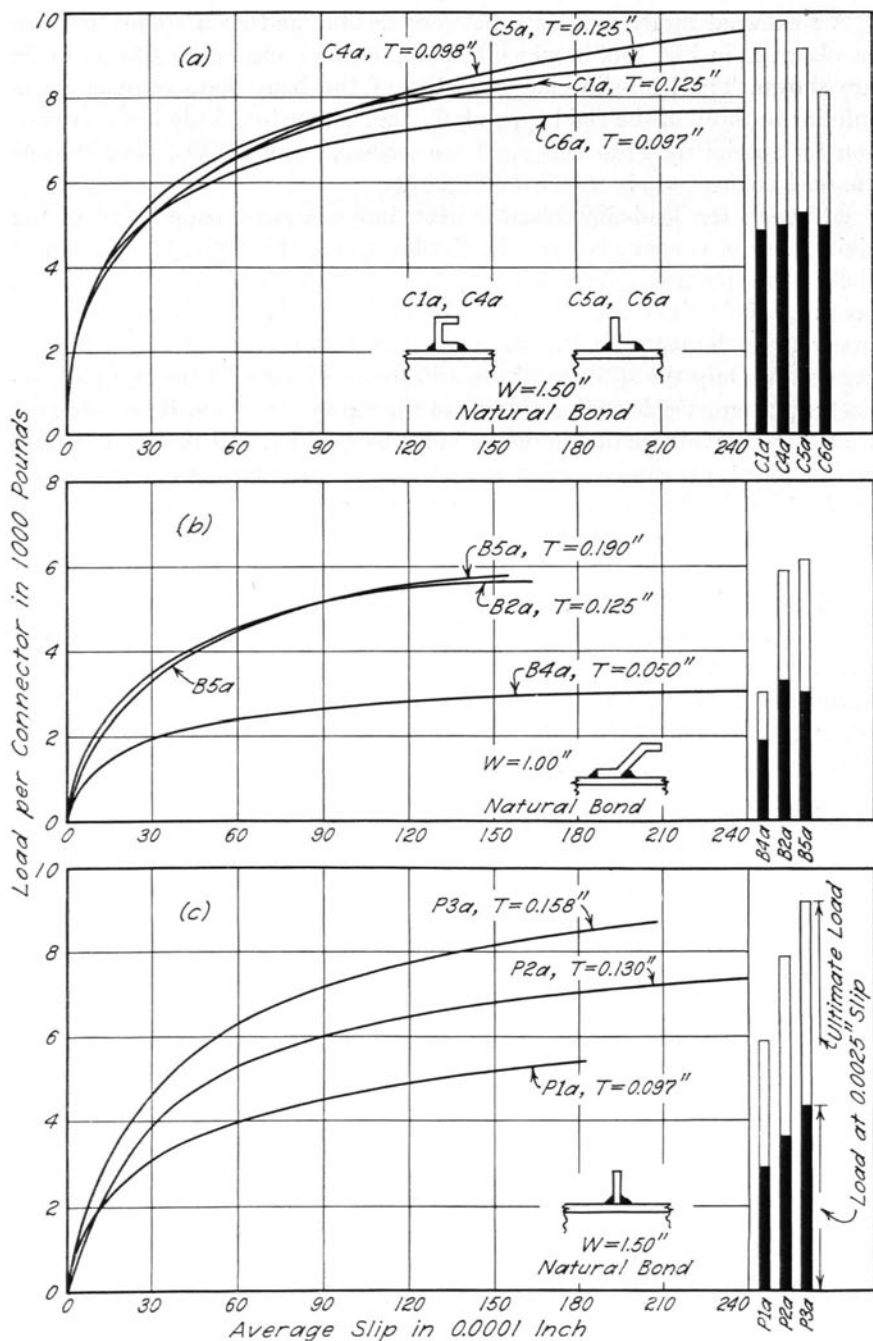
Fig. 16. *Effect of Thickness of Flexible Web of Connectors*

The third group of variables that may enter the picture are the bond conditions between the slab and the beam, and between the slab and the shear connectors. These variables were investigated in some detail.

Effect of Thickness of Connector Web. The effect of this variable was investigated on all four types of flexible connectors. The test results are plotted in Figs. 16 and 17. In these tests, the mortar strength varied from 3470 to 5440 psi.
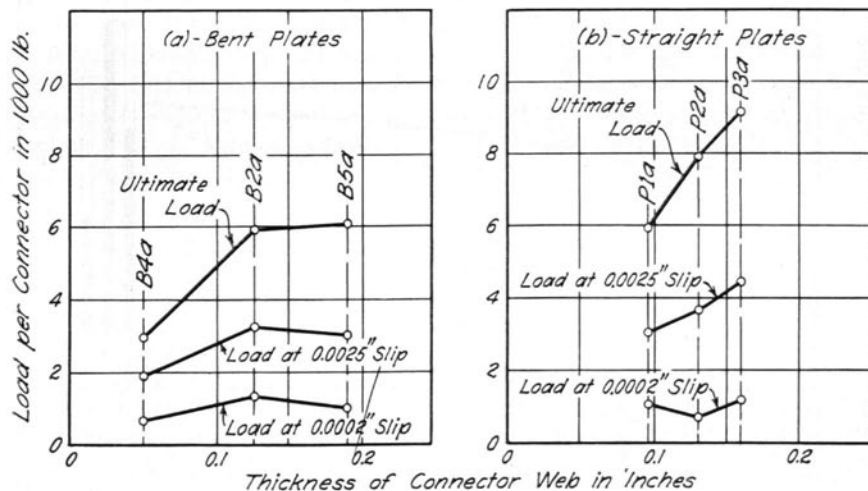

Fig. 17. *Variations of Capacity of Connectors with Changes in Web Thickness*

The load-slip curves for the channel-type connectors, both with and without the outstanding flange, are shown in Fig. 16a. Whether the comparisons are based on the general trend of these curves, on the load at 0.0025-in. slip, or on the ultimate loads, no consistent effect of the thickness of the flexible web is evident. Although the thicker web caused a slight decrease in the amount of slip for the channels with the outstanding flange cut off, the opposite is indicated for normal channels. It seems probable, therefore, that the slip of a channel connector is not influenced significantly by variations in the thickness of the web of the order of magnitude considered in these tests. This would lead to the conclusion that a fairly large part of the load is concentrated on the stiff portion of the channel—that is, on the channel flange welded to the beam.

Bent plates of three thicknesses were tested. Although in the tests of channel connectors the thickness of the web was the sole variable, in these tests the thickness of both the web and the flanges varied, since the bent-plate connectors were manufactured from plates of uniform thickness. Thus
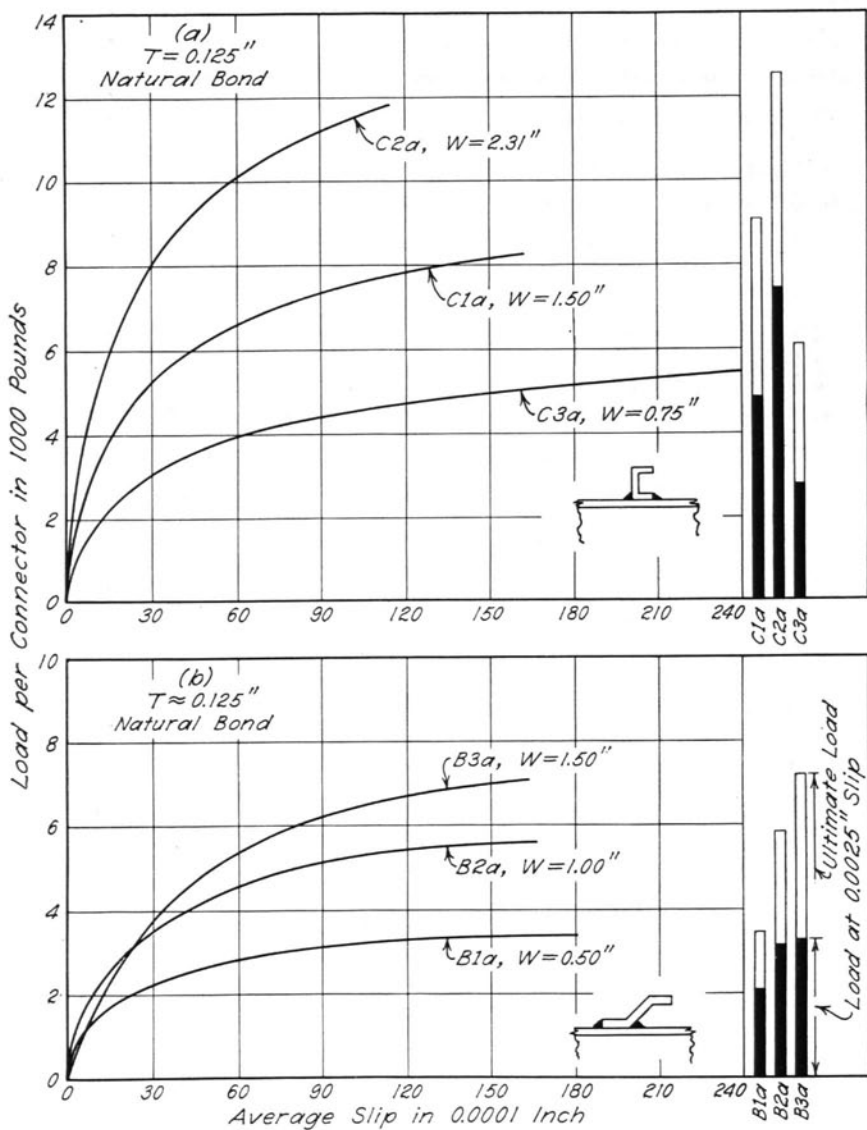
Fig. 18. *Effect of Width of Connectors*

the results of this group of tests were influenced by both variables. The load-slip curves in Fig. 16b show that the connectors 0.190 in. and 0.125 in. thick showed about the same load-slip characteristics, indicating that if any influence of the web thickness was present it was counterbalanced by the influence of the height of the stiff portion. The thinnest bent-plate connector, B4a, showed markedly different characteristics when compared with specimens B5a and B2a. This can be observed both in the load-slip curves and in the bar diagrams of Fig. 16b; it is clearly shown also in Fig. 17a, in which the load per connector is plotted against the thickness of the connector at slips of 0.0002 in. and 0.0025 in. and at the ultimate load. It is quite possible that the behavior of connector B4a differed fundamentally from that of the other bent-plate connectors because of the large flexibility of the flange welded to the I-beam. The difference could have been caused also by the rather large decrease in the web thickness, but in the light of the other results this seems unlikely.

While the channel connectors represent a type with a large and rigid stiff portion, in the straight-plate connectors only the weld is responsible for the increased stiffness of the connector at locations adjacent to the beam. It may be expected, therefore, that if the thickness of the web has any effect at all on the load-slip characteristics of a flexible connector this effect will be most significant in the straight-plate type of connector. The test results for plates of three different thicknesses are shown in Figs. 16c and 17b. Except for very low slips, at which the results are uncertain, the load-slip curves show decrease in slip with increasing thickness of the web. This is true both at a slip of 0.0025 in. and at the ultimate load. Fig. 17b indicates that a nearly straight line relationship exists between the load P on the connector and the thickness t of the plate. Thus the plate connector obviously does not act as a cantilever, for which the load P would vary as t^3; its behavior is more nearly like that of a dowel for which the load P varies with $t^{\frac{1}{2}}$.

Effect of Width of Connector. Two series of tests were made in which only the width of the connector was varied. Figure 18a contains load-slip curves for channel connectors of three different widths, in which the effect of width on the load-slip characteristics is obvious and quite marked. The relations between the width of the connector and the load at slips of 0.0002 in. and 0.0025 in. and at the ultimate load are shown more clearly in Fig. 19a. All three curves are almost straight lines. The linear relationship between the load and the width is not unexpected, inasmuch as the resistance of the connector to slip should vary linearly with its width regardless of whether this resistance is controlled by the flexural stress in the connector or by the compressive stress in the slab.

Fig. 18b contains the load-slip curves for a group of connectors of the bent Z-plate type with widths varying from $\frac{1}{2}$ inch to $1\frac{1}{2}$ inch. The variation of the ultimate load with width is present although not as marked as for the channel connectors. This variation is brought out more clearly by the curves in Fig. 19b from which it can be seen that the widest connector, B3a, has a much lower load at slips of 0.0002 in. and 0.0025 in. than would be expected. An inspection of the load-slip curve for B3a shows, however,
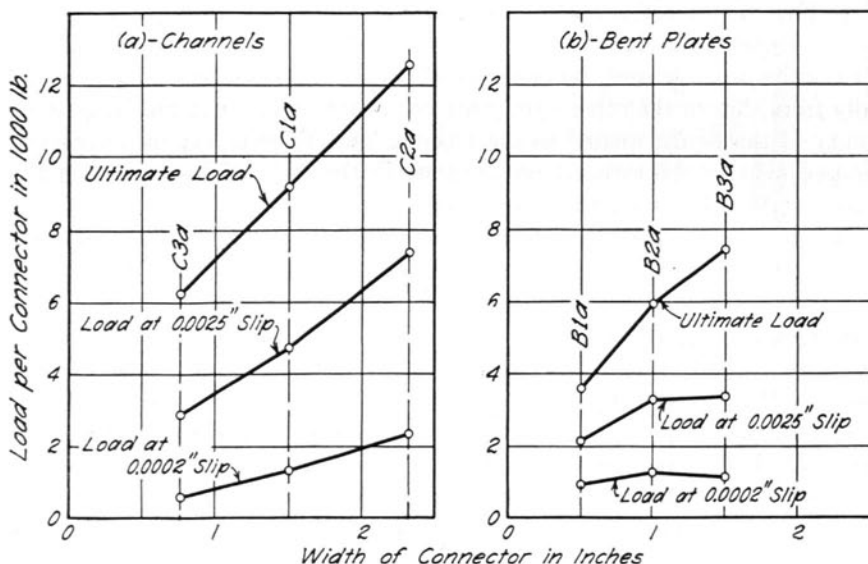
Fig. 19. Variations of Capacity of Connectors with Changes in Connector Width

that its shape is somewhat different from those of the other specimens. Whether the irregular shape of the curve for this specimen is accidental or whether it is a characteristic of the connector cannot be said on the basis of the data available.

Effect of Positive Anchorage. In order to prevent the mortar slab from pulling away from the steel I-beam, a positive anchorage is often required. Such an anchorage is provided by the upper flange of the channel—the outstanding flange. The effect of this flange can be studied by comparing the test results for specimens with the regular channel connectors and those with channel connectors having the upper flange cut off. The load-slip curves for specimens C1a and C5a, C4a and C6a, C1b and C5b, and C1c and C5c serve this purpose; they are shown in Figs. 13 and 20. The effect

of the outstanding flange, as brought out in Fig. 13, has been discussed in Section 16. It was found that the outstanding flange had little or no effect. As natural bond existed between the slab and the shear connectors in specimens C1a, C4a, C5a, C6a, it may be argued that the bond was at least partly responsible for these results. This hypothesis is to some extent confirmed by the curves in Fig. 20, from which a slight but definite advantage of the presence of the outstanding flange is obvious at higher loads. Bond
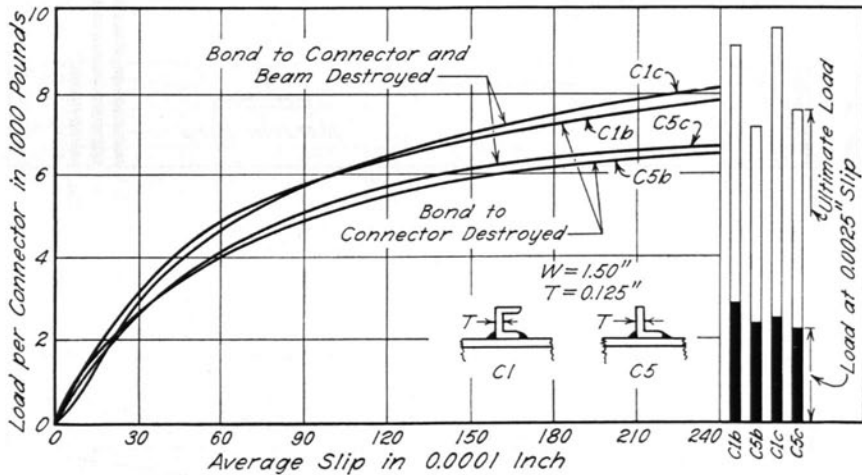
Fig. 20. Effect of Outstanding Flange

was prevented between the connector and the slab in all four specimens; in specimens C1c and C5c, also between the beam and the slab. It appears, however, that the bond conditions between the beam and the slab did not influence the effect of the outstanding flange.

Effect of Variations in Mortar Strength. The results of the tests to determine the effect of varying the strength of the mortar in the slab are shown in Figs. 21 and 22. The curves of Fig. 21 show in a general way the manner in which the load-slip characteristics are affected by the strength of the mortar. Figure 22, which furnishes data for a more quantitative study of these effects, shows that although there is a general decrease in the load at a given slip as the mortar strength is decreased, the relation is not quite linear. This suggests that the distribution of load on a connector might vary with variations in the strength of the mortar.

Effect of Width of Slab. The width of the slabs of the specimens used in these tests was rather arbitrarily made 6 in. It seemed desirable, therefore, that some study should be made of the effect of changing this width.

Fig. 21. Effect of Variations in Mortar Strength
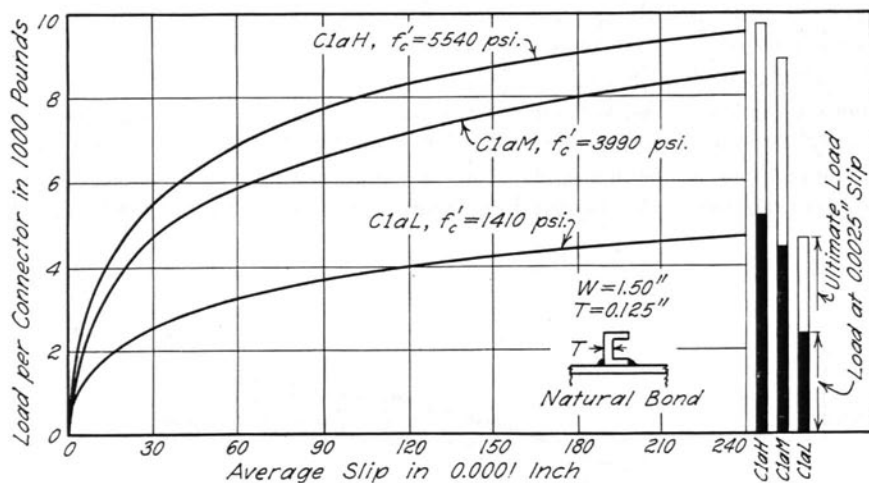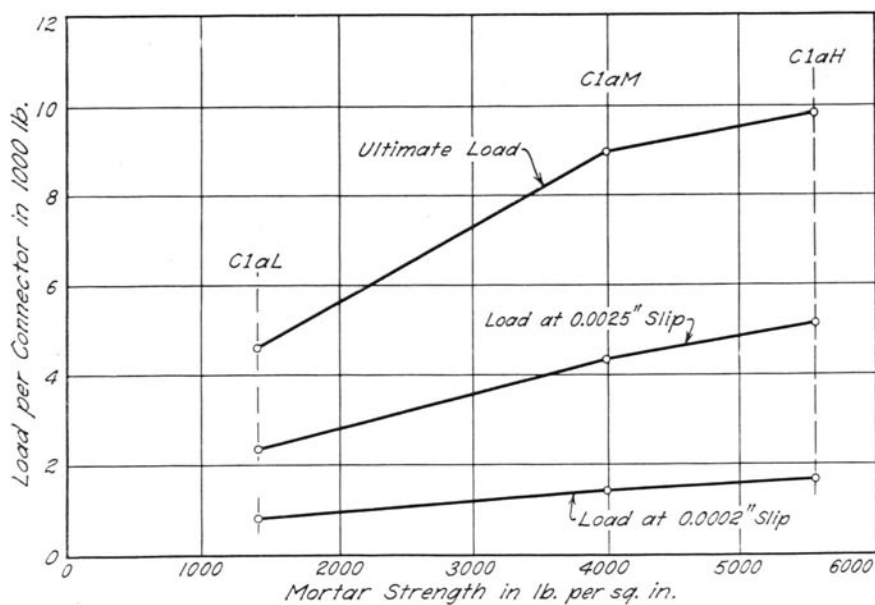
Fig. 22. Variations of Capacity of Connectors with Changes in Mortar Strength

Inasmuch as the width in an actual structure would be relatively greater than that chosen, one pair of specimens, C1d, was made with a slab width of 9 in. but similar in all other respects to specimens C1a. The average load-slip curve for these specimens is shown in Fig. 23 together with the corresponding curve for C1a. Specimen C1d (with a 9-in. slab) had slightly better load-slip characteristics than C1a, but the agreement between the two curves is quite good at low loads. Since it was not intended that the data obtained from these push-out tests should be applied directly to
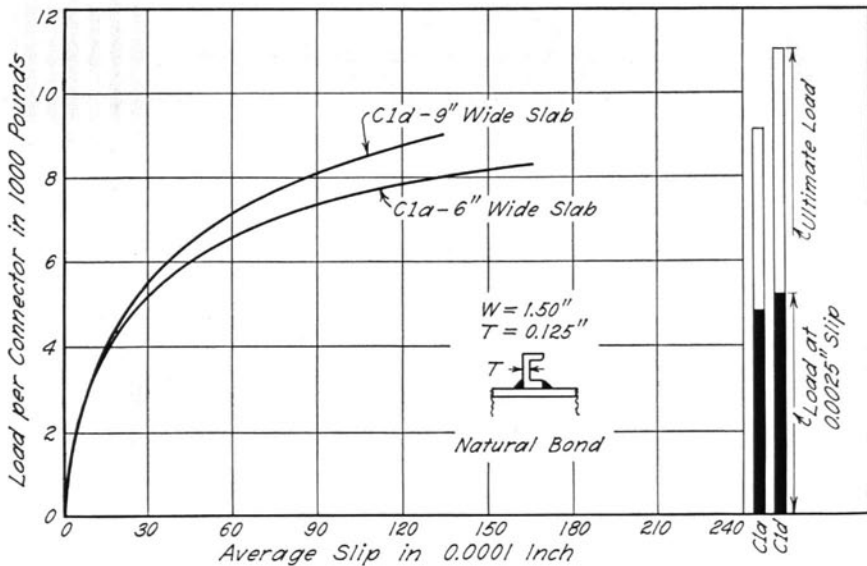
Fig. 23. Effect of Width of Mortar Slab

I-beam bridges, it is felt that the differences in load-slip characteristics caused by the 50-percent increase in the slab width are so small that the use of a 6-in. slab was justified and does not invalidate the conclusions drawn from these tests.

Effect of Method Used to Destroy Bond. Curves illustrating the effect of destroying the natural bond between the slab and the beam and connectors are shown in Figs. 24 and 25. Shear connectors of channels with and without outstanding flange, and bent Z-plates were tested. In the majority of the specimens bond was destroyed by a film of cup grease
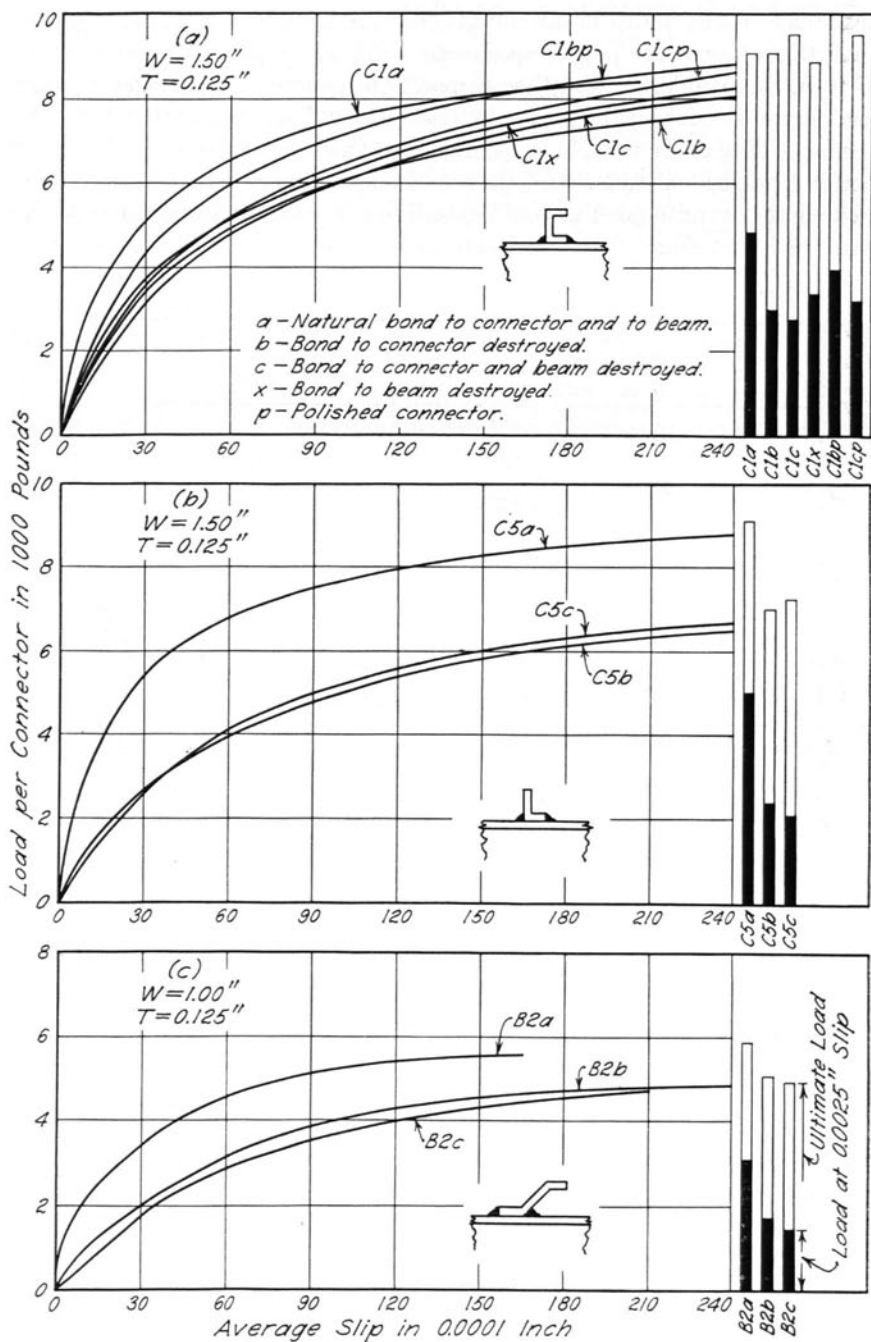
Fig. 24. Effect of Destroying Bond

applied to the surface of the steel. Although only a thin film was used, its thickness in terms of thousandths of an inch, which is the order of magnitude of the slip at small loads, was considerable. In two specimens an attempt was made to prevent bond between the slab and the connectors by polishing the surface of the latter.

In each of the three parts of Fig. 24, various specimens with bond destroyed are compared with specimens *a*, in which the natural bond existed at the beginning of the tests. An examination of the curves in Fig. 24a, b, and c shows that the slips at low loads increased considerably whenever the bond either to the connector or to the beam was destroyed. This initial slip was primarily responsible for the differences in the load-slip characteristics. It may also be observed from these curves and from the bar diagrams that the ultimate load was affected much less than the slip. Furthermore,
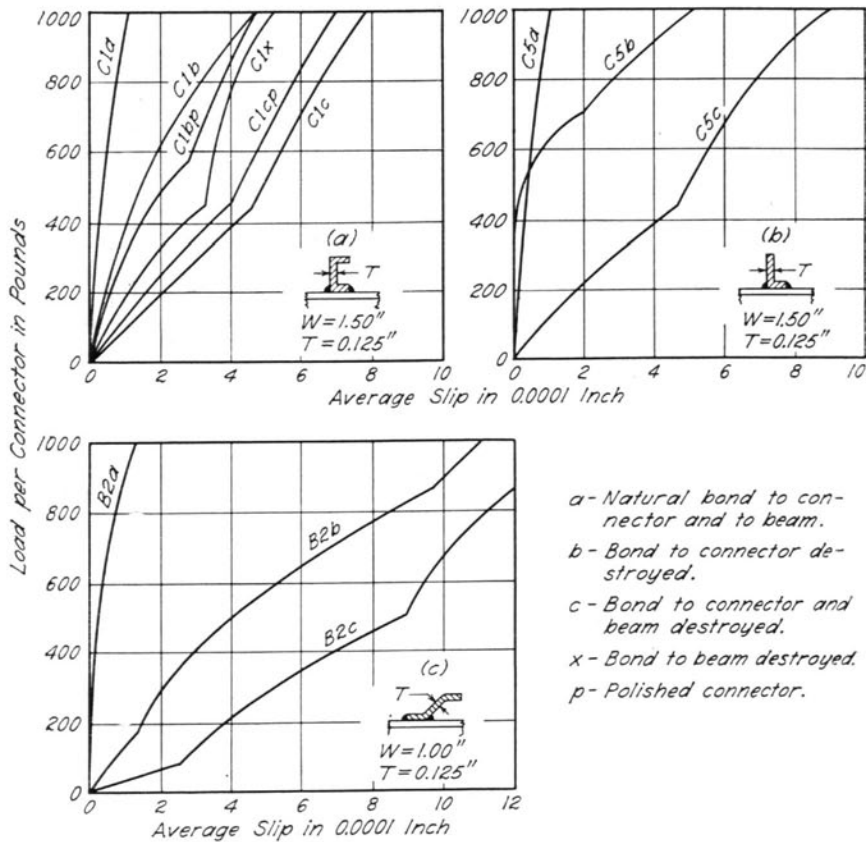
Fig. 25. *Effect of Destroying Bond; Slips at Low Loads*

by comparing specimens *b* (with bond only to connectors destroyed) and specimens *c* (with bond to both connectors and beam destroyed) it is found that larger slips were measured in the latter specimens. More data on the effects of destroying bond are given in Fig. 24a, where additional variations of bond conditions are represented by the curves for specimens C1x, C1bp, and C1cp, and in Fig. 25, where the lower parts of the load-slip curves are plotted on an enlarged scale.
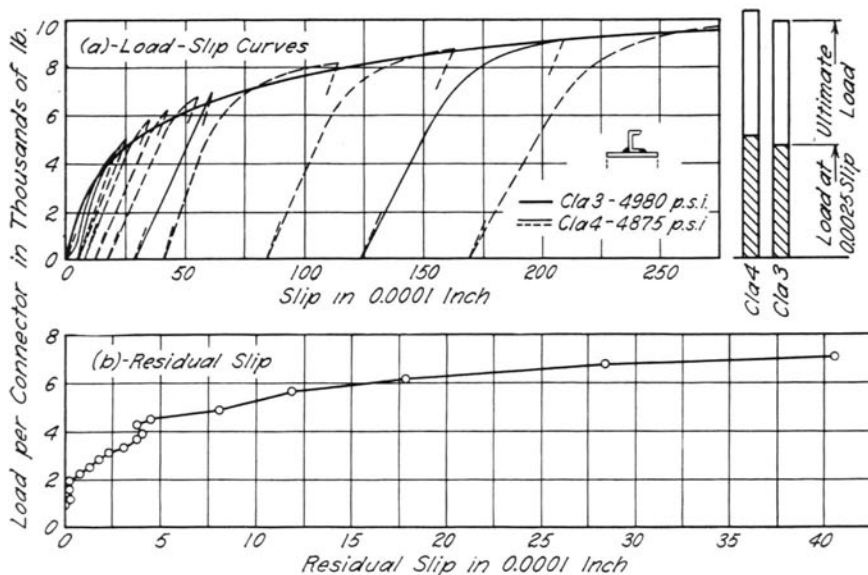
Fig. 26. *Effect of Releasing Load*

On the basis of Figs. 24 and 25 it is concluded that the most important factor is the bond between the beam and the slab. The bond to the shear connector is less important so long as no void exists between the connector and the slab. If, on the other hand, a continuous void exists under the connectors, large initial slips will occur.

18. Residual Slip After Release of Load

During the tests of two specimens, C1a4 and C1aH1, the testing procedure was changed; instead of increasing the load continuously from zero to the ultimate, the load was released several times during the test. The effect of releasing and reapplying the load on specimen C1a4 is shown in Fig. 26. The results for specimens C1aH1 were similar but are not presented in this bulletin.

In Fig. 26a, the load-slip curve for specimen C1a4 is compared with a similar curve for the companion specimen C1a3, which was tested with continuously increasing load. The curve for C1a4 consists of full and dashed lines: the full portions represent the behavior actually measured; the dashed lines show the estimated behavior for those cycles in which only slip at zero and maximum load was measured. It can be seen from the load-slip curves that the envelope curve for specimen C1a4 and the curve for C1a3 agree well. Thus the load-slip curves do not depend on whether the load is released and reapplied during the test or increased continuously from zero to the ultimate.

The residual slip is shown more clearly in Fig. 26b. It can be seen that practically all the slip was recoverable up to a load of about 2000 lb per connector. As the load was further increased the residual slip increased at an approximately constant rate. At a load of about 4000 lb per connector the residual slip was close to 0.0004 in. Beyond this load the slip increased at an increasing rate. The phenomenon may be explained by the following hypothesis regarding the behavior of the specimen: Up to about 2000 lb, both the steel of the connector and the mortar of the slab acted elastically. Beyond this load large permanent sets took place in the mortar, and the friction between the beam and the slab was responsible for the residual slip. At about a load of 4000 lb, first yielding in the shear connectors occurred. Above this load the residual slip was caused primarily by permanent deformations of the shear connectors.

19. Manner of Failure

In general, the failures of the push-out specimens can be divided into three groups: (1) As the maximum load was reached the mortar slab cracked suddenly in tension on the outside face; the crack was horizontal and occurred approximately at the level of the shear connectors. (2) After reaching the maximum load the slabs separated slowly from the beam and as a consequence the load dropped off; a separation as great as $\frac{1}{2}$ in. was observed in some specimens. (3) At the maximum load a break of one shear connector occurred at the bead of the weld or at the weld itself; this type of failure occurred with narrow and thin connectors.

The tensile failure of the slab was caused by the eccentricity of the compressive forces exerted by the shear connectors on the slab. The second type of failure was most probably caused by the lack of a positive anchorage against pulling the connectors out of the slab. The obvious reason for the third type of failure was overstressing of the weak shear connectors.

The first type of failure was a function of the type of specimen chosen and would not occur in a T-beam. The second and third types of failure are, however, primarily a function of the type of shear connector and thus

are likely to occur also in a T-beam. But even with this type of shear connector the failure in T-beams would occur at a slower rate than in push-out specimens, and the magnitude of the slip would be influenced by a redistribution of load from the overstressed connectors to the others. Thus the failures, and therefore also the ultimate loads and the corresponding slips indicated by the tests of the push-out specimens, have but little direct significance from the practical point of view. A comparison of the types of failure and an examination of the shapes of shear connectors after the failure are, however, of some value in illustrating the behavior of various types of shear connectors.

Views of six typical shear connectors after failure are shown in Fig. 27. All connectors were loaded from right to left. The shapes of the flexible connectors reveal that a large portion of the load must have been concentrated on a small length adjacent to the beam and that the free end was most probably subject to a load acting from left to right. This is best illustrated by the shape of the plate connector P2a where reverse curvature can be observed. The rigid connectors show only rotation in those tests in which the slab failed at relatively small slips; see the photograph of connector A1a, which is oriented in the same manner as connector A1 in Fig. 3. If, on the other hand, a slow failure by separation took place, the connectors were bent in a manner similar to that of T1a in Fig. 27. In addition, the wings of the angle of type A1 tended to spread, and the apex of the angle of type A2 caused vertical splitting of the slab.

For channel shear connectors the horizontal cracking of the slab occurred in all specimens, whereas for plate shear connectors this type of failure occurred only for the heaviest plates. With this type of failure, only slight separation of the slabs from the beam was observed, indicating that at loads close to the ultimate the outstanding flange functioned as an anchorage. In specimens with high strength mortar the tensile failures were rather abrupt; on the other hand, specimens C1aL with low-strength mortar failed slowly and noiselessly.

At the conclusion of all tests the mortar was found to be crushed in the area under the base of the connector. Whether this crushing occurred before, after, or simultaneously with the reaching of ultimate load is not known.

20. Dowel Analogy

When discussing the effect of web thickness on the load-slip characteristics of a plate connector, mention was made that the behavior of a channel may be similar to that of a dowel. Since several other test results also seemed to point in the same direction, the dowel analogy will be discussed briefly.

The action of a long elastic dowel embedded in an elastic medium is identical with the action of a semi-infinite beam on an elastic foundation.
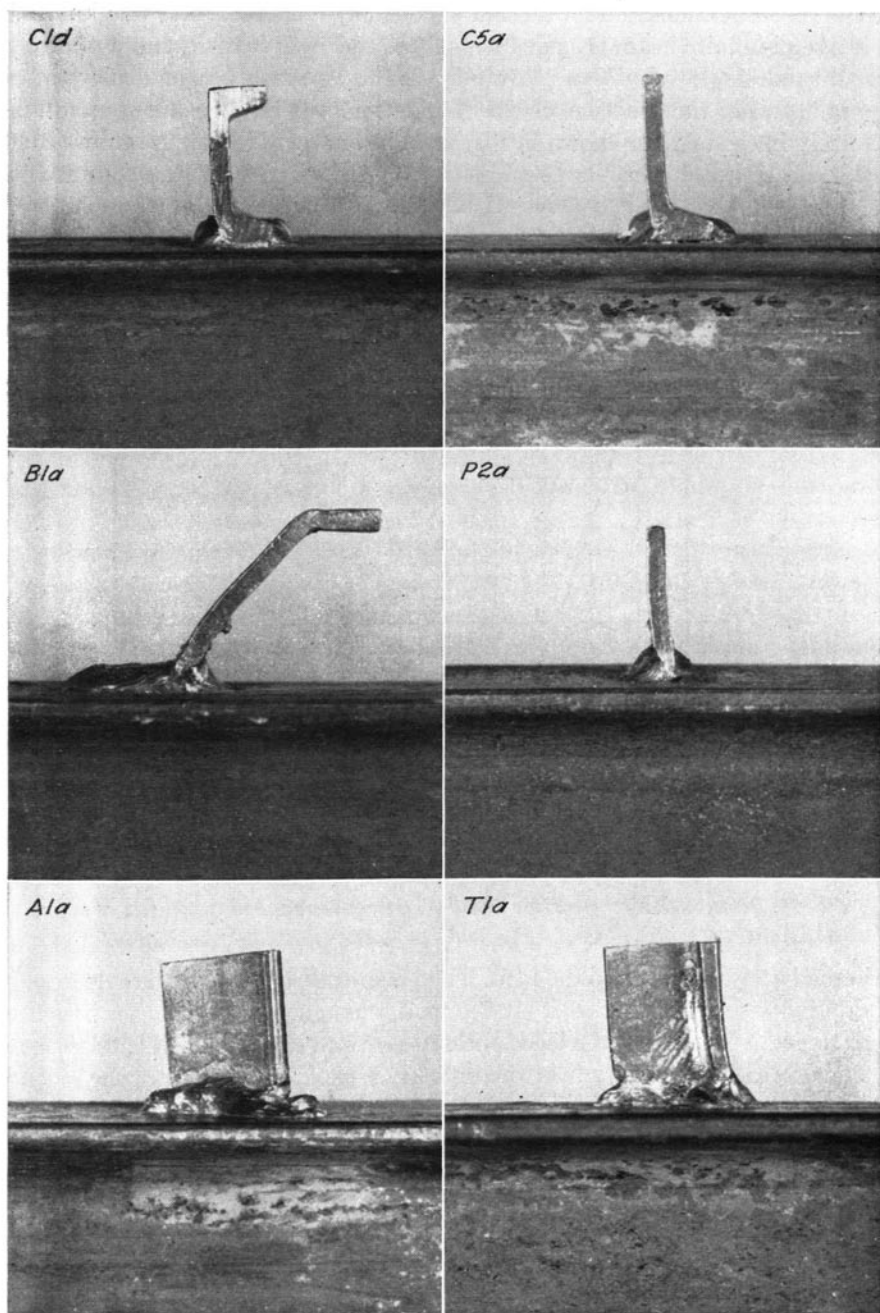
Fig. 27. Typical Shear Connectors After Testing

The theoretical solution for a beam of constant cross-section is well known.[2] If a semi-infinite beam is loaded at the free end by a load P, and if the free end cannot rotate but can move only in the direction perpendicular to its original axis, the reaction of the foundation will be distributed non-uniformly in the manner shown in Fig. 28. The curve on this figure shows that the dowel exerts very large pressures on the portion of the foundation
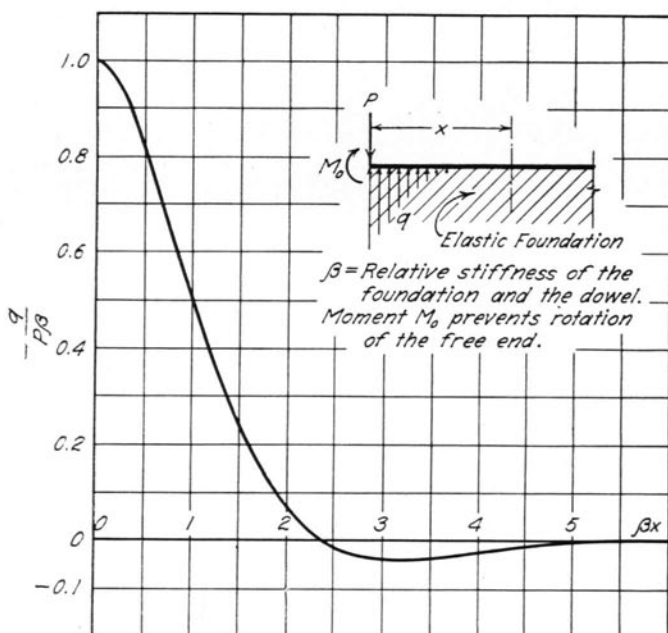
Fig. 28. Distribution of Reactive Load on Dowel Embedded in Elastic Medium

immediately adjacent to the load. The magnitude of this pressure decreases rapidly with the distance from the load, changing to a negative pressure at some distance from the load, and after several changes of sign, fades out. The decrease in magnitude of the pressure is rapid; at the end of the second wave it is virtually equal to zero.

Results of the tests of push-out specimens demonstrated clearly that the pressure exerted on the mortar by a shear connector is distributed non-uniformly along the height of the connector. It has been pointed out several times in the foregoing discussions that high pressures exist under the connector at locations adjacent to the beam. An examination of the deflected

[2] See, for example, Timoshenko: "Strength of Materials," Part II, D. Van Nostrand Co., New York, 1948, pp. 1-15.

shapes of the connectors indicated the presence of a reverse in direction of the pressure exerted on the mortar, and the study of the effect of the outstanding flange has shown that little or no rotation took place at the embedded end of the connector. Furthermore, the investigation of the effect of mortar strength on the load-slip curves indicated the possibility that changes in mortar strength affected the distribution of load; this suggests that the distribution of load might be dependent on the relative stiffness of the connector and the mortar. Although many of these indications were indefinite, and despite the fact that the non-uniformity of the shear connector cross-section and the elastic-plastic characteristics of concrete may have a profound influence on the distribution of the reaction, everything points toward a similarity in the behavior of a flexible shear connector and of a dowel.

21. Summary

Push-out tests were made on quarter-scale models of several different types of shear connectors for composite I-beam bridges. The object of these tests was to obtain information on the relative strengths and general behavior of various types of connectors, and to develop proper testing techniques in order that more extensive tests might be made on those types which appeared to be most effective. The variables studied include (1) type of connector, (2) width and thickness of connector, (3) mortar strength, and (4) condition of bond between the slab and the beam or connectors, and other miscellaneous variations. The method of testing was to load the specimen in such a manner as to produce a shearing force on the connector, and to measure the resultant slip between the slab and the beam. The results of these tests have been presented in the form of curves of load per connector versus average slip between the beam and the slab.

The most important results of the tests may be summarized as follows.

(1) The load-slip characteristics of the rigid type of connector are superior to those of the flexible type, but the differences were much less than would be expected from the very large differences in stiffness of the two types. Some indication was found that at a given slip the load carried by a stiff shear connector varied almost solely as a function of its bearing area.

(2) The flexible channel connector is superior to the straight plate and bent Z-plate types. Whether the outstanding flange of a channel has any beneficial effects in the prevention of uplift remains to be proved by other types of tests, since the push-out test is not suitable for this purpose.

(3) The load-slip characteristics are approximately linearly proportional to the width of the connector.

(4) Moderately large variations in the thickness of the web of a flexible connector have only a small effect on its load-slip characteristics.

(5) An increase in the compressive strength of mortar improves the load-slip characteristics of a flexible connector.

(6) The pressure exerted on the mortar by a flexible connector is distributed non-uniformly, with the highest values at locations close to the beam. It is believed that the action of a flexible connector is similar to the behavior of a dowel embedded in an elastic medium.

A considerable number of the push-out tests was devoted to the development of proper testing techniques. The results of this part of the tests are summarized briefly.

(a) Tests of push-out specimens represent a reliable method for comparative studies of various types of shear connectors.

(b) Ultimate loads obtained from the tests of push-out specimens have little if any practical significance.

(c) Destroying the bond between the steel beam and the mortar slab improves the uniformity of the test results.

(d) Destroying the bond between the shear connectors and the mortar slab introduces a new variable and is not recommended for future tests.

(e) Slab dimensions are apparently not critical as far as the width is concerned and so long as a sufficient cover is provided on each side of the shear connectors.

IV. STATIC TESTS OF T-BEAMS

22. Outline of Tests

The static tests of composite T-beams were designed primarily to permit study of the load-slip characteristics of this type of construction and of the effect of the load-slip characteristics of channel connectors on the degree of interaction obtained in a composite beam. Two beams of type A and one beam of type B, described in Section 9 and shown in Fig. 6, were tested during 1942–43.

Two principal variables were included in these tests: the mortar strength, and the stiffness of the shear connection. The first two beams, T1 and T2, were of the same type and differed only in the strength of the mortar. The

Table 6
Variations in T-Beams

| Beam Number | Beam Type* | Average Mortar Strength, psi† | Dimensions of Shear Connectors | | | | Spacing of Shear Connectors, in. |
			Height, in.	Flange Width, in.	Web Thickness, in.	Width, in.	
T1	A	4810	1.0	$\frac{3}{4}$	$\frac{1}{4}$	1.5	varying from
T2	A	1820	1.0	$\frac{3}{4}$	$\frac{1}{4}$	1.5	$3\frac{3}{4}$ to 2
T3	B	4420	1.0	$\frac{1}{2}$	$\frac{1}{16}$	1.0	4

* For types see Fig. 6.
† From Table 2.

mortar strength of beam T3 was similar to that of T1, but the shear connection on the beam was made considerably weaker. Table 6 gives the numerical values of the several variables. It is evident from this table that the weaker shear connection for beam T3 was accomplished both by use of weaker individual connectors and by almost doubling their spacing as compared with beams T1 and T2.

23. Description of Test Procedure

A detailed outline of the various static tests of the T-beams is given in Table 7. In most of the tests the beams were loaded only at midspan. However, one test on beam T3 was made with load at the quarter-point. In addition to the several static tests, one to three repeated-load tests were made on each beam. The number of repetitions varied from 50 to 100.

The arrangement of the testing and measuring apparatus has been described in Section 12. The usual procedure was to apply load through a

Table 7
Outline of Static Tests of T-Beams

Test No.	Age at Test, Days	Position of Load	Locations* of Measured			Load Increment, lb	Maximum Load, lb
			Strains	Slips	Deflection		
Beam T1							
1	56	Midspan	All	All	None	650	2600
2	56	Midspan	All	All	None	650	2600
3	56	Midspan	None	None	None	2600 repeated 100 times	
			All	All	None	2600	2600
4	65	Midspan	All	All	Midspan	650	6500
5	72	Midspan	All	All	Midspan	No Load	
			None	None	None	6500 repeated 50 times	
			All	All	Midspan	6500	6500
			None	None	None	6500 repeated 50 times	
			All	All	Midspan	1300–650	13000
Beam T2							
1	39	Midspan	All	All	Midspan	650	2470
2	60	Midspan	All	All	Midspan	1300	5200
			None	None	None	5200 repeated 100 times	
3	60	Midspan	All	All	Midspan	5200	5200
4	88	....	All	All	Midspan	No load-after crack found	
	98	Midspan	All	All	Midspan	2600	5200
5	110	Midspan	All	All	Midspan	1300	10200
Beam T3							
0	14	....	Top of Slab	None	None	Shrinkage Measurements	
	25	....	Top of Slab	None	None		
1	31	Midspan	All	All	Midspan	650	2600
2	35	East ¼-pt.	All	All	Midspan	650	2600
					¼-pt.	650	2600
3	40	Midspan	All	All	Midspan	650	2600
4	40	Midspan	None	None	None	1950 repeated 100 times	
		Midspan	All	All	Midspan	1300	8700

* See Fig. 10.

dynamometer in increments of 650 or 1300 lb and to measure strains, slips, and deflection for each increment of load. A complete set of readings at no load was taken before and after each test. The load increment of 1300 lb was chosen to correspond to a single H-20 rear wheel load plus 30 percent impact for a quarter-scale model.[1]

In the repeated-load tests, no measurements were made except at the beginning and end of the complete cycle of loading. The shrinkage measurements referred to for beam T3 are described in Section 28.

[1] Computed as $(1/4)^2 \times 16,000 \times 1.30 = 1300$ lb.

24. Manner of Presentation of Test Data

The test data on the general behavior of composite mortar and steel T-beams are presented in Figs. 29–35. Since the data obtained were extremely uniform for all the tests on each beam it has been considered sufficient to present the results for only one typical test. For beams T1 and T3 the final tests were chosen, while the data presented for beam T2 are those obtained in test No. 2. This early test was chosen because of a shrinkage crack which occurred after the test was made and which influenced the results of the later tests as discussed in Section 28.

Theoretical curves for strain, slip, and deflection are also given for purposes of comparison. These curves are of three types. Two are for the limiting cases of complete or no interaction between the slab and the beam. Their values were computed by the ordinary theory of flexure as applied to the particular case. The third curve gives the theoretical values for incomplete interaction between the beam and the slab. These were computed by the theory described in the Appendix. The degree of interaction between the beam and the slab was evaluated on the basis of slips measured on the same beam. Thus a comparison of the test data with the theoretical curves for incomplete interaction shows only whether the theory is consistent with the actual behavior of the structure.

The two elements of a composite steel and mortar T-beam are used most effectively if no slip can take place at the contact surfaces of the slab and the beam. Thus the values for complete interaction represent one limit for capacity and deformations of a composite beam. On the other hand, the structure is weakest if slip at the contact level can take place freely, that is, for no interaction. The corresponding deformations and capacity represent, therefore, another limit. The values of the deformations and capacity of an actual structure should lie between these two limits.

25. Effect of Slip on Composite Action

Slip. The effect of an imperfect shear connection is to permit slip and thus to decrease the degree of composite action between the beam and the slab. As the slip not only gives the best physical picture of the effect of imperfect shear connection but is also more sensitive than deflections and strains to changes in the degree of interaction, the results of slip measurements are presented first. The distribution of slip is shown in Fig. 29 and the load-slip curves for the end connectors are shown in Fig. 30. In these figures the test data are shown as circles; the theoretical values for incomplete interaction, as full lines.

Each of the three parts of Fig. 29 shows the distribution of slip on one half of one of the T-beams for various magnitudes of load applied at mid-
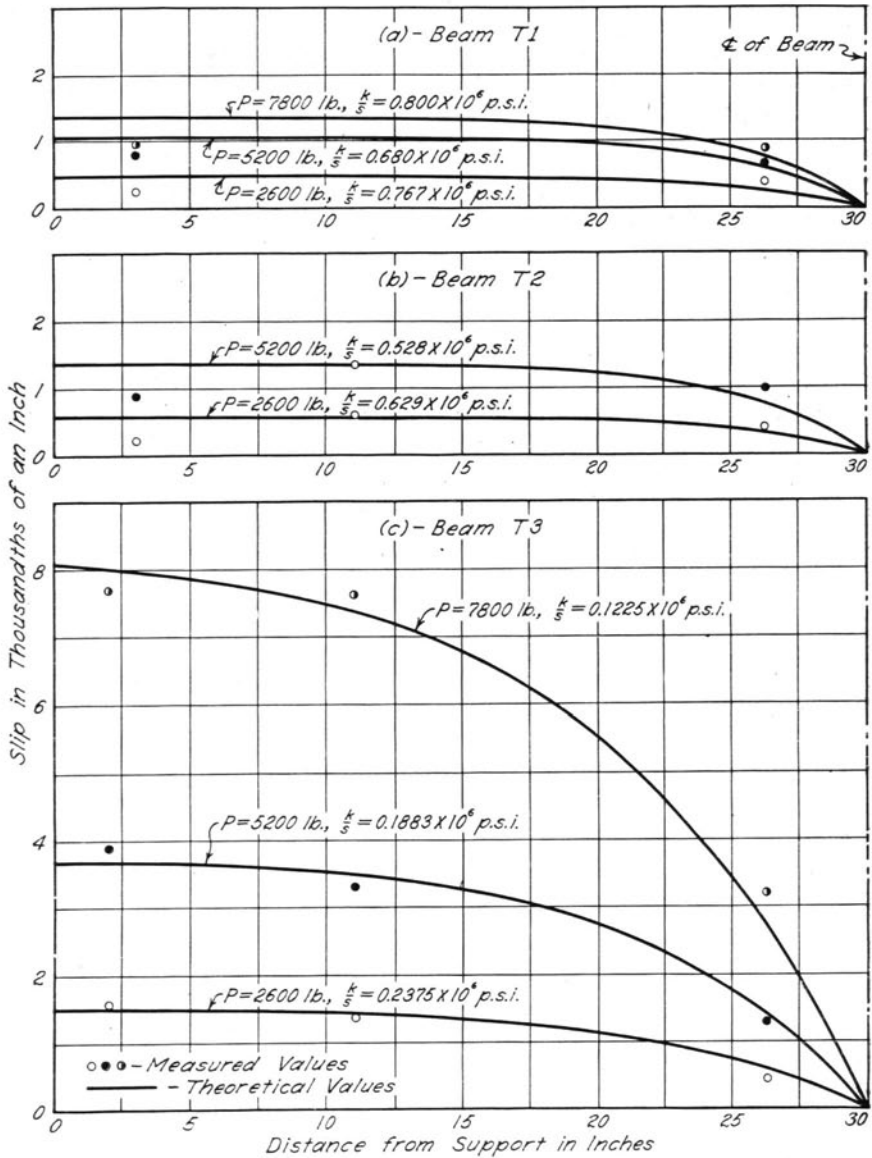
Fig. 29. Slip Distribution at Various Loads

span. The test data are supplemented by theoretical curves which were computed for the purpose of determining the modulus of the shear connectors; the method used is described in Section 54 of the Appendix. The theory on which these theoretical curves are based required that the spacing of the connectors be constant, provided that all connectors are equally strong. Actually, the spacing between the shear connectors was constant only for beam T3; in the computations for T1 and T2 an average spacing was used instead of the actual values. The introduction of this additional approximation may be responsible, at least in part, for the differences between the theoretical curves and the test data, since the theoretical curves could be fitted better to the data for beam T3 than to the data for beams T1 and T2. Inasmuch as each of the curves was fitted to the test data, the resulting modulus k of the shear connectors was different for each load. However, for loads below yielding of beams or shear connectors the differences were small and the average ratios of the modulus k to the connector spacing s were taken as the basis for all subsequent calculations. The average values of k/s for the three beams are as follows:

$$\text{Beam T1: } k/s = 0.762 \times 10^6 \text{ lb/in.}^2$$
$$\text{Beam T2: } k/s = 0.608 \times 10^6 \text{ lb/in.}^2$$
$$\text{Beam T3: } k/s = 0.241 \times 10^6 \text{ lb/in.}^2$$

The ratio k/s represents the stiffness of the shear connection. A comparison of the k/s values for beams T1, T2, and T3 shows how much the stiffness of the shear connection is influenced by changes in the mortar strength and by changes in the spacing and stiffness of individual shear connectors. The strength of the mortar in T1 was 2.4 times that of the mortar in T2. The corresponding ratio of the stiffnesses of the shear connections is 1.3. A strengthening of the shear connection by decreasing the spacing of the individual connectors from 4 in. to an average of 2.64 in. and by increasing the thickness of the channel web from $\frac{1}{16}$ to $\frac{1}{8}$ in. and the width from 1 to $1\frac{1}{2}$ in. resulted in a 316 percent increase in the ratio k/s, as indicated by comparing the results for beams T1 and T3.

In all comparisons of beams T1 and T3 the effects of the different spacings, web thicknesses, and widths of the shear connectors are all involved. Some data on how the stiffness of the connection is affected by the individual variables is given in Fig. 30, where the load-slip curves for the end connectors of beams T1, T2, and T3 are compared. At a load of about 1400 lb per connector the theoretical values of the end slip are 0.00106 in., 0.00135 in., and 0.00150 in. for the three beams respectively. As these values do not include the influence of the spacing of connectors, comparison of the slips for T1 and T3 shows the combined effect of the web thickness and connector width. The slip for T1 is somewhat less than 50 percent less
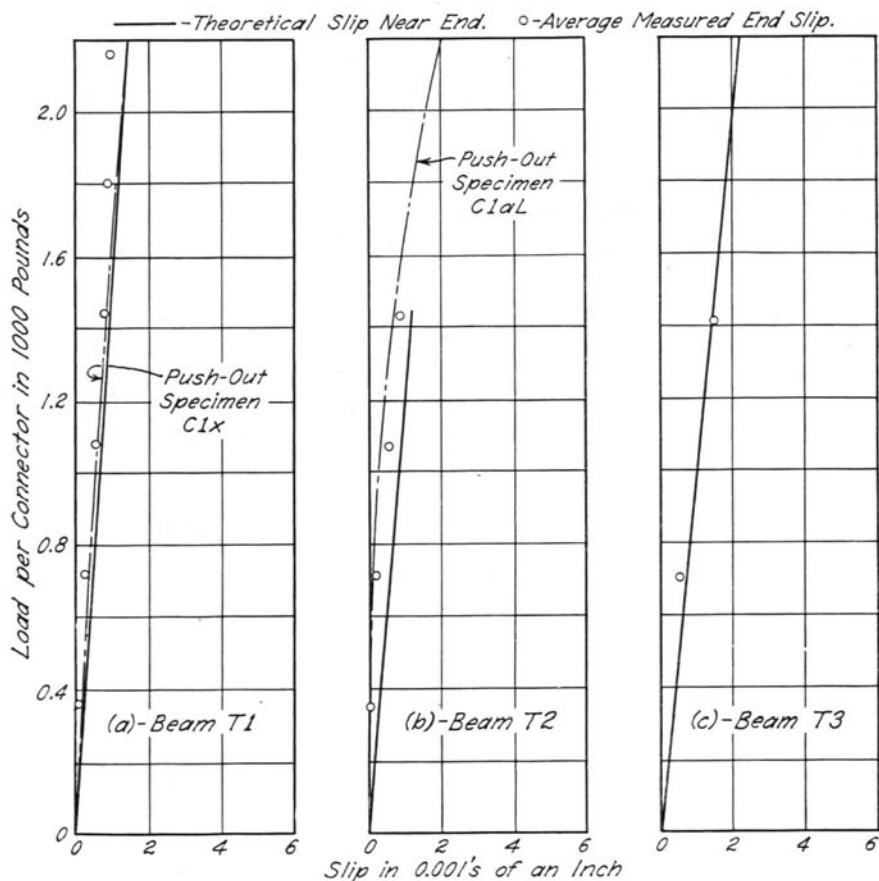
Fig. 30. Load-Slip Curves for End Connectors

than that for T3. If we accept from the push-out test data a proportionality between the load-carrying capacity of a connector and the width of the connector, the entire difference in slip can be accounted for by the difference in width of connector. Then, obviously, the effect of a change in the web thickness must be very small.

Load-slip curves obtained from the tests of push-out specimens C1x and C1aL are given in Figs. 30a and b. Specimen C1x and beam T1 had comparable connectors and mortar strengths, and specimen C1aL corresponded to beam T2. The load-slip curves for the push-out specimens are of the same order of magnitude as the test data for the T-beams, but the percentage differences are fairly large.

Strain and Deflection. As a result of slip between the beam and slab, the strains and deflections for a composite beam are generally greater than those computed on the basis of complete interaction, but are smaller than those for no interaction. This relation is illustrated in Figs. 31, 32, and 33.

The slab strains shown in Fig. 31a are not particularly significant, since they depend to a great extent on the modulus of elasticity of the mortar, which is only imperfectly determined from cylinder tests. Since the slab stresses commonly do not control the design, they are of little importance. In all the theoretical calculations the initial tangent modulus, determined from the stress-strain curves for the control cylinders, was used. For beam T2, having a low strength mortar, a changing secant modulus should have been used instead of the initial constant one. This discrepancy was responsible for a large part of the difference between the theoretical and measured values for that beam. For the other beams, the secant modulus was practically the same as the initial tangent modulus for the range of strains encountered in these tests.

The steel strains shown in Fig. 31b are for the bottom flange of the I-beam close to midspan and correspond to the stresses which would usually govern the design of this type of beam. At the higher loads the measured strains are slightly greater than those computed for complete interaction, and in general are in fairly good agreement with the theory for incomplete interaction. The effect of the decrease of interaction on strains may best be evaluated on the basis of theoretical computations. This is done in Table 8a, which shows that even for the weakest beam, T3, the increase in steel strain due to incomplete interaction is only 7 percent—only about one-sixth the increase for no interaction. For the other beams the increase in strains is only about one-fourteenth that for no interaction.

In Fig. 32 the measured deflections at midspan are compared with the computed ones. All computed deflections include deflection due to shear which was usually about 7 percent of the total. Since the theory for incomplete interaction and the test data are in very good agreement, the numerical evaluations of the effects of incomplete interaction were made on the basis of theoretical computations. They are presented in Table 8b, in which the theoretical differences between deflections at midspan computed from the theories for complete, incomplete, and no interaction are given. Although the increases in deflection due to incomplete interaction are greater than the corresponding increases in strain, the ratios of these increases to those for no interaction are about the same for both deflection and strain. For example, the increase in deflection of beam T3 for the case of incomplete interaction was about one-eighth as much as the increase for no interaction. This ratio of one-eighth is comparable to the value of one-sixth for strain.

——— -Theoretical Values.   o-Measured Values.

(a)-Load-Strain Curves for Top of Slab $3\frac{3}{4}''$ from Midspan

(b)-Load-Strain Curves for Bottom of I-Beam $3\frac{3}{4}''$ from Midspan
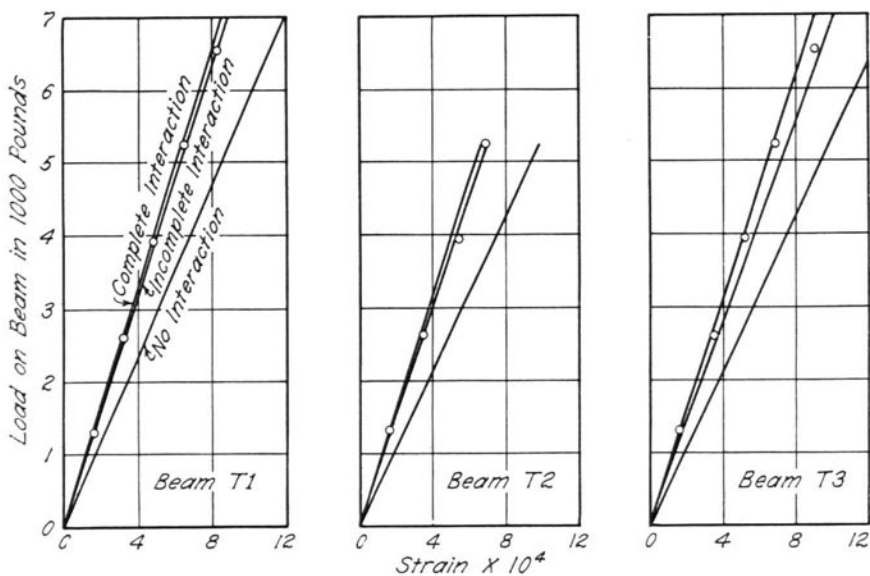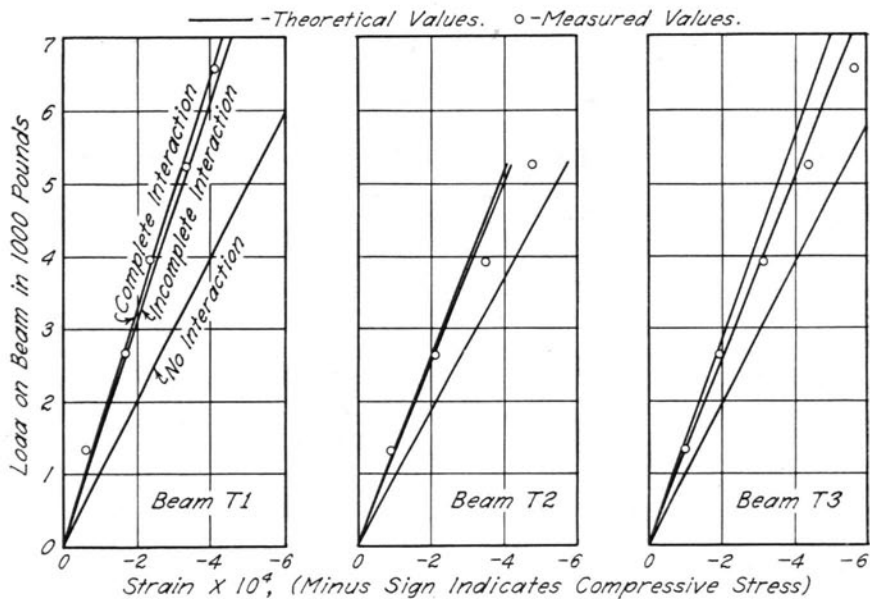
Fig. 31. Load-Strain Curves for T-beams

Table 8

Theoretical Differences in Strains and Deflections for Complete, Incomplete, and No Interaction

Concentrated load at midspan. Strains 3¾ in. from midspan. Deflections at midspan.

Beam Number	Relative Values in Percent Based on Values for Case of Complete Interaction					
	(a) Bottom Flange Strains			(b) Deflections at Midspan		
	Complete Interaction	Incomplete Interaction	No Interaction	Complete Interaction	Incomplete Interation	No Interaction
T1	100	103	140	100	109	272
T2	100	103	146	100	109	268
T3	100	107	144	100	122	268

Perhaps the clearest picture of the effect of lack of interaction is obtained by studying the distribution of strains throughout the depth of the composite section. In Fig. 33 the measured strains on the top and bottom of the slab and on the upper and lower flanges of the I-beam are compared with the strains at those points computed for complete, incomplete, and no composite action. The effect of slip in producing a difference in strain at
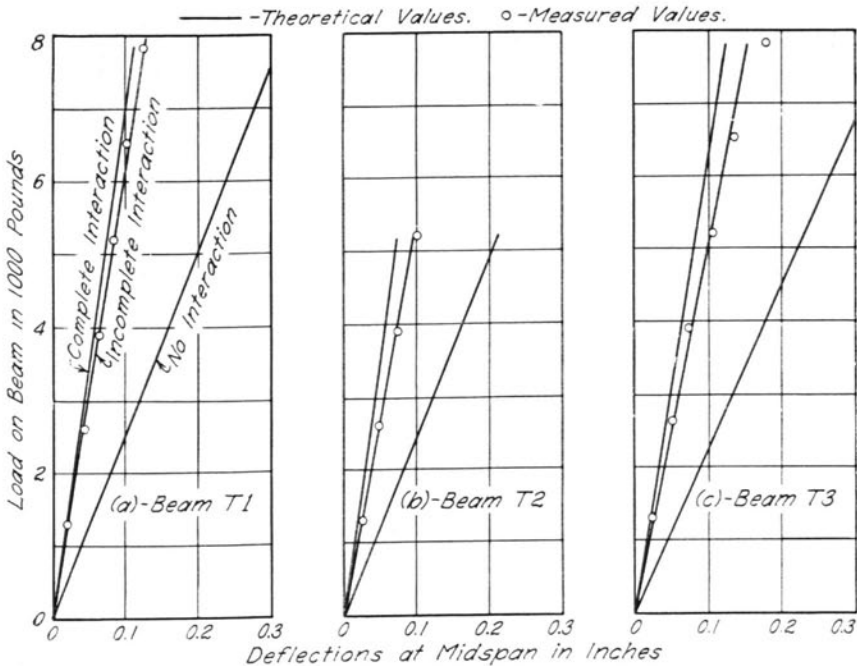
Fig. 32. Load-Deflection Curves for T-beams
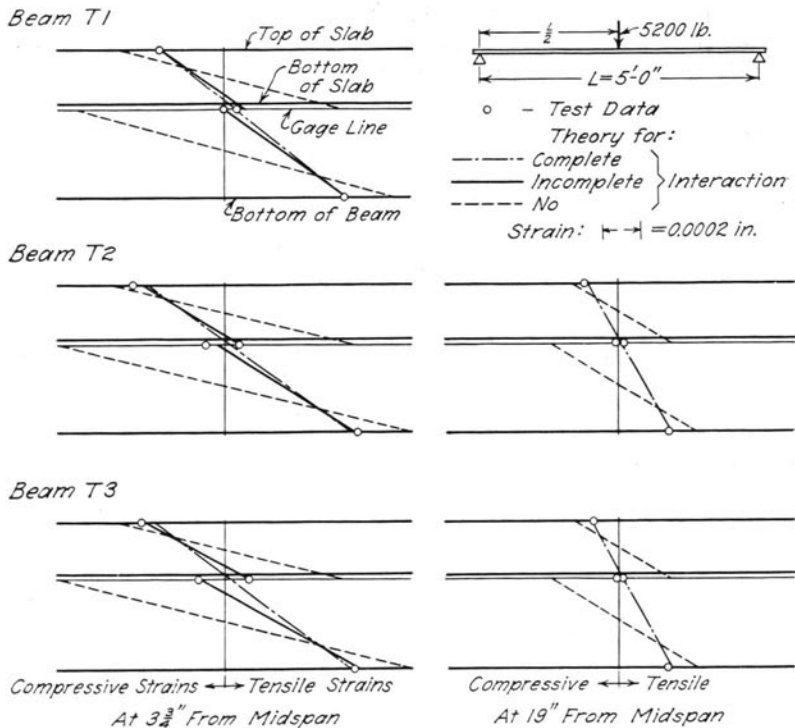
Fig. 33. Strain Distribution

the junction of the two elements is clearly shown in this figure. Theoretically, the slopes of the lines connecting the points representing the measured strains should be equal in the slab and in the I-beam, but different from the slope of the line for complete interaction. For the test data these slopes are not always equal, but the inequalities can generally be explained on the basis of the probable errors in the measured strains; the strains on the bottom of the slab and on the upper flange of the I-beam are quite small and are usually only two or three times as large as the probable error of measurement. The distribution of measured strain at a point 19 in. from midspan, also shown in Fig. 33, is not significantly different from the distribution computed for complete interaction. In other words, complete composite action apparently existed at this location, whereas it did not exist at the location only $3\frac{3}{4}$ in. from the load.

Summary. The data in Figures 29–33 show conclusively that the shear connection was not perfect in any of the beams tested, that slip occurred, and that strains and deflections were increased over the values which would

exist for complete composite action. The fact is also brought out that although slip occurred at all points along the length of the beam, the effect of such slip on the strains was confined to a short length of the beam on either side of the load. The amount of slip which occurred and the decrease in interaction which accompanied it were appreciably greater for beam T3 than for the other two beams. This increase was attributed to the greatly decreased stiffness of the shear connection used in that beam. A comparison of the data for beams T1 and T2 indicates that the degree of interaction obtained in beam T2 was slightly less than for T1, due to the lower strength mortar used in beam T2. However, the effect was quite small as compared to the large variation in mortar strength between the two beams.

The theory for composite beams with incomplete interaction is consistent with the test data for all three beams. Therefore the theory gives a satisfactory representation of the behavior of composite beams with incomplete interaction and may be used for theoretical studies of the effects of an imperfect connection.

26. Distribution of Strain Across the Slab

It was assumed in all calculations for strain and deflection that the full width of the slab was effective in resisting moment. In the tests of beam T3 the validity of this assumption was checked by measuring the distribution of strain across the width of the slab. This distribution was determined at points $3\frac{3}{4}$ in. and 19 in. from midspan of the beam on gage lines spaced transversely at a distance of 4 in. The results of a typical test are shown in Fig. 34, in which it is seen that the distribution of strain was substantially uniform across the width of the slab.
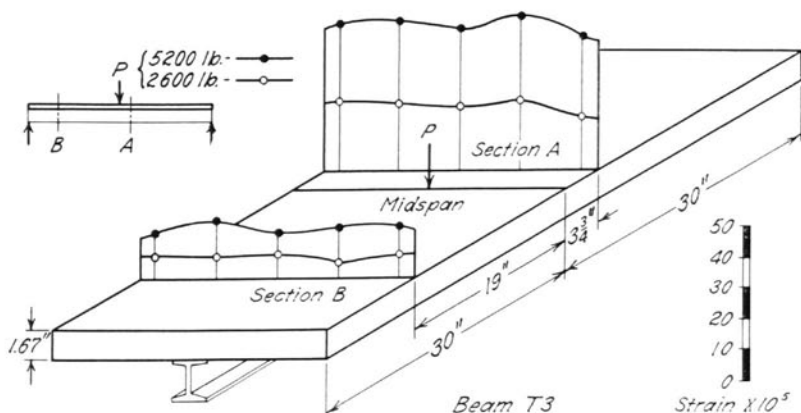

Fig. 34. Distribution of Strain Across Top of Slab

It is believed that the results of these measurements, which indicate full participation of the slab, justify the assumption that in an ordinary I-beam bridge as well as in a T-beam of the type tested, a full panel of the slab may be considered to act with the I-beam in resisting bending.

27. Effect of Repeated Loading

In order to determine whether the load-slip characteristics of the connectors and the composite beam were entirely elastic, at least one repeated-load test was made on each T-beam. The procedure in each of these tests was as follows. First a load test was made in which the load to be repeated was applied in increments. This load was then released and a set of slip and strain readings were made. The desired load was then applied and released 100 times without any reading being made. After this was done, another set of readings at zero load was taken, followed by a second load test in which strain, slip, and deflection were measured for each increment of load. The actual loads used in these tests are given with other pertinent data in Table 7.

It was possible to determine two things from the repeated-load tests. First, the amount of residual strain or slip present after 100 applications of the load could be ascertained from the readings made at zero load before and after the repeated loading. Second, the effect of repeated loads on the load-strain and load-slip characteristics could be obtained from a study of the load tests which preceded and followed the repeated-load test.

The following statements can be made with regard to the results of these tests.

(1) For the tests with loads of 2600 lb on T1, 5200 lb on T2, and 1950 lb on T3, there was no significant residual slip or strain, and neither the load-slip nor the load-strain characteristics of the beam were noticeably affected by the repeated loading.

(2) For the test with a load of 6500 lb on T1 there was no residual slip at any point, and there was a noticeable residual strain only at the gage lines at midspan. The repeated loading had no effect on either the load-slip or the load-strain characteristics.

(3) Since, for the tests mentioned in (1) above, the loads per end connector were approximately 720 lb and 1430 lb for beams T1 and T2 respectively, the fact that there was no effect of repeated loading is in agreement with the results of the push-out tests in which there was found to be no residual slip for loads per connnector of less than about 2000 lb (see Fig. 26b). The load per connector for the load of 6500 lb on beam T1 is about 1810 lb. The results mentioned in (2) above are also seen to be consistent with the results of the push-out tests.

28. Effect of Shrinkage Crack

When beam T2 was 88 days old a transverse crack occurred in the slab at a point about 2 in. west of midspan. It extended across the entire width of the slab and through the entire thickness, and was obviously the result of shrinkage. The width of the crack was about 0.003 in. on the south half of the slab and about one-half to two-thirds as much on the north half. As soon as the crack was noted, a complete set of strain and slip readings was made with no load on the beam, and was compared with the last set of readings which had been made with no load on the uncracked beam. This comparison indicated that the cracking of the slab had released tensile stresses in the slab and compressive stresses in the beam, and that slip of a magnitude commensurate with the width of the crack had occurred in the neighborhood of midspan. In general, the effects noted agreed completely with the assumption that the crack was due to shrinkage. It will be recalled that the slabs of all the T-beams had been given two coats of paint in order to prevent their drying out. However, the strength of the mortar in this beam was evidently so low that this precaution was not sufficient to prevent cracking.

The effect of the crack on the behavior of the T-beam is shown by the curves in Fig. 35. In this figure the results of test 5, made after the crack occurred, are compared with the results of test 2, made before the crack occurred. In test 5 it was noted that the crack was completely closed at the top of the slab at a load of 2600 lb. The strains in the bottom flange of the I-beam near midspan are compared in Fig. 35a. It can be seen in this figure that until the crack closed at 2600 lb the strain at a given load was about 23 percent greater after cracking than before. For loads greater than 2600 lb the two load-strain curves are parallel. The reason for the increased strain is that the section of the composite beam was considerably reduced by the presence of the crack. The beam strains at a distance of 19 in. from midspan are not compared in this figure, but they were not affected by the crack. This behavior would be expected, since the presence of a number of shear connectors between this location and midspan would tend to restore the slab to full effectiveness.

The load-deflection curves before and after cracking are shown in Fig. 35b. The effect here is similar to that for beam strains except that the increase in deflection for loads less than 2600 lb is about 53 percent as compared to about 23 percent increase for strain.

The presence of the crack had a very marked effect on the slip between the slab and the beam. At some distance from midspan, the amount of slip at a given load was greater after cracking than before (Fig. 35c). On

the other hand, the slip near the crack (Fig. 35d) was greatly reduced and
was reversed in direction until a load sufficient to close the crack was
reached.

Figure 35a and Fig. 35b show also theoretical values for full and no inter-
action. In both test 2 and test 5 there was less than perfect composite
action. In test 2 this was due chiefly to slip permitted by an imperfect shear
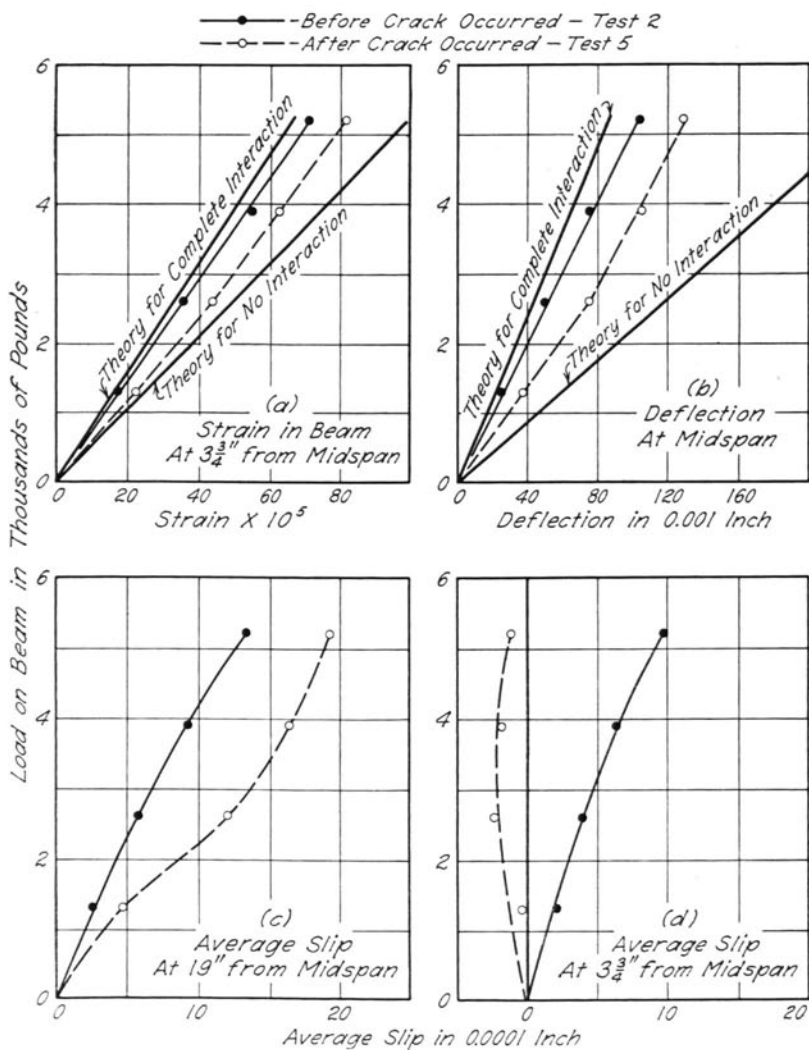connection. In test 5 it was due to a combination of this cause and the

Fig. 35. *Effect of Shrinkage Crack, Beam T2*

presence of the shrinkage crack. Comparison of the data for the two tests shows that the effect of a shrinkage crack was far greater than the effect of imperfect shear connection. However, the effect of the crack in these tests was not sufficient to produce strains or deflections greater than those for the limiting case of no interaction.

The formation of the shrinkage crack in beam T2 raised the question of the presence of shrinkage strains in the other beams and the possible effects of their presence on the interpretation of the results. With this in mind a careful study of the strain readings at zero load for beam T1 was made, but no evidence was found of the presence of any shrinkage strains in the slab. A similar study for beam T2 indicated the presence of large shrinkage strains. These strains were apparently uniform along the length of the beam and were somewhat smaller on the bottom of the slab than on top. Between the ages of the beam of 39 and 60 days the strain readings at zero load changed by an amount equal to a compressive strain of 0.00014 on the bottom of the slab and 0.00024 on the top of the slab. The total shrinkage strains at the age of 88 days were probably considerably more than these values.

In the tests on beam T3 a number of measurements of strain in the slab were made to determine the magnitude of the shrinkage strains. These measurements were first made when the slab was 14 days old and were continued until the beam was tested to failure at an age of 40 days. The measured strains were uniform across the width of the slab and along the length of the beam, and were reasonably uniform throughout the depth of the slab. The strains continued to increase, although at a slightly decreasing rate with time, until the beam was broken; the average total strain for the 26-day period was 0.00035 in. The initial tangent modulus of elasticity for the mortar in this beam was 3,440,000 psi, and the stress corresponding to a strain of 0.00035 is about 1200 psi. The total shrinkage strain, including the first 14-day period, was probably larger than that measured in these tests. However, 7 of these 14 days constituted the period of moist curing; in addition, the effect of creep has not been considered.

The presence of shrinkage strains in beams T2 and T3 has been proved, and the effect of the resulting crack in beam T2 has been discussed. The effect of shrinkage strains on the results obtained in the tests of beam T3 cannot be evaluated, but it is believed that comparisons based on load-strain, load-slip, and load-deflection curves from short time tests will not be affected appreciably by their presence.

29. Tests to Failure

The final test on each beam consisted of a test to failure in which load was applied in increments until the ultimate capacity of the beam was reached. The initial failure of all beams was by yielding of the steel in the

bottom flange of the I-beam. As load greater than that which caused yielding was applied, and as additional deflection was produced by continued jacking at the ultimate load, the actions of the various beams were quite different. A brief description of the test to failure for each beam follows.

Beam T1. First yielding of the I-beam occurred in the lower flange at midspan at a load of 8450 lb. This was followed by yielding at the gage lines $3\frac{3}{4}$ in. from midspan at a load of 9100 lb and by the formation of visible strain lines on the lower flange at a load of 9750 lb. At a load of 10,400 lb a crack in the paint at the junction of the slab and the I-beam indicated the presence of a large amount of slip as well as a tendency for the slab to pull vertically away from the beam. The first tension cracks in the bottom of the slab appeared at a load of 11,700 lb. As the loading continued the tension cracks on both sides penetrated beyond mid-depth of the slab. At 13,000 lb the separation crack indicated a definite vertical separation of the slab from the beam. The load of 13,000 lb was never exceeded, but jacking was continued and additional deflection was produced until a total deflection of 0.75 in. was obtained. In the process of obtaining this much deflection a compression failure occurred on top of the slab at midspan. Although the strains and deflections were undoubtedly increased by the lack of complete interaction, the performance of this beam indicated that interaction was present to a considerable extent at all loads including the maximum attained. This is best illustrated by comparing the maximum load of 13,000 lb with the theoretical ultimate load of 13,400 lb for complete interaction.

Beam T2. The test to failure on this beam was performed after the slab had cracked, and certain quantitative results are affected by the presence of this crack. The first yielding of the I-beam at the gage lines $3\frac{3}{4}$ in. from midspan occurred at a load of slightly less than 9000 lb. The first additional crack in the slab was visible at about this same load, and a crack at the junction of the slab and the I-beam was visible on both sides of the beam over its full length. The maximum load carried by the beam was 10,200 lb. However, additional deflection to a maximum of 1.5 in. was produced by continuing to jack at the maximum load. While this was being done, the following events occurred. Additional transverse cracks formed in the bottom of the slab. The separation crack between the slab and the I-beam opened wider. Cracks in the top of the slab, parallel to and over the I-beam, began to form, probably caused by a splitting or shearing effect of the connectors. A compression failure on top of the slab at midspan occurred. The lower maximum load for this beam was primarily due to the lower strength of the slab. The increase in slip was also due to the lower strength of the mortar in the slab, since the load-slip characteristics of the connector are affected by that variable. The theoretical ultimate load for complete interaction was computed as 10,800 lb.

Beam T3. At a load of 5200 lb a crack in the paint at the junction of the slab and the I-beam was visible for the full length of the beam on both sides. The presence of such a crack, which had first begun to form at an even lower load, indicated a large amount of slip and a corresponding decrease in the degree of composite action. The shape of the load-slip curve indicates that yielding might have been present in several or even in all shear connectors. First at a load of 6500 lb and then at a load of 7800 lb the deflection of the slab began to increase at such a rate that it was difficult to maintain the load at a constant value while readings were being made. At 7800 lb the first crack in the bottom of the slab was observed. The steel in the I-beam began to yield at the gage lines $3\frac{3}{4}$ in. from midspan at a load slightly greater than 7800 lb, and the maximum load of 8700 lb was reached shortly thereafter. Jacking was continued at the maximum load until a deflection of 1.06 in. was obtained at midspan. While this was being done, the separation and slip between the slab and the I-beam continued to increase, additional cracks formed on the bottom of the slab, and cracks formed on top of the slab parallel to the beam and at an angle to the beam, forming a "V" pointed toward the end. As a result of the excessive deflection produced after the maximum load was reached, a secondary failure of the shear connection on the east half of the span was produced. As nearly as could be determined from the observations made during testing, the failure consisted of excessive deflection of the connectors, followed or preceded by a compression failure of the slab in front of the connectors and by shear failure of the slab along lines parallel to the beam. This latter type of failure was indicated by the formation of longitudinal cracks on top of the slab. It should be emphasized, however, that this failure was the result of excessive deflection after the maximum load was reached, and that it occurred only on one-half of the beam; there was little slip or separation noted for the other half at any time. At the maximum load the maximum slip noted at any point of the beam was less than 0.03 in. This slip, however, was sufficient to cause a pronounced decrease in the amount of interaction, and thus to reduce the maximum load considerably below that which was carried by beam T1 and below the theoretical ultimate of 12,700 lb for complete interaction. The difference in maximum load for these two beams must be attributed to the difference in the shear connections. In this respect it should be remembered that the connectors for T3 were not only one-half as thick as those for T1, but were also only $\frac{2}{3}$ as wide and were spaced at an average spacing 1.5 times as great. Because of these changes it is somewhat difficult to evaluate the effect of the decreased thickness, but it is believed that its effect on the ultimate strength of the beams was not as important as that of the width and spacing.

30. Action of Shear Connectors

One of the objectives of the static tests of T-beams was to study the action of the channel connectors and to determine their suitability for the type of structure considered. It has been shown very clearly in the previous sections that in all beams tested the channel shear connectors provided almost complete interaction up to first yielding in the I-beams. After first yielding had occurred, the slips began to increase rapidly, and pronounced differences were observed in the behavior of the three beams.

The shear connection of beam T1 proved to be very efficient for the entire range of loading up to the maximum load. It is probable that the end connectors of this beam did not start to yield until the last increment of load was applied, and it is believed that the ultimate capacity of this beam was not affected by the small decrease of interaction. Beam T2 failed first by cracking of the slab, possibly as the result of the splitting or shearing effect of the connectors. The size and spacing of the shear connectors used in beams T1 and T2 were evidently adequate to provide full composite action up to failure as demonstrated by the behavior of these connectors in beam T1. However, the splitting and shearing observed in beam T2 emphasize that a sufficiently strong mortar slab must be used if the shear connectors are to develop their full strength.

In beam T3, the shear connectors began to yield before the beam yielded or at approximately the same time. Relatively large slips took place at all points along the beam, indicating that failure was most probably brought about by excessive deflection of the shear connectors. The ultimate capacity of this beam was affected considerably by the decrease in interaction.

Any specific information obtained from small-size T-beam tests concerning the shear connectors is valid only for the particular structures tested unless it can be expressed in terms of some factors independent of the physical properties of the beam. Slip, which was discussed at length in previous sections, is not suitable for this purpose because its magnitude depends not only on the stiffness of the connector but also on the ratio of horizontal to vertical shear at the junction of the slab and the beam. A slip acceptable in one structure may be prohibitively large for another. Neither can any of the other measured quantities be used for this purpose.

The theory for imperfect interaction, however, gives a quantity which offers a fairly good basis for the comparison of various beams. The quantity C, given by Eq. 13 of the Appendix, is a dimensionless quantity which involves the properties of the slab, the beam, and the shear connectors, the spacing of the shear connectors, and the span length of the beam. As the coefficient C appears in all theoretical expressions for composite beams with incomplete interaction it can be used for the desired purpose. C is inversely proportional to the modulus k of the shear connector; hence it is more convenient to use the value $1/C$.

The $1/C$-values for the three beams tested were as follows: 20.8 for T1, 18.4 for T2, and 6.97 for T3. Thus the limit between a good and poor connection lies somewhere between $1/C = 6.97$ and $1/C = 18.4$; beams with a $1/C$-value greater than this limit may be considered as composite beams with complete interaction.

The question whether the push-out tests furnish an acceptable procedure for determining the load-slip characteristics and thus also the modulus k of a shear connector may be answered tentatively by the curves in Fig. 30, supplemented by the results of the theory. It can easily be shown theoretically that for beams with $1/C$-values larger than about 10 the bottom flange strains and deflections change only slightly even if the modulus k is doubled. Thus the modulus k obtained from push-out tests need not be determined with great accuracy in order that the theory for incomplete interaction yield a satisfactory prediction of the behavior of most practical structures. The slopes of the curves in Fig. 30 obtained from the push-out tests and T-beam tests are in good agreement, and it may therefore be concluded that the values from the push-out tests would be sufficiently accurate for use with the theory.

The question whether a positive vertical anchorage between the slab and the I-beam is needed was answered in part by the tests to failure. In each beam a definite tendency for vertical separation of the slab from the beam was observed at high loads. It seems reasonable to expect that this separation would have been more serious and would have occurred at lower loads if the upper flange of the channel shear connectors had not tied together the two elements of the composite beams. The tendency for separation justifies also a requirement that the shear connectors should not be placed too far apart.

31. Summary

Static tests of composite mortar and steel T-beams were made on $\frac{3}{4}$-scale models. The object of these tests was to determine the effect of an imperfect shear connection on the behavior of these beams and to determine the effectiveness of channel shear connectors. Only two variables were included in these tests: (1) mortar strength and (2) strength of the shear connection. All tests were made with a single concentrated load applied to the slab. In all cases the natural bond between the slab and the beam was destroyed during the first test.

The significant results of the static tests of T-beams are summarized below.

(1) In the T-beam tests all of the shear connectors used permitted some slip at even the smallest loads. As a result, the measured strains and deflections for the T-beams were slightly greater than those computed for perfect composite action but in every case were much smaller than those computed for no composite action.

(2) The strains and deflections measured in the T-beam tests agreed well with those computed on the basis of an analysis of the action of a composite T-beam with incomplete interaction.

(3) Though the lack of complete interaction had measurable effects on the strains and deflections the strain in the bottom flange of the I-beam, which would usually govern the design of a composite T-beam, was affected only negligibly for loads up to those producing yielding. It may therefore be concluded that composite beams provided with adequate shear connection may safely be designed on the basis of full interaction.

(4) It may be concluded from the results of these tests that an adequate shear connection will be obtained if the value of $1/C$ as defined in the Appendix is not less than about 20.

(5) Comparisons of the results for beams T2 and T1 indicate that the use of an unusually low-strength mortar may result in splitting or shearing failure of the slab around the connectors.

(6) The load-slip characteristics of the connectors used in the T-beams compared satisfactorily with those obtained from the push-out tests of comparable connectors.

(7) Measurements made on beam T3 indicated that the distribution of strain across the width of the slab was uniform. This fact is believed to justify the assumption that, in an I-beam bridge of usual dimensions as well as in the T-beams tested, a full panel of the slab may be considered to act with the I-beam in resisting bending.

(8) The T-beam tests indicated a need for positive vertical anchorage of the slab to the beam.

V. REPEATED-LOAD TESTS OF T-BEAMS

32. Outline of Tests

The repeated-load tests of composite T-beams were made in order to investigate the nature of the fatigue failure of this type of beam and also as an indirect means for the study of strains in channel shear connectors. A total of 85 specimens was divided intò five series. The first three series were designed primarily to investigate the effects of the following variables: thickness of the flexible web of the connectors, strength of the mortar, and thickness of the connector flange welded to the beam. The remaining two series were added in order to gain a better understanding of the characteristics of the fatigue failures that had been obtained in the preceding tests. These tests were carried out during 1944–1948.

A list of the T-beam specimens tested in fatigue is given in Table 9. In this table each of the five series—R,M, F, E, and G—is divided into groups according to the variables considered; for example, Series R is divided into groups A, B, C, and D. Channel web thicknesses were $\frac{1}{16}$ in. and $\frac{1}{8}$ in., flange thicknesses were 0.06 in., 0.12 in., and 0.20 in., and the mortar strengths ranged from about 1000 psi to 6000 psi. The thickness of both the flange and the web was measured for the connectors on each beam, but since the variations were too small to be significant only nominal values are listed in Table 9.

The tests were carried out in such a manner as to obtain one load-cycle curve for each group of beams. Specimens of one group, equal in all respects except for minor differences in the strength of mortar, were subjected to loads of magnitude between 1670 and 7000 lb. The load for each specimen was constant throughout the test. The magnitudes of the test loads are given in Table 9.

Series R. The 33 beams of Series R were tested primarily to study the effect of varying the thickness of the connector web. Only 25 specimens from this series are reported in this bulletin; the remaining 8 specimens were defective in various ways. In addition to variations in the web thickness, the mortar strength was varied from 1770 to 4320 psi and the test loads varied from 3000 to 7000 lb.

Series M. This series, consisting of 20 beams, included variations in mortar strength only. The various strengths of mortar were designated as

Table 9
Properties of T-Beams Tested in Fatigue

Beam Number	Beam Type*	Shear Connector		Average Mortar Strength, psi	Load, lb
		Web Thickness, in.	Flange Thickness, in.		
Series R					
R1A	C	$\frac{1}{16}$	0.20	4000	7000
R2A	C	$\frac{1}{16}$	0.20	4100	6000
R3A	C	$\frac{1}{16}$	0.20	3400	5000
R4A	C	$\frac{1}{16}$	0.20	3600	5000
R5A	D	$\frac{1}{16}$	0.20	3320	4000
R6A	C	$\frac{1}{16}$	0.20	4000	4000
R7A	D	$\frac{1}{16}$	0.20	3940	3000
R1B	C	$\frac{1}{16}$	0.20	1900	5000
R2B	D	$\frac{1}{16}$	0.20	2950	5000
R3B	C	$\frac{1}{16}$	0.20	1950	4000
R4B	D	$\frac{1}{16}$	0.20	2200	4000
R5B	C	$\frac{1}{16}$	0.20	1910	3900
R6B	C	$\frac{1}{16}$	0.20	2280	3500
R7B	C	$\frac{1}{16}$	0.20	1800	3000
R1C	D	$\frac{1}{8}$	0.20	3600	7000
R2C	C	$\frac{1}{8}$	0.20	2860	6000
R3C	D	$\frac{1}{8}$	0.20	4230	6000
R4C	C	$\frac{1}{8}$	0.20	4320	6000
R5C	C	$\frac{1}{8}$	0.20	3800	5000
R1D	D	$\frac{1}{8}$	0.20	2030	7000
R2D	D	$\frac{1}{8}$	0.20	1950	6000
R3D	C	$\frac{1}{8}$	0.20	2280	6000
R4D	D	$\frac{1}{8}$	0.20	2670	6000
R5D	C	$\frac{1}{8}$	0.20	1810	5000
R6D	C	$\frac{1}{8}$	0.20	1770	4000
Series M					
M1L	D	$\frac{1}{16}$	0.20	1720	4275
M2L	D	$\frac{1}{16}$	0.20	1410	3820
M3L	D	$\frac{1}{16}$	0.20	1270	3450
M4L	D	$\frac{1}{16}$	0.20	1660	3270
M5L	D	$\frac{1}{16}$	0.20	1390	2900
M6L	D	$\frac{1}{16}$	0.20	1940	2770
M7L	D	$\frac{1}{16}$	0.20	1070	2610
M8L	D	$\frac{1}{16}$	0.20	1270	2385
M1M	D	$\frac{1}{16}$	0.20	3410	5950
M2M	D	$\frac{1}{16}$	0.20	2620	5290
M3M	D	$\frac{1}{16}$	0.20	2440	5250
M4M	D	$\frac{1}{16}$	0.20	2730	4230
M5M	D	$\frac{1}{16}$	0.20	3110	3400
M6M	D	$\frac{1}{16}$	0.20	3150	3330
M7M	D	$\frac{1}{16}$	0.20	2840	3220
M1H	D	$\frac{1}{16}$	0.20	5240	6450
M2H	D	$\frac{1}{16}$	0.20	5810	5210
M3H	D	$\frac{1}{16}$	0.20	5350	5120
M4H	D	$\frac{1}{16}$	0.20	6200	3890
M5H	D	$\frac{1}{16}$	0.20	6550	3890

Table 9—Concluded

Beam Number	Beam Type*	Shear Connector		Average Mortar Strength, psi	Load, lb
		Web Thickness, in.	Flange Thickness, in.		
			Series F		
F1A	D	$\frac{1}{16}$	0.06	4510	6000
F2A	D	$\frac{1}{16}$	0.06	3580	5500
F3A	D	$\frac{1}{16}$	0.06	3780	4500
F4A	D	$\frac{1}{16}$	0.06	3400	4500
F5A	D	$\frac{1}{16}$	0.06	3660	3500
F6A	D	$\frac{1}{16}$	0.06	4090	3500
F7A	D	$\frac{1}{16}$	0.06	4010	3200
F8A	D	$\frac{1}{16}$	0.06	2220	2800
F1B	D	$\frac{1}{16}$	0.12	3840	5800
F2B	D	$\frac{1}{16}$	0.12	3920	5350
F3B	D	$\frac{1}{16}$	0.12	3920	4600
F4B	D	$\frac{1}{16}$	0.12	3530	4150
F5B	D	$\frac{1}{16}$	0.12	3500	3400
F6B	D	$\frac{1}{16}$	0.12	3550	3100
F7B	D	$\frac{1}{16}$	0.12	3380	3100
F1C	D	$\frac{1}{16}$	0.20	3300	5450
F2C	D	$\frac{1}{16}$	0.20	3390	5075
F3C	D	$\frac{1}{16}$	0.20	2960	4500
F4C	D	$\frac{1}{16}$	0.20	3220	3900
F5C	D	$\frac{1}{16}$	0.20	3220	3100
F1L	D	$\frac{1}{16}$	0.12	2220	4240
F2L	D	$\frac{1}{16}$	0.12	2580	3670
F3L	D	$\frac{1}{16}$	0.12	2650	2760
F1H	D	$\frac{1}{16}$	0.12	5050	5775
F2H	D	$\frac{1}{16}$	0.12	5230	3420
			Series E		
E1	D	$\frac{1}{16}$	0.20	2700	4995
E2	D	$\frac{1}{16}$	0.20	1850	2500
E3	D	$\frac{1}{16}$	0.20	1830	2260
E4	D	$\frac{1}{16}$	0.20	1970	2100
E5	D	$\frac{1}{16}$	0.20	2230	1670
			Series G		
G	D	$\frac{1}{16}$	0.20	2460	2880

* See Fig. 6. In type C all shear connectors face toward midspan; in type D all shear connectors face the same way.

low, medium, and high, corresponding to ultimate compressive strength of about 1500, 3000, and 5000 psi. The test load varied from 2385 to 6450 lb.

Series F. This series consisted of 26 beams. Twenty-one of these were tested in order to determine the influence of variations in thickness of the shear connector flange welded to the beam. Only 20 tests are reported, however, as one of the beams was tested only with a static load. The mortar strength of these beams ranged from 2220 to 4510 psi. The remaining five beams were tested in order to extend the studies of the effect of mortar strength. They were made with shear connectors corresponding to those of group B, and their slabs were made with mortar of low and high strengths. The high-strength mortar was designed for 5000 psi; the low-strength mortar had an average cylinder strength of about 2500 psi. The test loads varied from 2760 to 6000 lb.

Series E. The maximum number of cycles applied to the beams of Series R, M and F was about 2,000,000. As the load-cycle curves indicated that the endurance limit was not reached at this number of repetitions of load, five additional beams were tested in an attempt to find the endurance limit. All beams of Series E were identical except for their mortar strengths, which varied from 1830 to 2700 psi. Test loads varied from 1670 to 4995 lb.

Series G. The fifth series contained only one specimen. The criterion of failure in the previous series was an end slip of 0.01 in. It was the purpose of this last series to determine whether this slip occurred immediately after the first fracture of a connector or only after several connectors had been broken in slow succession.

33. Description of Test Procedure

The program of testing for each beam was divided into three parts as follows:

(1) *Initial Static Test.* Before the repeated-load test was begun a static test was run in which a load equal to that used in the fatigue test was applied at midspan of the beam in increments of 500 or 1000 lb. For each increment, strains were measured at midspan. The load applied to the beam was measured with a 10,000-lb dynamometer, and a reading was also taken on the dynamometer located in the connecting rod of the testing machine. Slip between the slab and the beam was measured on each side of the beam at each end by means of 0.001-in. dial indicators, and center deflection was measured by a deflectometer bearing against the floor of the laboratory.

(2) *Repeated-Load Test.* The beam was subjected to repeated application of a load varying from a maximum value to a minimum value which was usually between 300 and 500 lb. At frequent intervals the magnitude of the load was checked by means of the fatigue machine dynamometer and

readings were taken of deflection and slip. Failure of the beam was gradual, and after some study it was decided to consider failure to have occurred when the average slip at one end of the beam had exceeded 0.01 in. In order to end the test at the established amount of slip, microswitches located at each end of the beam automatically stopped the testing machine motor when a slip of 0.01 in. had occurred.

(3) *Final Static Test.* At the conclusion of the repeated-load test, the beam was again-loaded statically in increments of 500 to 1000 lb until failure occurred, usually by yielding of the I-beam. In this test, strains, deflections and slips were measured.

After the static test to failure, the mortar slab was carefully broken off the beam, and the shear connectors were examined for evidence of fatigue failure. It should be pointed out that the deformations produced in the test to failure were never sufficiently large to cause a static failure of the connectors or to obscure the manner in which they failed in fatigue.

The final static test was omitted in some cases.

34. Test Results

The results of the test are presented in Tables 10–13 and in Figs. 36–46, including the results of both the initial static tests and the repeated-load tests. The results of the static tests are discussed in this section; most of the results of the tests in fatigue are presented in the following sections dealing with the effects of particular variables encountered in the tests.

Initial Static Tests. These tests were made in order to obtain initial data for each beam which could be used as a basis for evaluating the effect of repetition of the load. The preloading in this test also generally insured that the bond between the steel beam and the mortar slab was broken before starting the fatigue test. Except for a few specimens in Series R the full load cycle of the initial static test was repeated three times; in each case the reported measurements are for the third loading.

In Figs. 36–38 the end slips are plotted against the load applied to the beam at midspan. Each part of these figures represents one group of specimens similar in all respects. The only differences within each group were the magnitudes of the highest load applied and minor variations in the cylinder strength of the mortar. A study of these curves shows that the scatter of the load-slip curves is large. It does not follow the small variations in mortar strength within any group, but it follows to some degree the magnitude of the highest load applied; a large increase of slip at low loads can be observed in specimens loaded to very high loads. It is believed that this increase of slip resulted from permanent deformations of the mortar which took place before the third application of the static load, from which these data were obtained.
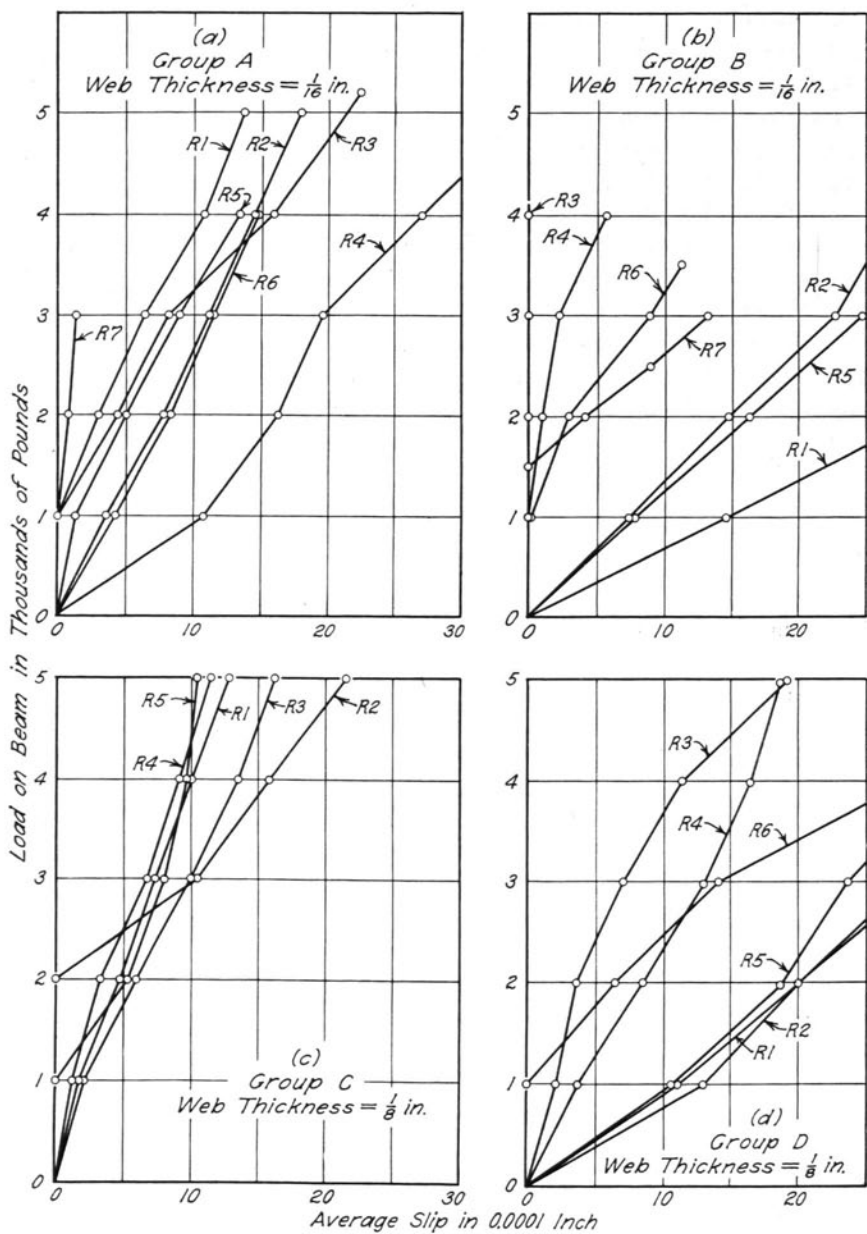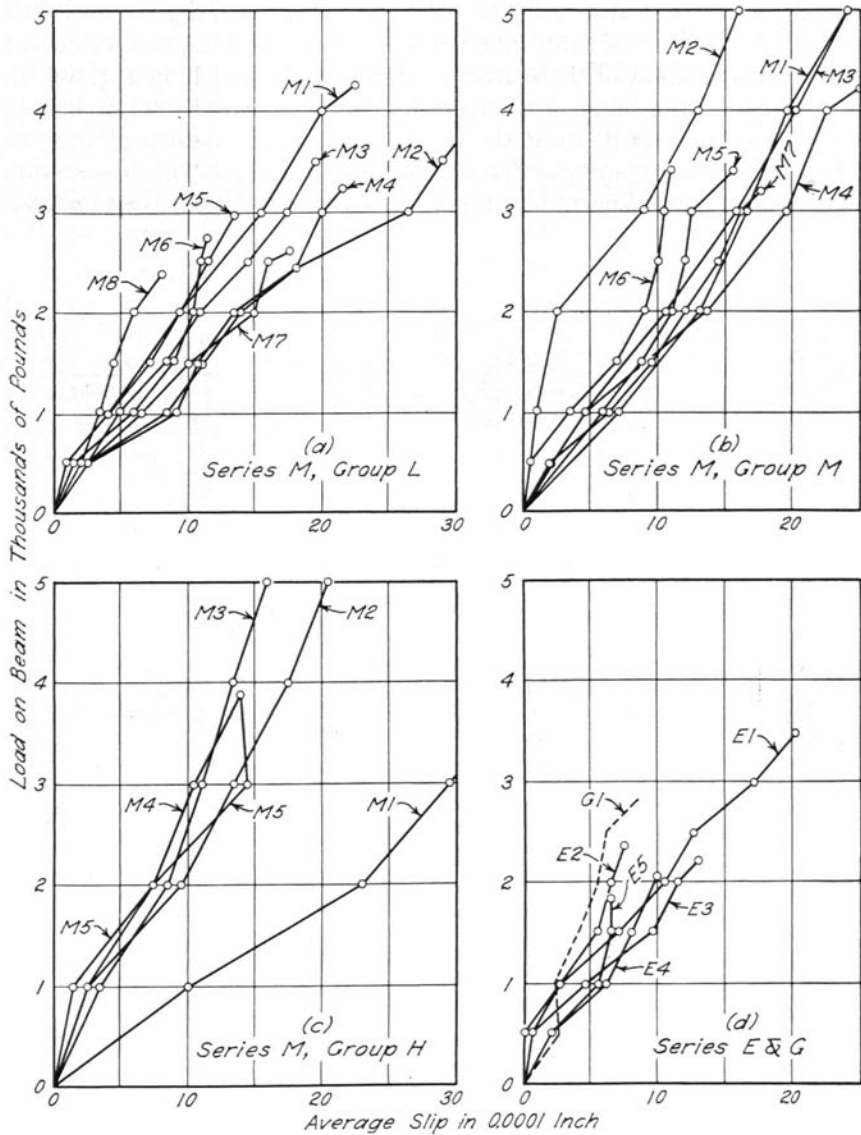
Fig. 36. Initial Load-Slip Curves, Series R

Fig. 37. Initial Load-Slip Curves, Series M, E, and G

A considerable scatter may be observed in the load-slip curves of all groups; the least consistent data are those shown in Figs. 36a, b, d, and 38a. An explanation of the scatter in groups A, B, and D in Fig. 36 can be found from the shape of the load-slip curves. It seems evident that in several specimens of Series R the bond either was not destroyed at all or was destroyed only partly at the time of the static tests. This observation is confirmed by the repeated-load tests. The presence of some bond between
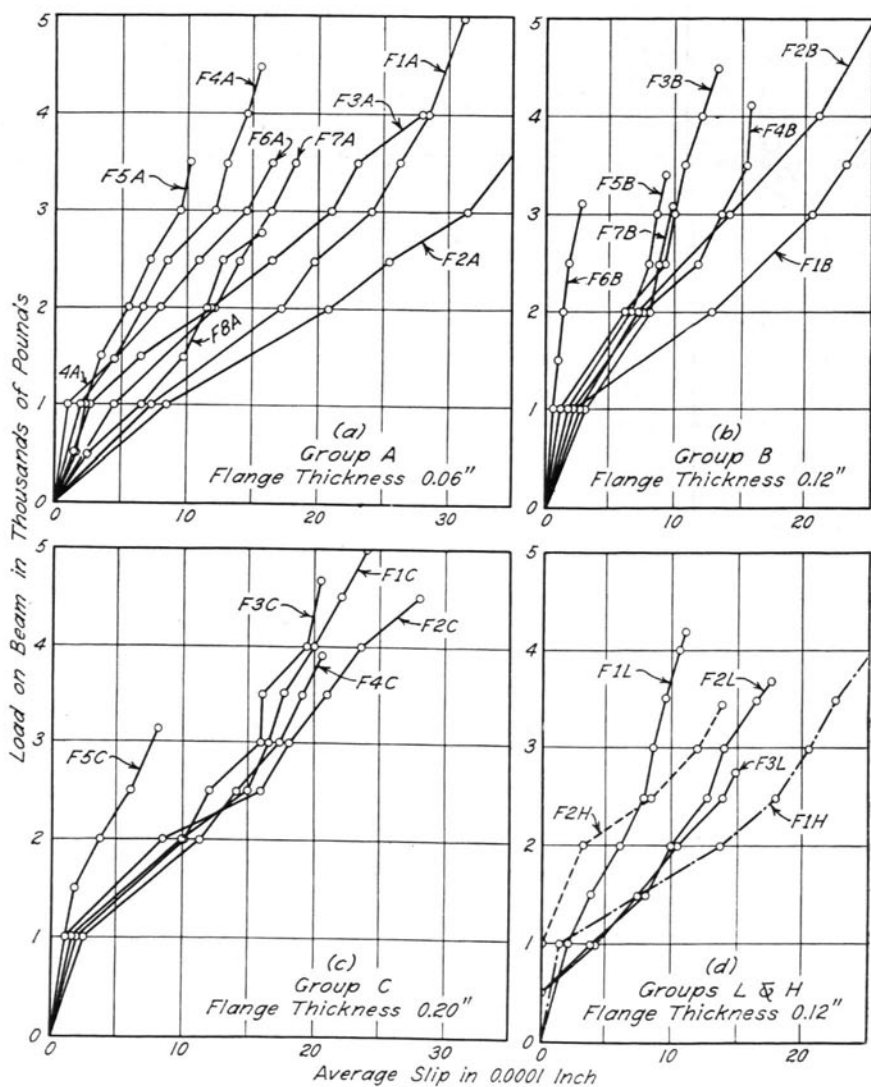

Fig. 38. Initial Load-Slip Curves, Series F

the slab and the beam was undoubtedly responsible for an increase of the degree of interaction. Thus the degree varied from one beam to the other; as a result, the magnitude of slip also varied from one beam to the other. It seems certain that in most of the specimens of the other series the bond was broken before the third static test was performed. Thus the large scatter of the results of group A in Fig. 38a must have been caused by some other factor. It should be noted that specimens F1A, F2A, and F3A (which show the largest slips) are those loaded to the highest load. Furthermore, all specimens of this group had shear connectors with flanges only 0.06 in. thick. It seems most probable that a very large concentration of stress was present under the flanges welded to the beam and, as a result, large permanent deformations of the mortar took place during the first or second application of static load. This difference in permanent deformations provides an explanation for the differences between the slips of the various specimens of this group.

Because of the low uniformity of the results within the single groups of beams it is rather difficult to compare the results of the various groups and to evaluate the effects of the many variables. In general, the scatter within the groups was at least as large as the influence of these variables.   Nevertheless, some general trends can be traced as described in the following paragraph.

The uniformity of the data is definitely influenced by large variations in concrete strength and by the thickness of the connector flange welded to the beam. It may be seen from Fig. 36 that more consistent results were obtained in the tests of groups A and C with the higher mortar strengths, and this same tendency can be detected in Fig. 37. Similarly, in Fig. 38 it may be observed that the data become more consistent as the flange thickness increases from 0.06 in. in group A to 0.20 in. in group C. No similar effect of the thickness of the shear connector web can be observed in Fig. 36 which contains curves for connectors with $\frac{1}{16}$ and $\frac{1}{8}$-in. webs. A comparison of the general trends in Figs. 36 and 38 indicates also that the slip increases with a decreasing strength of mortar and decreases slightly with an increasing thickness of the web of the shear connectors. Both of these influences are very small and are obscured by the non-uniformity of the test results.

It was brought out in the description of the test procedure that strains and deflections were measured in these tests in addition to slips. These measurements gave more uniform results than did those of slips, and the variations fell within the usual range of experimental errors. Inasmuch as neither the strains nor the deflections of the beam had any direct bearing on the static behavior of the shear connectors or on their strength in fatigue, they are not presented here.

Tests in Fatigue. The data obtained from repeated loading of the T-beams are presented in Tables 10–13, and also in Figs. 39–46 primarily
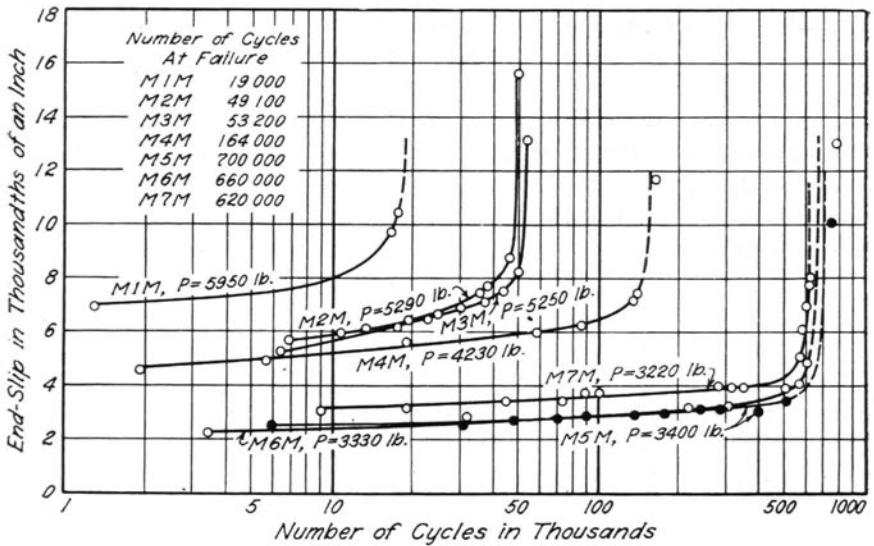
Fig. 39. Slip-Cycle Curves for Group M of Series M

as plots of load versus the logarithm of the number of cycles at failure. The loads are the maximum test loads; the reported number of cycles is that at failure. In addition to the actual test loads corrected loads are given; the corrections have been made on the basis of mortar strength and the thickness of shear connector web.

Although during the conduct of the tests an end slip of 0.01 in. was used as the criterion of failure, additional studies of the manner of failure were made and a slightly different criterion has been adopted in this bulletin. For every specimen for which sufficient data existed, slip was plotted against the number of cycles as illustrated by typical curves in Fig. 39. It is evident from these curves that a slip of 0.01 in. does not represent the beginning of structural damage. Neither does it represent closely the major decreases in interaction which are indicated on the curves by a sharp increase in slip. Actually a slip of 0.01 in. corresponds rather closely to final failure of the shear connection, but generally occurs at a slightly smaller number of cycles. Further study showed that somewhat more consistent comparisons were obtained if the number of cycles corresponding to the vertical part of the curves in Fig. 39 was used; hence this criterion has been employed in preparing the load-cycle curves herein.

As the slip usually became excessive at one end of the specimen only, the curves in Fig. 39 represent the slips at the end which failed. Up to the sharp change in the rate of increase of slip, the slips measured at the two ends of the same specimen were in good agreement.

Final Static Test. In the final static test, performed after the repeated-load test, all slips, strains and deflections showed a considerable increase over the corresponding values found in the initial static tests. They were, however, smaller than the corresponding values given by the theory for no interaction, a fact which indicates that the shear connection was not broken completely. This supposition was confirmed by the examination of the shear connectors when the slab was broken off the beam. Although with the exception of some of the specimens which did not fail in fatigue, several completely or partly broken connectors were found on each beam, there were always a number of undamaged connectors remaining.

The location of the fracture of the connectors varied from beam to beam. A study of these failures is presented in Section 40.

35. Effect of Mortar Strength

The effect of mortar strength on the fatigue life of the shear connection in a mortar and steel composite T-beam was studied primarily on the basis of data from Series M which was designed for this purpose. However, some additional data on this effect could be obtained from the results of Series R and F. The test data for Series M are summarized in Table 10, and those for Series R and F in Tables 11 and 12 respectively.

Table 10
Results of Repeated-Load Tests: Series M

All shear connectors $1 \times \frac{3}{8} \times \frac{3}{16}$-in. channels, $1\frac{1}{2}$ in. long

T-Beam Number	Mortar Strength f_c', psi	Correction Factor, k^*	Test Load P, lb	$\frac{P}{k}$, lb	Number of cycles
M1L	1720	0.89	4275	4800	45 000
M2L	1410	0.86	3820	4440	135 000
M3L	1270	0.84	3450	4110	209 000
M4L	1660	0.89	3270	3670	692 000
M5L	1390	0.86	2900	3370	1 030 000
M6L	1940	0.92	2770	3010	2 062 000†
M7L	1070	0.81	2610	3220	579 000
M8L	1270	0.84	2385	2840	2 075 000†
M1M	3410	1.03	5950	5780	19 000‡
M2M	2620	0.97	5290	5450	49 100
M3M	2440	0.96	5250	5470	53 200
M4M	2730	0.98	4230	4320	164 000
M5M	3110	1.01	3400	3370	700 000
M6M	3150	1.01	3330	3300	660 000
M7M	2840	0.99	3220	3250	620 000
M1H	5240	1.18	6450	5470	11 300‡
M2H	5810	1.23	5210	4240	144 000
M3H	5350	1.19	5120	4300	229 000
M4H	6200	1.26	3890	3090	1 052 000
M5H	6550	1.28	3890	3040	1 881 000

* From Curve 1 in Fig. 42.
† Did not fail.
‡ Estimated value.

All specimens of Series M were made with identical shear connections; the only variable was the mortar strength. The series was divided into three groups with widely different mortar strengths. The results from Table 10 are plotted in Fig. 40a as solid circles, triangles, and squares. This figure included also data from groups A and B of Series R and group C of Series F, the specimens of which were made with the same kind of shear connectors as those of Series M. These are represented by the open symbols. In Fig. 40a the actual load applied at midspan of the beam is plotted against the logarithm of the number of cycles at failure. It can be seen that the number of cycles required to produce failure of two specimens of widely different strengths but subjected to an equal load was greater for the specimen with higher mortar strength. A distinct decrease of the fatigue strength with a decreased strength of mortar can be observed. A similar phenomenon is brought out by Fig. 41a, which shows the results for specimens of groups C and D of Series R. Specimens of these groups were made with shear connectors consisting of $1 \times \frac{3}{8} \times \frac{1}{8}$-in. channels while those in Fig. 40a had shear connectors consisting of $1 \times \frac{3}{8} \times \frac{1}{16}$-in. channels. The effect of mortar strength for both types of specimens is defined quantitatively in Fig. 42, in which correction factors k are plotted against the compressive strength of the control cylinders. Two curves are shown in this figure: one for channels with $\frac{1}{16}$-in. web thickness and the other for those with $\frac{1}{8}$-in. webs. Both curves were found by trial and error, in order to reduce all results to a mortar strength of 3000 psi. Just why these curves take the form shown cannot be determined conclusively from the available evidence. A possible explanation may be that in specimens with high strength mortar the mortar acts very much as an elastic material, whereas the mortars of low strength are subject to large plastic deformations. If this is true, then in the first case the fatigue strength of the T-beams depends primarily on the fatigue strength of the steel of the shear connectors, while with low strength mortars the deformation and strength of the mortar are of primary importance.

Corrected loads P/k from Series M and R and from group C of Series F are plotted against the number of cycles at failure in Figs. 40b and 41b. Comparison of these figures with Figs. 40a and 41a shows that the correction factors reduced the scatter considerably. This holds true especially for the specimens of Series M. The data obtained from Series F fall generally below those from Series M and the data from Series R show far more scatter than any other series. It has been pointed out in Section 34 that, on several beams of Series R, bond between the slab and the beam has not been destroyed in the initial static tests and was present at least for a part of the duration of the repeated-load tests. This explains in part the scatter of Series R. The data for the following specimens were entirely
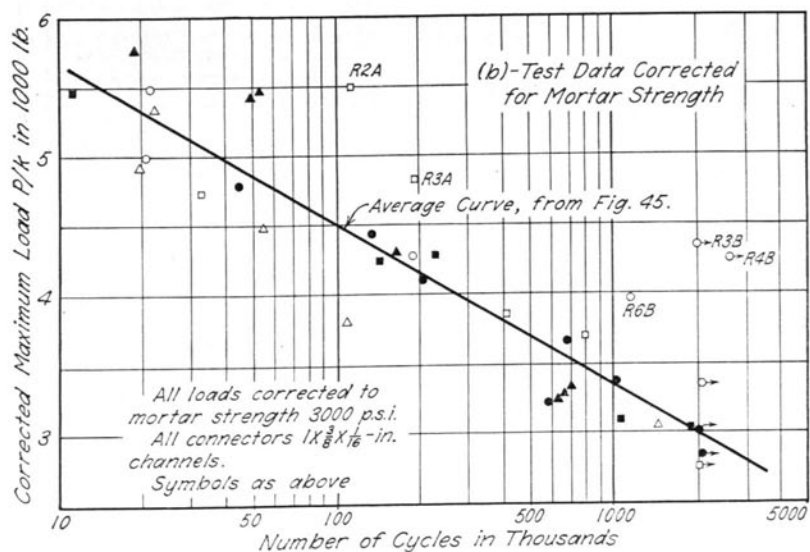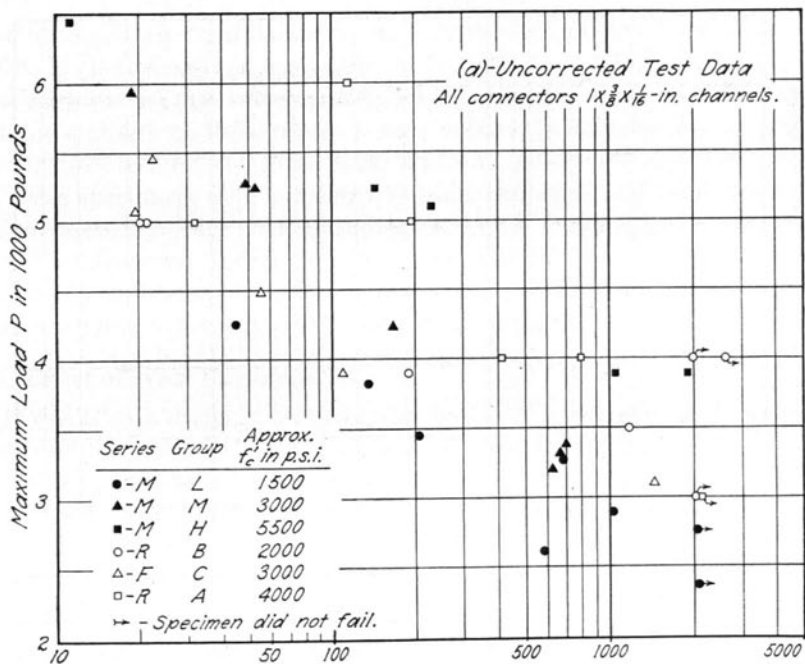
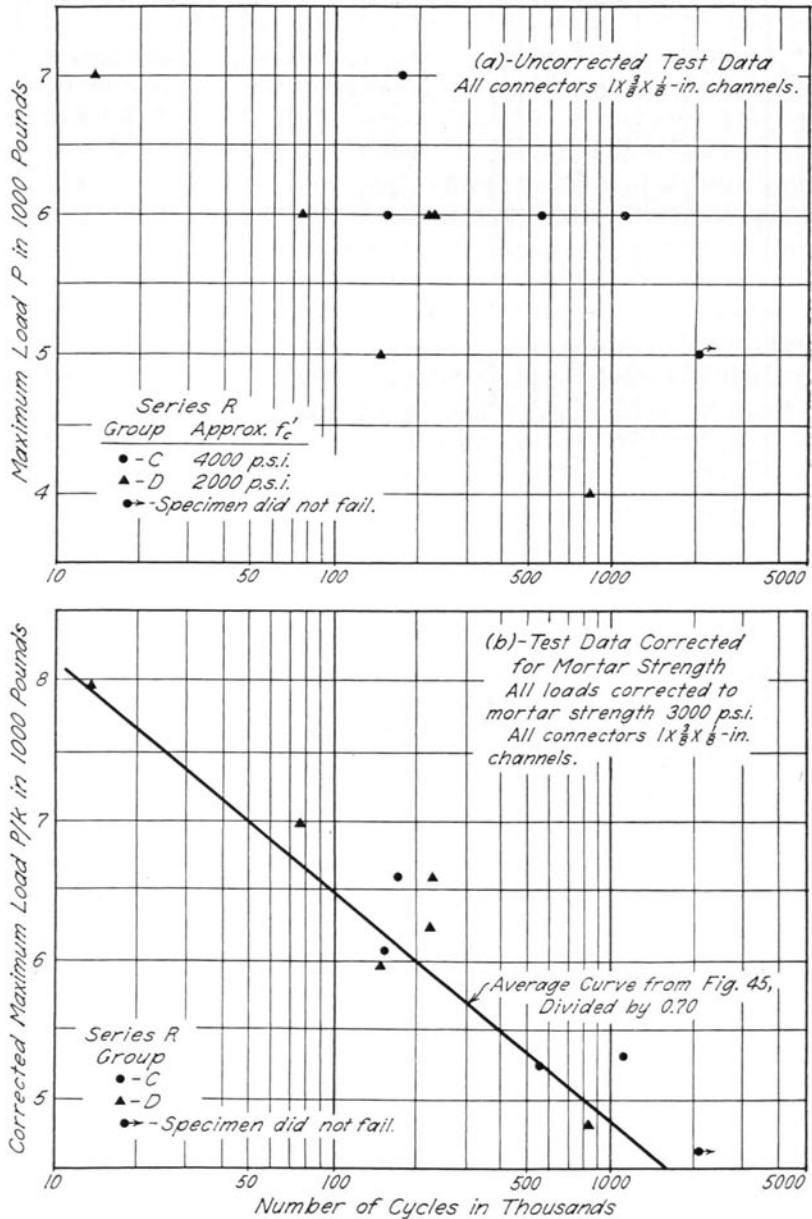Fig. 40. Variation of Number of Cycles at Failure with Mortar Strength,
1/16-in. Channels

Fig. 41. Variation of Number of Cycles at Failure with Mortar Strength,
1/8-in. Channels

out of line: R1A (not shown on the figure), R2A, R3A, R3B, R4B, and R6B. With the possible exception of R2A and R3A, bond was present at the time the fatigue test began in all these beams. Therefore the higher fatigue strength of these beams is only apparent, since during the part of the fatigue test in which the bond was not broken the shear connectors of these specimens were subjected to much smaller loads than those that would normally exist after breaking the bond. In specimen R3B no slip could be observed during the entire test, and this specimen did not fail. Obviously, full bond was present throughout the test. A similar phenomenon was observed in connection with specimen R4B.

36. Effect of Web Thickness

Series R was designed primarily to study the effect of the thickness of the connector web on the fatigue life of T-beams. The results are presented in Table 11 and Fig. 43. Channel connectors of two different web thicknesses were used: $\frac{1}{16}$ in. in groups A and B, and $\frac{1}{8}$ in. in groups C and D. To eliminate the effects of the variations of mortar strength, the corrected loads P/k are plotted in Fig. 43. Specimens R1A, R2A, R3B, and R4B are omitted from this figure because the presence of some initial bond obscured the results of the tests made on these specimens.

The data in Fig. 43a show very clearly that the effect of increasing the thickness of the web is to increase the fatigue strength of the T-beams.
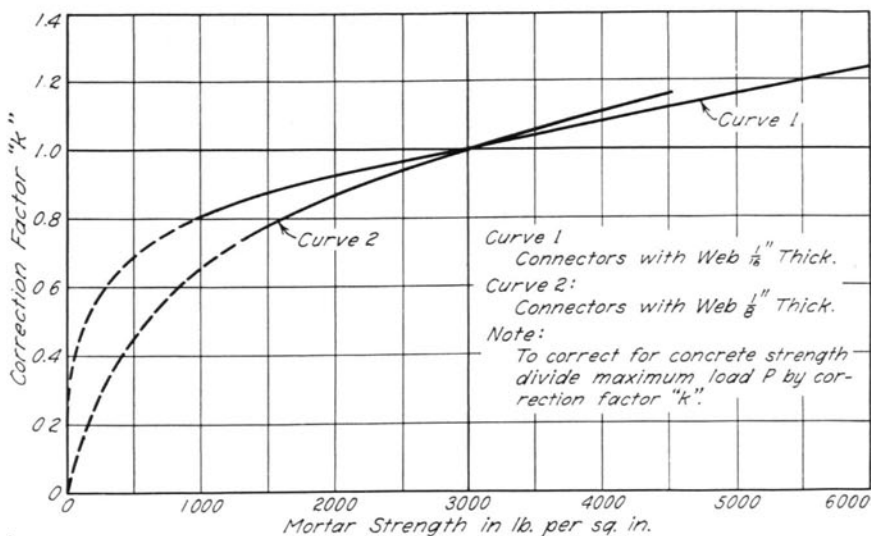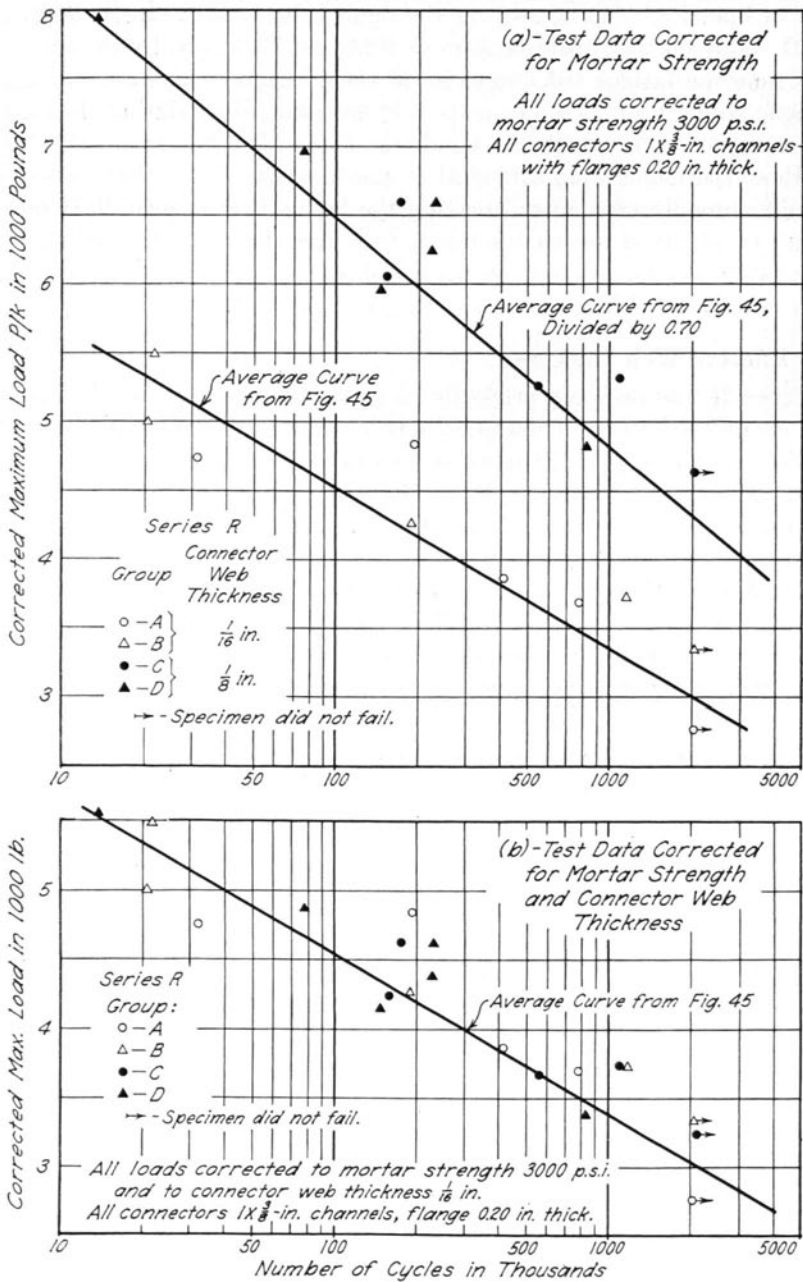

Fig. 42. Correction Factors for Mortar Strength

Fig. 43. *Variation of Number of Cycles at Failure with Connector Web Thickness*

Quantitatively the difference between the beams with the heavier connectors and those with the lighter connectors is about 30 percent. This difference is illustrated in Fig. 43b in which the loads for beams of groups A and B are the same as in Fig. 43a, but the loads of groups C and D are multiplied by a coefficient equal to 0.7 in addition to the correction for mortar strength. Thus it is seen that the reduction of connector web thickness from $\frac{1}{8}$ in. to $\frac{1}{16}$ in. reduced the fatigue strength of the shear connection by only about 30 percent. Since the section modulus of the channel web was reduced by 75 percent the decrease in thickness must have been accompanied by an appreciable reduction of the moment at the section at which fracture occurred. In accordance with the dowel concept, such a reduction would result from the change in pressure distribution caused by the reduction in stiffness of the connector.

Table 11
Results of Repeated-Load Tests: Series R

Shear connectors of groups A and B $1 \times \frac{3}{4} \times \frac{1}{8}$-in. channels, $1\frac{1}{2}$ in. long
Shear connectors of groups C and D $1 \times \frac{3}{4} \times \frac{1}{16}$-in. channels, $1\frac{1}{2}$ in. long

T-Beam Number	Mortar Strength f'_c, psi	Correction Factor, k^*	Test Load P, lb	$\dfrac{P}{k}$, lb	$0.7\dfrac{P}{k}$, lb	Number of Cycles
R1A	4000	1.08	7000	6480	....	21 400†
R2A	4100	1.09	6000	5500	....	116 000†
R3A	3400	1.03	5000	4850	....	194 000†
R4A	3600	1.05	5000	4760	....	31 700
R5A	3320	1.03	4000	3880	....	408 000
R6A	4000	1.08	4000	3700	....	784 000
R7A‡	3940	1.08	3000	2780	....	2 035 000¶
R1B	1900	0.91	5000	5490	....	21 700†
R2B	2950	1.00	5000	5000	....	20 500
R3B	1950	0.92	4000	4350	....	2 000 000¶
R4B‡	2200	0.94	4000	4260	....	2 634 000¶
R5B	1910	0.91	3900	4290	....	190 000†
R6B	2280	0.94	3500	3720	....	1 191 000
R7B	1800	0.90	3000	3330	....	2 051 000¶
R1C	3600	1.06	7000	6600	4620	173 000
R2C	2860	0.99	6000	6060	4240	153 000
R3C‡	4230	1.13	6000	5310	3720	1 100 000
R4C	4320	1.14	6000	5260	3680	553 000
R5C	3800	1.08	5000	4630	3240	2 032 000¶
R1D	2030	0.88	7000	7950	5570	13 600
R2D‡	1950	0.86	6000	6980	4890	76 800
R3D	2280	0.91	6000	6590	4610	230 000
R4D‡	2670	0.96	6000	6250	4380	223 000
R5D	1810	0.84	5000	5950	4170	147 000
R6D	1770	0.83	4000	4820	3370	817 000

* From curves in Fig. 42.
† Uncorrected maximum applied number of cycles.
‡ Connectors made of hard grade steel.
¶ Did not fail.

37. Effect of Flange Thickness

Although both the push-out tests and the static T-beam tests of shear connectors suggested a large concentration of stress adjacent to the flange welded to the beam, none of these tests included the thickness of this flange as an independent variable. It was hoped, therefore, that the fatigue tests would bring out the importance of this factor and thus throw additional light on the behavior of channel shear connectors. Three groups— A, B, and C—of Series F were designed for this purpose. The test results
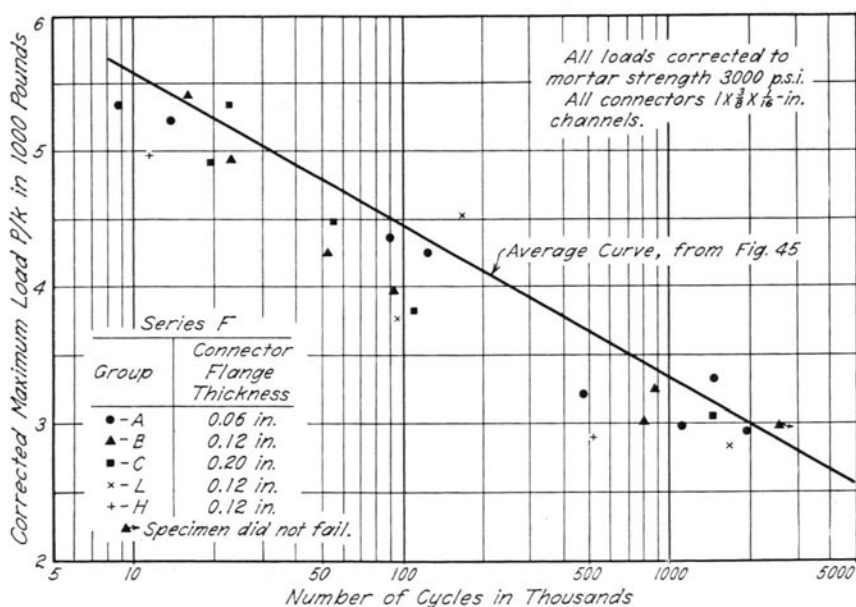
Fig. 44. Variations of Number of Cycles at Failure with Connector Flange Thickness

are summarized in Table 12 and shown in Fig. 44, where loads corrected for mortar strength are plotted against the number of cycles at failure. The shear connectors in all specimens were $1 \times \frac{3}{8} \times \frac{1}{16}$-in. channels $1\frac{1}{2}$ in. long with flanges 0.06, 0.12, and 0.20 in. thick (see Fig. 7), each flange thickness being used in all specimens of one group. It can be seen that all the results fall in the same band and that no consistent variation with thickness of the flange can be observed.

The maximum stress in a connector, on which the fatigue strength depends, is a function both of the magnitude of the load taken by the web and of the distribution of this load. If the failures of all three kinds of connectors were of the same type, the results of these tests would indicate

Table 12
Results of Repeated-Load Tests: Series F

All shear connectors $1 \times \frac{3}{4} \times \frac{1}{16}$-in. channels, $1\frac{1}{2}$ in. long; shear connector flange thickness 0.06 in. in group A, 0.12 in. in groups B, L, and H, 0.20 in. in group C

T-Beam Number	Mortar Strength f'_c, psi	Correction Factor, k^*	Test Load P, lb	$\dfrac{P}{k}$, lb	Number of Cycles
F1A	4510	1.12	6000	5360	8 800†
F2A	3580	1.05	5500	5240	13 900†
F3A	3780	1.06	4500	4250	125 000
F4A	3400	1.03	4500	4370	90 000
F5A	3660	1.05	3500	3330	1 457 000
F6A	4090	1.09	3500	3210	470 000
F7A	4010	1.08	3200	2960	1 975 000
F8A	2220	0.94	2800	2980	1 100 000
F1B	3840	1.07	5800	5420	16 000
F2B	3920	1.08	5350	4950	23 000
F3B	3920	1.08	4600	4260	51 900
F4B	3530	1.04	4150	3990	92 900
F5B	3500	1.04	3400	3270	890 000
F6B	3550	1.04	3100	2980	2 562 000‡
F7B	3380	1.03	3100	3010	800 000
F1C	3300	1.02	5450	5340	22 400†
F2C	3390	1.03	5075	4930	19 800
F3C	2960	1.00	4500	4500	54 900
F4C	3220	1.02	3900	3820	110 800
F5C	3220	1.02	3100	3040	1 430 000†
F1L	2220	0.94	4240	4510	165 000
F2L	2580	0.97	3670	3780	96 300
F3L	2650	0.97	2760	2850	1 684 000
F1H	5050	1.16	5775	4980	11 300†
F2H	5230	1.18	3420	2900	518 000

* From Curve 1 in Fig. 42.
† Estimated value.
‡ Did not fail.

either that (1) both the magnitude and the distribution of the loads on the webs of the channels of all three types were equal or (2) the variations in magnitude and distribution were compensating in such a manner that the fatigue strengths were not affected. The large differences in the thicknesses of the flange and the corresponding very small differences in the slips (Fig. 38) indicate that the unit pressure on the mortar under the flange was not greatly different for the three types of connectors. As the thickness of the flange varied, the magnitude of the load transmitted through the web also varied. It is believed, therefore, that both the distribution and the magnitude of the load transmitted through the web of the connectors with flanges 0.12 and 0.20 in. thick varied in such a way that their effects canceled. It will be shown subsequently that the failures of connectors with flanges 0.06 in. thick differed fundamentally from those of the two other types of connectors.

The correction factor k used to eliminate the variation in mortar strength was taken from Curve 1 of Fig. 42. It can be seen from Table 12, however, that the strength of the mortar did not vary greatly in groups A, B, and C. Therefore two additional groups of specimens were tested in order to find whether the factor k depended on the thickness of the connector flange and whether the effects of flange thickness depended on the mortar strength. Three beams of group L and two beams of group H were made with shear connectors having flanges 0.12 in. thick, and with low- and high-strength mortars respectively. Although the specimens in these groups were too few to provide conclusive data, there was some indication that a reduction in flange thickness from 0.20 in. to 0.12 in. produced some reduction in fatigue strength for these beams in which the mortar strengths were higher or lower than those used in the main series. These results are, of course, in contradiction to those of the more extensive tests of groups A, B, and C of Series F.

38. Load-Cycle Curves and Endurance Limit

The results of all repeated-load tests of T-beams are shown in Fig. 45. In this figure, by use of the factors previously described, all loads are corrected to a concrete strength of 3000 psi and to a connector web thickness of $\frac{1}{16}$ in. The heavy line is an average load-cycle curve, which is in fair agreement with the results throughout the range of the tests. The two broken lines are for loads 15 percent greater or less than the average values. Practically all the test data fall within these limits. The five specimens above the upper line were those that were believed to have bond present during at least a part of the repeated-load test.

The five specimens of Series E were tested to determine the existence of an endurance limit or load below which the beam could withstand an indefinitely large number of cycles of loading. The results are included in Table 13 and shown in Fig. 45. Four of the five specimens failed at a num-

Table 13
Results of Repeated-Load Tests: Series E and G

All shear connectors $1 \times \frac{3}{8} \times \frac{1}{16}$-in. channels, $1\frac{1}{2}$ in. long

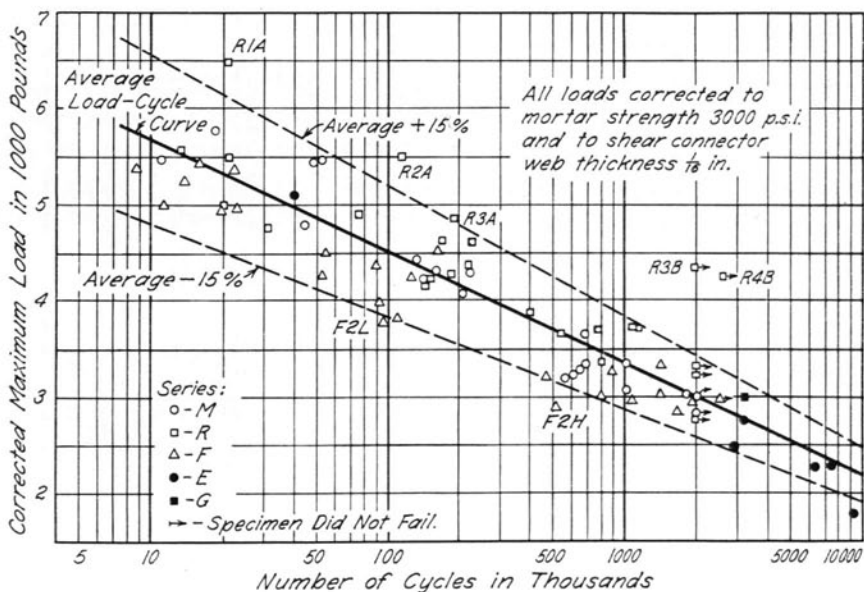| T-Beam Number	Mortar Strength f_c', psi	Correction Factor, k*	Test Load P, lb	$\dfrac{P}{k}$, lb	Number of Cycles
E1	2700	0.98	4995	5100	40 000
E2	1850	0.91	2500	2750	3 200 000
E3	1830	0.91	2260	2480	2 897 000
E4	1970	0.92	2100	2280	7 450 000
E5	2230	0.94	1670	1780	9 400 000
G	2460	0.96	2880	3000	3 200 000

* From Curve 1 in Fig. 42.

Fig. 45. Corrected Load-Cycle Curve for All Repeated-Load Tests

ber of cycles greater than the maximum of 2,000,000 imposed in the other tests, and the maximum number of cycles reached before failure was 9,400,000. It seems likely that the nature of the failure of shear connectors in composite T-beams is such that no endurance limit will be found for loads that might be considered normal.

39. Sequence of Fracture of Shear Connectors

In the repeated-load tests of Series R, M, F, and E the criterion of failure was a slip between the slab and beam of approximately 0.01 in. It was found, however, that for the T-beams used in these tests this amount of slip occurred only after several of the shear connectors had fractured and after a rather extensive breakdown in composite action took place. This or a similar criterion of failure was entirely satisfactory for interpreting the results of tests which were made primarily to compare the effects of several variables on the action of channel shear connectors. It was recognized, however, that actual fatigue failure of the connectors must begin at a considerably smaller number of cycles than that corresponding to a slip of 0.01 in., and that the cracking and fracture of the various shear connectors is a progressive phenomenon.

One specimen, constituting Series G, was tested in an attempt to determine the stage of the test at which each of the several shear connectors
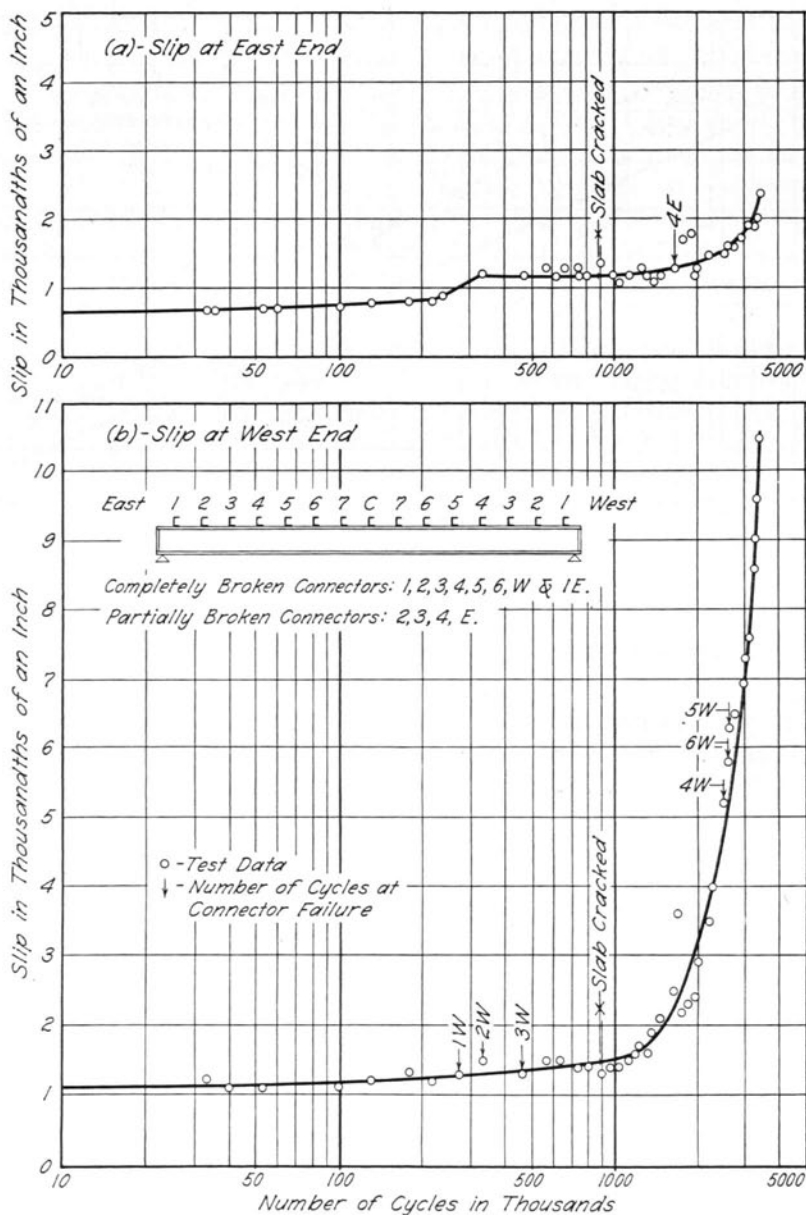
Fig. 46. Slip-Cycle Curves for Beam G

failed by fracture. Each shear connector on this beam had attached to it in the fillet of the channel a small loop of No. 36 enameled copper magnet wire. The wire was cemented in place with DuPont Cement No. 5458 (Duco cement), and the two ends of the loop of wire were carried from the shear connector to the top flange of the I-beam and down over the edge of the flange to a point on the web of the beam. At this point the wires from all the shear connectors were connected in series, using a No. 22 copper wire with plastic insulation. The No. 36 wires were protected from damage by a thin coating of Fairprene synthetic rubber cement.

The series circuit of magnet wires was then connected through a battery to an electromagnetic relay which was inserted in the circuit of the holding coil of the start-stop switch controlling the electric motor on the repeated-load testing machine. Thus, if one of the wires attached to the shear connectors was broken, presumably as a result of fracture or the formation of a crack in the connector, the relay would be tripped and the motor stopped. When this occurred, the circuit was checked with an ohmmeter to determine which wire had been broken, and the broken wire was then by-passed and the test continued until another break occurred.

The results of the test of beam G are shown in Fig. 46 and in Table 13. The beam failed at 3,200,000 cycles. At this stage, six of the shear connectors at the west end of the beam (flanges turned out) were completely fractured, and all these fractures had been indicated by the magnet wire circuit. At the other end of the beam, the end connector was fractured and the next three from the end were cracked partly through the web. Only one of these failures, however, was indicated by the magnet wire, that of the fourth connector from the east end. Failure of the first and third connectors was not indicated because their wires were inadvertently cut out of the circuit before the connectors cracked or fractured. The crack in the second connector was not indicated because it did not extend entirely across the width of the connector and had not intersected the magnet wire at the end of the test. The number of cycles at which failures of the individual connectors were indicated by the magnet wire are marked in Fig. 46.

In general, the test results were satisfactory. They confirmed the belief that the sharp change in the slip-cycle curves does not represent the first damage in fatigue and that the first fracture occurred at a much lower number of cycles. Furthermore, this test illustrated well the progressive character of fatigue failure of shear connectors. The results of this test cannot be used quantitatively, however, as it is not known just what stage in the failure of the shear connector is indicated by the failure of the magnet wire, even though an exploratory test indicated that a break in the wire is produced by the formation of a microscopic crack in the specimen.

40. Types of Connector Failures

At the conclusion of the tests of each T-beam the slab was carefully broken off the beam and the connectors were examined. With the exception of eight beams which did not reach the limiting slip of 0.01 in., and of specimens F1A and F2A, several broken shear connectors were found in every beam. Shear connectors with incipient cracks were found in all beams except R7A, R3B, and R5C. Specimens F1A and F2A had connectors with flanges only 0.06 in. thick and were loaded with the highest loads; the lack of damage to the connectors indicates, therefore, that excessive slip resulted from very large inelastic deformations of the mortar at a number of repetitions of load insufficient to produce failure of the metal.

In nearly all beams the largest damage occurred for connectors located close to the supports. In the 16 specimens with all shear connectors facing toward midspan the damaged connectors were fairly evenly distributed on both ends. On the other hand, in the remaining 60 beams with all connectors facing the same way the failure of connectors facing toward midspan was predominant, though not exclusive. An explanation may be that the connectors facing away from midspan were stiffened by the block of mortar enclosed between the flanges of the channel connector.

The types of failures observed on the shear connectors are illustrated in Fig. 47. All connectors with flanges 0.20 and 0.12 in. thick fractured through the web of the channel, as shown in Fig. 47a. Failures of connectors with a flange thickness of 0.06 in. were of several types as shown in Fig. 47b and summarized in Table 14. Thus the types of fatigue failures of all connectors included in these tests may be divided into two large groups: (1) those for channels with relatively stiff flanges and (2) those for channels with relatively flexible flanges.

Channels with Stiff Flanges. Both the 0.12-in. and the 0.20-in. thick flanges were much thicker than the webs of the respective connectors. Therefore the flange could bend only a negligible amount and the web was practically fixed against rotation at the fillet between the web and the flange welded to the beam. The fillets on one side and the bead of the weld on the other side of the web acted as severe stress raisers. This explains the failures through the channel web.

The point of incipient failure could be either in the fillet or at the top of the heel weld depending on the relative dimensions of the weld and connector. Both types of incipient failure were observed.

Channels with Flexible Flanges. In all connectors with flanges 0.06 in. thick the flanges were slightly thinner than the connector web. In addition, the welds for these connectors were machined down to a height of 0.06 in. (see Fig. 47b). Thus the restraint against rotation at the heel of the channel was small, and bending of the flange welded to the beam could
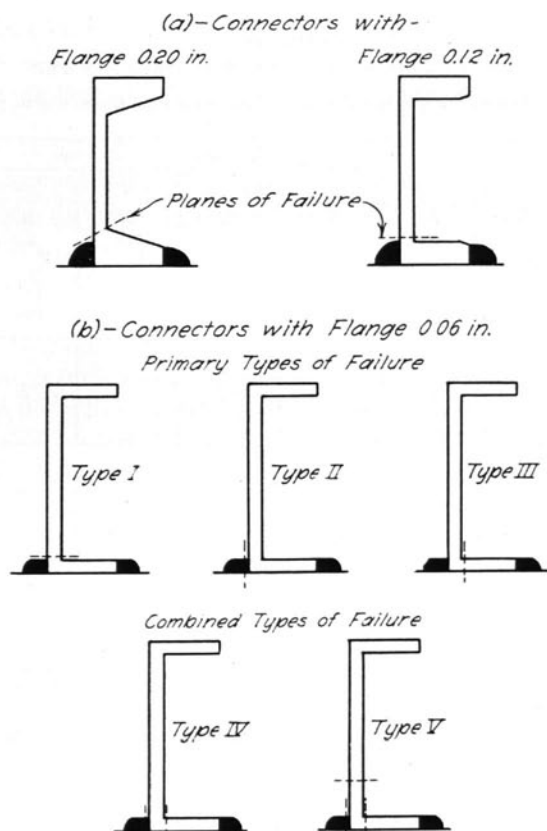
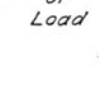*Fig. 47. Types of Connector Failures*

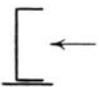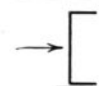be expected. As a result, three primary types of failure occurred in this kind of connector. It can be seen from Fig. 47b that some of the connectors failed by a horizontal crack through the web (Type I), some by a vertical crack through the weld (Type II), and others by a vertical crack through the flange (Type III). A large number of specimens failed with combined types of fracture, shown as Types IV and V.

The total numbers of connectors in Series F which failed with the various types of fracture are summarized in Table 14. It can be seen that two types of failure, II and III, were definitely influenced by the direction of the load; Type I was observed the same number of times for both directions of loading. The type of failure was probably influenced also by the height of the weld.

All the connectors which failed by fracture of Type I had a relatively high heel weld. The stiffness added by an increased weld was probably

Table 14

Types of Connector Failures, Specimens F1A–F8A

All shear connectors $1 \times \frac{3}{4} \times \frac{1}{16}$-in. channels, $1\frac{1}{2}$ in. wide with flanges 0.06 in. thick

Direction of Load	Number of Connector Failures				
	Primary Types			Combined Types	
	I	II	III	IV	V
←	13	—	12	12	3
→	13	7	—	6	5

Characteristics of types of failures:

Type I: High heel weld. Failure by horizontal crack beginning at fillet.

Type II: Low heel weld. Vertical crack at heel weld only. Fillet undamaged except for possible incipient crack. Web not pulled out but bent toward inside.

Type III: High heel weld. Vertical crack at fillet only. Channel not torn out nor fillet damaged.

Type IV: Low heel weld. Vertical cracks formed at fillet and weld. Web torn out, leaving groove between flange and weld.

Type V: Low heel weld. Vertical crack at fillet and weld. Channel torn out, leaving groove. Web broken off or cracked at about one-quarter of the connector height.

responsible for this type of failure, a type similar to that of the connectors with stiff flanges.

Fractures of Type II were observed only on specimens loaded on the back face of the channel. The channel tended to rotate around the toe of the flange and tensile stresses were developed in the weld at the heel. The result was a vertical failure by separation of this weld from the channel.

Failures of Type III were caused only by load acting toward the inner face of the channel connector. In this case tensile bending stresses took place in the flange welded to the beam which explains the failure by a vertical crack through this flange.

Failures of Types IV and V were caused by continued loading after primary failure occurred. This seems to be obvious from the composite character of these failures and also from the location of connectors on which failures of Types IV and V were observed. These connectors were usually located at the ends of the T-beams, and several connectors damaged by one of the first three types of failures were located between them and the undamaged connectors. It is believed that both of these types of failure started with a vertical crack of Type II or III. As the loading continued, a second vertical crack was developed on the opposite face of the web.

From this time on the web was free to rotate at the broken end and the section of maximum stress shifted from the fillet upwards. As a result a horizontal crack through the web developed at some distance up from the beam.

41. Action of Shear Connectors

The only data on shear connectors obtained from both the push-out tests and the static tests of T-beams were the load-slip characteristics. While it is recognized that the load-slip characteristics of a shear connector are of primary importance from the standpoint of the degree of interaction between the beam and the slab of a composite T-beam, it is obvious that these data are insufficient for the design of flexible connectors. The static tests gave some indirect qualitative data on the distribution of the load along the connector but did not give any direct information regarding the steel stresses. The fatigue tests filled this gap in a qualitative manner.

The data on fracture of shear connectors tested in fatigue show that the critical moment section of a channel shear connector is located at or near the fillet of the flange welded to the beam. If the flange is relatively stiff as compared with the connector web, the web is the only part of the connector subject to flexure. It is therefore important to find out how much of the total load is carried by the flexible web and how that load is distributed along the web. This question, however, could not be answered from these tests; it was left for an investigation of full-size connectors in which strains could be measured in the connectors themselves.

The relatively small effect of web thickness on the fatigue strength of channel connectors seems to indicate that the heavier the web the larger the part of the total load that it carries. This behavior is in agreement with the dowel concept of the action of the flexible portion of a channel shear connector.

The fatigue tests seem to indicate that the thickness of the flange has little effect on the strength of shear connectors. This indication is in direct contradiction to what would be expected from the dowel theory. The evidence available from the data of Series F can be accepted, however, only in part, since the results for connectors with flanges 0.06 in. thick are not comparable with those for the other connectors because of their fundamentally different behavior. This leaves only two different thicknesses of flange, and it is quite possible that the equal strengths were coincidental as has been discussed in Section 37.

The data presented in Section 35 indicate that the maximum stress in the shear connectors decreased with increasing mortar strength. This effect is greater for low strength than for high strength mortars. In general the effect of the mortar strength does not seem to be very large in the range of practical values.

42. Summary

The results of repeated-load tests on 76 quarter-scale model T-beams have been described. The object of these tests was to obtain general information on the effects of repeated loading on channel type shear connectors. Three variables were included: (1) mortar strength, (2) thickness of the webs of the shear connectors, and (3) thickness of the flanges of the shear connectors. All tests were made with a single concentrated load applied at midspan. The magnitude of the maximum load varied from 1070 to 7000 lb, the minimum load was maintained between 300 and 500 lb.

It is recognized that the results obtained from the fatigue tests of the small-scale models cannot be applied directly to full-size beams. The general information, however, is of some value when considering actual structures. Moreover, the repeated-load tests were of special value in that the strength of channel shear connectors in fatigue is believed to be primarily a function of the maximum stresses produced in the web of the channel. For this reason the data obtained in the fatigue tests provide some information, although mostly indirect, on the possible distribution of load between the flexible web and the more rigid flange.

The results of the repeated-load tests of the small-scale composite T-beams are summarized as follows.

(1) The fatigue failure of the shear connection between the slab and beam of a composite T-beam is progressive in character. The end connectors fail first and the damage progresses toward the load.

(2) A large and rapid decrease in the degree of interaction takes place only after several connectors have been broken. This decrease in interaction is accompanied by a decrease in the load-carrying capacity of the beam.

(3) In a channel shear connector with the flanges stiffer than the web, the maximum steel strains occur at the fillet of the flange welded to the beam and the fracture occurs on a section extending from this fillet to the edge of the weld on the back face of the channel.

(4) An increase in the thickness of the channel web produced an increase in the fatigue strength of the composite beams. However, the increase in fatigue strength was very much less than the increase in section modulus of the channel web.

(5) The fatigue strength of composite beams with channel shear connectors was increased by an increase in the compressive strength of the mortar slab. The effect of the strength of mortar was smaller for high strengths than for low strengths.

(6) The results of the repeated-load tests confirmed the concept of a dowel-like action of channel shear connectors. An exception was the anomalous behavior of the beams having connectors with various flange thicknesses.

(7) In spite of the fact that an attempt was made to destroy the natural bond between the mortar slab and the beam in all specimens, there were several beams in which the bond was effective throughout the initial static tests and during part or even all of the repeated-load tests. The fatigue life of these beams was increased appreciably over that of the beams without bond and in some of these beams there was no failure of the shear connectors whatsoever.

VI. SUMMARY OF TEST RESULTS

43. Preliminary Remarks

Laboratory tests were made on a large number of quarter-scale push-out and T-beam specimens. The push-out specimens were made with various types of rigid and flexible connectors; the T-beam specimens were made with channel shear connectors only.

The push-out tests were designed primarily to compare the behavior of various types of shear connectors and to permit the selection of the particular type most deserving of additional study. The static tests of T-beams were planned primarily to study the action of composite beams with channel shear connectors. The fatigue tests were also used for this purpose and in addition provided data regarding the strength characteristics of channel shear connectors.

The results of the several series of tests have been summarized at the end of each of the preceding chapters. These results are brought together and discussed further in the following sections. The behavior of shear connectors proper and that of composite steel and mortar T-beams with channel shear connectors are discussed separately.

44. Shear Connectors

Considerable information regarding the behavior of shear connectors and the factors that influence their behavior has been obtained from these tests. This information, generally only qualitative in nature, is brought together and discussed briefly in the following paragraphs.

Comparison of Types of Connectors. From the standpoint of load-slip characteristics the rigid type of shear connector was found to be superior to the flexible type. The differences, however, were much less than would be expected from the very large differences in stiffnesses of the two types. It should be emphasized that the selection of a suitable type of shear connector for use in composite beams requires the consideration of other factors besides the load-slip characteristics. For example, the ability of a channel to tie the slab down to the beam may be of sufficient importance to outweigh its slight deficiency in preventing slip.

Among the several types of flexible shear connectors, the channel with one flange welded to the beam appeared to be superior to the types made up from bent or straight plates. It seems likely that the behavior of a

rolled Z-section or even of a rolled angle section would be similar in many respects to that of a channel.

Factors Affecting Behavior of Channel Shear Connectors. It has been shown conclusively that the behavior of channel shear connectors of the type used in most of these tests is affected by three major variables: (1) the width of the connector, (2) the thickness of the channel web, and (3) compressive strength of the mortar slab.

The load-slip characteristics of channel shear connectors and also of the other types tested were approximately linearly proportional to the width of the connector normal to the direction of the load.

The fatigue strength of channel shear connectors was increased by an increase in thickness of the web. The increase, however, was much less than the increase in the section modulus of the web.

The fatigue strength and load-slip characteristics of channel shear connectors were improved by an increase in the compressive strength of the mortar slab. This effect was greatest for low mortar strengths.

Concept of Dowel-Like Action. The results of both the T-beam tests and the push-out tests involving flexible shear connectors led to the hypothesis that the behavior of this type of connector is similar to that of a flexible elastic dowel embedded in an elastic medium. This hypothesis is sufficient to explain qualitatively the relative effects of changes in the channel web thickness and in the strength of the mortar slab. According to this concept a change in web thickness or in mortar strength changes the relative stiffness of the equivalent dowel and elastic medium and thus changes the distribution of load on the shear connector. As a result, the moment at the critical section of the channel is changed and its strength is affected. The maximum compressive stress in the slab is also changed by a change in load distribution, and consequently the load-slip characteristics may be affected.

Behavior of Channel Shear Connectors in Fatigue. Channel shear connectors in T-beams subjected to fatigue loadings failed usually by fracture of the connector web on a line through the fillet closest to the beam. Although exceptionally high compressive stresses in the mortar adjacent to the connector would be expected on the basis of the dowel hypothesis, failure of the mortar slab was believed to have occurred only in those few cases where very low mortar strengths were used. It is probable that a state of multiaxial compression exists in the slab adjacent to the connector and as a result the relatively large stresses are not as damaging as they would be for the case of simple compression.

Applicability of Results from Push-out Tests. On the basis of comparisons between the results of push-out and T-beam tests, it is believed that the load-slip characteristics for channel shear connectors determined from

the push-out tests are representative of those for similar connectors in composite T-beams. This conclusion must be limited, however, to a range of slip corresponding to only moderate decreases in interaction. The ultimate loads obtained in the push-out tests were in all cases accompanied by such large slips as to have no application in the design of composite beams. Moreover, for most specimens, it is believed that the ultimate load was to a large extent a function of the design and dimensions of the specimen rather than of the shear connectors.

45. Composite Beams

All the composite beams in these tests were made with channel shear connectors, and with a few exceptions the bond between the slab and the I-beam was destroyed before the testing was begun. In practically all cases the beams were loaded with a single concentrated load at midspan. Subject to these restrictions on the scope of the tests, the characteristics and behavior of composite beams for both static and fatigue loading are discussed in the following paragraphs.

Degree of Composite Action. Complete composite action was achieved only for those few beams in which the bond between the beam and the slab was not destroyed. In all other beams, in which shear was transferred only through the shear connectors, a decrease in the degree of interaction was always observed. However, the effect of this decrease on the stresses which would govern the design was so small that for all practical purposes the beams could have been designed for the assumption of full composite action.

Nearly full composite action was maintained up to the ultimate capacity of the beam if an adequate shear connection was provided. For the case of an excessively weak shear connection, the degree of composite action was reduced at the higher loads and the ultimate capacity of the beam was consequently lowered. It was also brought out by the tests that the ultimate capacity of a beam with otherwise adequate shear connectors may be impaired by premature splitting of the slab resulting from the use of very low strength mortar.

Theory of Imperfect Interaction. The theory developed and described in the Appendix provides a satisfactory qualitative description of the behavior of composite beams. Moreover, the theory may be used together with values of the connector modulus from push-out tests to predict with good accuracy the magnitude and effects of imperfect interaction.

In terms of the dimensionless constant, C, which is developed in the theoretical analysis, the results of the tests of T-beams may be interpreted to indicate that an adequate shear connection is one for which the value of $1/C$ is greater than about 20.

Fatigue Failure of Composite Beams.   Composite T-beams tested in fatigue failed in the shear connection. The failure was progressive, beginning with the end shear connectors and progressing toward the load at midspan. The overall effects of fatigue failure of the shear connection on the strains and deflections for a composite beam were not evident until several shear connectors had fractured; failure of a single connector, however, probably leads eventually to failure of the beam, since the load formerly carried by that connector is transmitted to the remaining ones and thus increases their load and stress. There was no evidence of an endurance limit for the composite beams used in these tests for numbers of load applications up to about ten million.

Bond as Shear Connection.   In a few of the T-beams tested in fatigue the bond between the slab and the beam was not destroyed. The results of these tests indicated that bond is an extremely effective shear connection as long as it is present. The connection provided by bond is very stiff and permits little slip. Consequently, most of the shearing load is carried by the bond and very little by the shear connectors.

It must be emphasized, however, that the bond is not always reliable. It offers little resistance to vertical separation of the slab and the beam, and such separation as might be caused by warping of the slab due to temperature or shrinkage effects or by the effects of loading will result in the almost complete loss of the bond. It seems probable, however, that if the slab is securely anchored to the beam against vertical movement the bond may be maintained permanently and that the shear connectors may be greatly relieved of load.

46. Significance of Results

The conclusions stated and discussed in the preceding two sections are in general only qualitative. Moreover, even the few quantitative statements should be considered as tentative in view of the character and limitations of a test program involving quarter-scale models.

The test program described in this bulletin was intended to be exploratory. It was not expected that the tests would yield definite answers to the many questions regarding shear connectors and composite beams. It was hoped, however, that the large number of specimens which could more conveniently be tested by the use of small-scale models would permit a narrowing of the range of variables and would provide improved insight into the nature of the problem. Obviously this test program—involving 64 push-out specimens and 88 composite T-beams—would have been impracticable except with the use of small-scale models.

It is believed that the test program reported herein has yielded much information on the behavior of shear connectors and composite beams.

In view of the exploratory nature of the tests, however, it is not surprising that conclusive answers were not obtained to all questions and that in some cases additional questions were raised by the results of these tests. For the most part the questions still remaining appear to be answerable only by tests of full-size shear connectors and full-size composite beams.

The concept of dowel-like action, which appears to be a fundamental factor in the behavior of individual channel shear connectors, can be investigated satisfactorily only by tests in which the distribution of strain in the web of the channel can be measured. For this purpose it would seem, push-out tests of full-size connectors would provide the needed data.

Full-size tests of T-beams are desirable for several reasons. For one thing, the shear connectors used in the small-scale beams were not exact scale models of possible full-size connectors, and some questions regarding the interpretation of the tests may exist. Moreover, the properties and dimensional relations of the quarter-scale T-beams differed in many respects from those of the full-size beams forming a part of a composite I-beam bridge. This difficulty can be overcome in part by the use of the theoretical analysis which employs a dimensionless constant to represent the properties and dimensions of the beam. However, tests of full-size beams would provide more conclusive evidence regarding the validity of the theoretical analysis.

APPENDIX: ANALYSIS OF COMPOSITE T-BEAMS WITH INCOMPLETE INTERACTION

47. Introduction

The connection between the slab and beam of a composite steel and concrete T-beam is usually not perfect; that is, it allows some slip to take place along the contact surfaces. When the small-size T-beam tests reported in this bulletin were begun there was no rational way of taking this slip into account. It was desired, therefore, to develop a theoretical analysis of a composite T-beam with incomplete interaction. The original solution of this problem was obtained by N. M. Newmark and reported in an unpublished progress report in 1943. This solution was presented and compared with the results of several tests of composite T-beams in a previous paper.[1] The same solution is presented in more detail herein.

48. Notation

The subscripts used with the notation of this Appendix have the following meanings:

s = slab
b = beam
L = section to the left of the load
R = section to the right of the load
o = composite beam with no interaction
Primed symbols designate values for composite beam with complete interaction.

The following notation is used:

A_s, A_b = cross-sectional areas of the slab and the beam respectively

A = cross-sectional area above the section at which horizontal shear is computed

c_s, c_b = distances between the respective centroidal axes of the slab and the I-beam and their contact surfaces

E_s, E_b = moduli of elasticity of slab and beam, respectively

$$\frac{1}{\overline{EA}} = \frac{1}{E_s A_s} + \frac{1}{E_b A_b}$$

$$\Sigma EI = E_s I_s + E_b I_b$$

$$\overline{EI} = \Sigma EI + \overline{EA}z^2$$

$$C = \frac{s}{k}\frac{\pi^2 \overline{EA}\ \Sigma EI}{L^2 \overline{EI}}$$

---

[1] N. M. Newmark, C. P. Siess, I. M. Viest, "Tests and Analysis of Composite Beams with Incomplete Interaction," Proceedings of the Society for Experimental Stress Analysis, Vol. 9, No. 1, 1951.

F, F_L, F_R, F' = horizontal direct forces acting at the centroids of the slab and the beam

G_b = shearing modulus of material of beam

I_s, I_b = moments of inertia of slab and beam respectively

k = modulus of a shear connector = Q/γ (lb/in.)

K = first moment of the area A with respect to the centroidal axis of the I-beam

L = span length of composite beam

M = external moment applied to composite beam

M_s, M_b = moment of flexural stresses in slab and beam respectively

P = concentrated load

q = horizontal shear per unit length of beam at any horizontal section

$q_c, q_{cL}, q_{cR}, q_c'$ = horizontal shear per unit length of the beam at the contact surface of the slab and the beam

Q = load on a connector

s = spacing of shear connectors

$s_s = y_s/\Sigma EI$

$s_b = y_b/\Sigma EI$

t = thickness of the web of the I-beam

u = distance of the concentrated load P from the left support

v = unit shearing stress

V = vertical shear

x = distance of a cross-section from the left support

y, y_L, y_R, y' = flexural deflections

y_s, y_b = vertical distances from the centroidal axis of the slab and the beam

$\bar{y}$ = vertical distance from the centroidal axis of the composite T-section

z = distance between the centroidal axes of the slab and the beam

$\gamma, \gamma_L, \gamma_R$ = slip between slab and beam

$\delta, \delta', \delta_o$ = shearing deflections

$\epsilon_s, \epsilon_s', \epsilon_b, \epsilon_b'$ = strains in slab and beam, respectively

τ = angle of shear distortion.

49. Analysis of Composite T-beams

The type of structure considered in this analysis is shown in Fig. 48a. It is a T-beam consisting of an I-beam and a slab tied together by a shear connection which transfers horizontal shear from one element to the other. The principal assumptions made in this analysis are as follows.

(1) The shear connection between the slab and the I-beam is assumed to be continuous along the length of the beam. If it is desired to consider individual shear connectors, as is done here, the assumed condition is approximated only if the connectors are of equal capacities and are equally spaced along the beam; that is,

$$\frac{k}{s} = \text{const.} \tag{1}$$

where k is the so-called modulus of the connector and s is the spacing between the connectors. If the connectors are not equally spaced, this assumption will be satisfied only if the capacities of the connectors vary directly as their spacing.

$$M = M_s + M_b + Fz$$

(a)-Cross Section   (b)-Forces   (c)-Strain Distribution
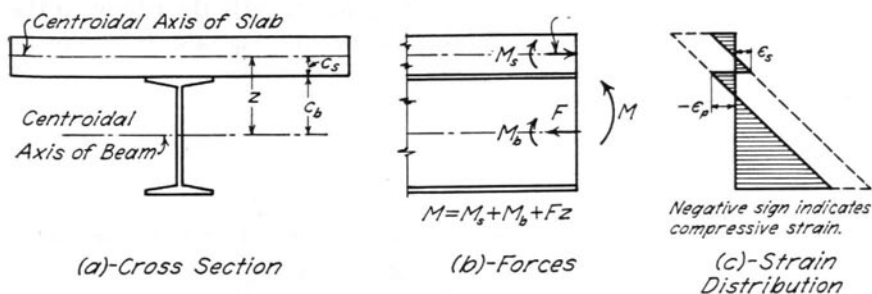
Fig. 48. Composite T-beam with Incomplete Interaction

(2) The amount of slip permitted by the shear connection is directly proportional to the load transmitted:

$$\gamma = \frac{Q}{k} \tag{2}$$

where Q is the load transmitted by a connector. For individual connectors this requires that the load-slip curve for a connector be a straight line, the slope of which is called the modulus k of the connector.

Other assumptions made in this analysis are as follows:

(3) The distribution of strains throughout the depth of the slab and I-beam is linear.

(4) The I-beam and the slab are assumed to deflect equal amounts at all points along their lengths.

The degree of composite action attained depends on the effectiveness of the shear connectors in preventing relative movement between the slab and the I-beam. If no movement or slip is permitted, interaction will be complete and the resisting moment of the T-beam may be computed from

the ordinary equations of mechanics using the properties of the transformed section.[2] If the beam and slab are not interconnected and slip takes place freely, there is no interaction and the resisting moment of the two elements is simply the sum of their individual resistances, developed at equal deflections.

The relative movement between the slab and the I-beam is slip which is given by Eq. (2) or, if the total load on a connector is expressed in terms of the load q_c transmitted per unit length of the beam and in terms of the spacing, s, of the shear connectors,

$$\gamma = \frac{q_c s}{k} \tag{3}$$

The rate of change of slip along the length of the beam is equal to the difference between the strain in the slab and the strain in the I-beam at the level at which slip occurs. Using the notation of Fig. 48c this may be written as

$$\frac{d\gamma}{dx} = \epsilon_b - \epsilon_s \tag{4}$$

in which dx is measured along the length of the beam.

Strains ϵ_b and ϵ_s may be expressed in terms of internal forces and moments acting on the T-beam at any section. When the composite T-beam is subjected to a positive bending moment, the shear connectors exert forces which produce compression in the slab and tension in the I-beam. These forces act at the location of the shear connector, but on each element may be replaced by a couple and a force acting at the centroid of the element. The couples may be added algebraically to the moments that would exist in the I-beam and slab due to the external moment if there were no shear connectors. If this is done, the resultant internal forces and moments acting on the T-beam at any section, and resisting the external moment, are as shown in Fig. 48b. They consist of the moment M_s in the slab, the moment M_b in the I-beam, and the forces F acting at the centroids of the slab and the I-beam. From the assumption that the distribution of strains throughout the depth of the slab and the I-beam is linear it follows that

$$\epsilon_b = \frac{F}{E_b A_b} - \frac{M_b c_b}{E_b I_b} \tag{5a}$$

$$\epsilon_s = -\frac{F}{E_s A_s} + \frac{M_s c_s}{E_s I_s} \tag{5b}$$

[2] See, for example, N. M. Newmark and C. P. Siess, "Design of Slab and Stringer Highway Bridges," Public Roads, Vol. 23, No. 7, p. 162, 1943.

where E_b and E_s are the moduli of elasticity, I_b and I_s are the moments of inertia, and A_b and A_s are the cross-sectional areas of the I-beam and the slab respectively. A positive sign indicates a tensile strain.

The load per unit of length q_c which is transmitted between the slab and the I-beam is equal to the change in the force F along the length of the beam. This may be written as

$$q_c = \frac{dF}{dx} \tag{6}$$

and from Eq. (3)

$$\frac{d\gamma}{dx} = \frac{s}{k}\frac{dq_c}{dx} = \frac{s}{k}\frac{d^2F}{dx^2} \tag{7}$$

Substituting Eq. (5) and (7) in Eq. (4) one obtains

$$\frac{s}{k}\frac{d^2F}{dx^2} = \frac{F}{E_bA_b} - \frac{M_bc_b}{E_bI_b} + \frac{F}{E_sA_s} - \frac{M_sc_s}{E_sI_s}$$

$$= F\left(\frac{1}{E_bA_b} + \frac{1}{E_sA_s}\right) - \left(\frac{M_bc_b}{E_bI_b} + \frac{M_sc_s}{E_sI_s}\right) \tag{8}$$

From statics, the total resisting moment of the T-beam is:

$$M = M_b + M_s + Fz \tag{9}$$

where the distance z is shown in Fig. 48a. Since it is assumed that the slab and the beam deflect alike at all points, that is, they have equal curvatures, the moments M_s and M_b are related as follows:

$$\frac{M_b}{E_bI_b} = \frac{M_s}{E_sI_s}$$

Furthermore, from Eq. (9)

$$\frac{M_b}{E_bI_b} = \frac{M_s}{E_sI_s} = \frac{M - Fz}{\Sigma EI} \tag{10}$$

where

$$\Sigma EI = E_bI_b + E_sI_s$$

Substituting from Eq. (10) into Eq. (8) yields

$$\frac{s}{k}\frac{d^2F}{dx^2} = F\left[\frac{1}{E_bA_b} + \frac{1}{E_sA_s} + \frac{z^2}{\Sigma EI}\right] - \frac{Mz}{\Sigma EI}$$

which may be written as

$$\frac{d^2F}{dx^2} - F\frac{k}{s}\frac{\overline{EI}}{\overline{EA}\ \Sigma EI} = -\frac{k}{s}\frac{Mz}{\Sigma EI} \tag{11a}$$

where the following expressions are introduced for convenience:

$$\overline{EI} = \Sigma EI + \overline{EA}z^2$$

$$\frac{1}{\overline{EA}} = \frac{1}{E_s A_s} + \frac{1}{E_b A_b}$$

To obtain the solution of the differential equation (11a) it is necessary to express the external moment M in terms of the distance x of the section from the left support. The following solution is obtained for a concentrated load P acting on a simply-supported beam at a distance u from the left support.

For a section to the left of the load P, that is, when $x < u$, the moment is

$$M = P\frac{x}{L}(L - u)$$

and correspondingly, Eq. (11a) will have the form

$$\frac{d^2F_L}{dx^2} - F_L\frac{k}{s}\frac{\overline{EI}}{\overline{EA}\ \Sigma EI} = -\frac{k}{s}\frac{P(L - u)z}{L\ \Sigma EI}\ x \tag{11b}$$

For a section to the right of the load P— when $x > u$—the moment is

$$M = P\frac{u}{L}(L - x)$$

and Eq. (11a) will have the form

$$\frac{d^2F_R}{dx^2} - F_R\frac{k}{s}\frac{\overline{EI}}{\overline{EA}\ \Sigma EI} = -\frac{k}{s}\frac{Puz}{L\ \Sigma EI}(L - x) \tag{11c}$$

The differential equations (11b, c) can be solved for known end conditions.[3] For this case the end conditions are:

at $x = 0$ $F_L = 0$

at $x = L$ $F_R = 0$

at $x = u$ $\dfrac{dF_L}{dx} = \dfrac{dF_R}{dx}$ and $F_L = F_R$

The solutions for the force F are:

---

[3] See, for example, the solution of a similar equation relating to another type of action, however, in Timoshenko, "Theory of Elastic Stability," McGraw-Hill, New York, 1936, p. 3.

for $x < u$

$$F_L = \frac{\overline{EAz}}{\overline{EI}} \, PL \left\{ \left(1 - \frac{u}{L}\right) \frac{x}{L} \right. $$

$$\left. - \frac{\sqrt{C}}{\pi} \frac{\sinh\left[\frac{\pi}{\sqrt{C}}\left(1 - \frac{u}{L}\right)\right]}{\sinh\frac{\pi}{\sqrt{C}}} \sinh\left(\frac{\pi}{\sqrt{C}}\frac{x}{L}\right) \right\} \quad (12a)$$

and for $x > u$

$$F_R = \frac{\overline{EAz}}{\overline{EI}} \, PL \left\{ \frac{u}{L} \left(1 - \frac{x}{L}\right) \right. $$

$$\left. - \frac{\sqrt{C}}{\pi} \frac{\sinh\left(\frac{\pi}{\sqrt{C}}\frac{u}{L}\right)}{\sinh\frac{\pi}{\sqrt{C}}} \sinh\left[\frac{\pi}{\sqrt{C}}\left(1 - \frac{x}{L}\right)\right] \right\} \quad (12b)$$

where

$$C = \frac{8}{k} \frac{\pi^2}{} \frac{\overline{EA} \, \Sigma EI}{L^2 \overline{EI}} \quad (13)$$

is a dimensionless expression introduced for convenience.

If the modulus of the shear connectors is infinitely large, the slip will be zero and there will be complete interaction between the slab and the I-beam. The force F' for complete interaction can be obtained by setting $C = 0$ in Eq. (12), or directly from statics. The result is [4]

$$F' = \frac{\overline{EAz}}{\overline{EI}} \, M \quad (14)$$

Thus, the ratio of the horizontal force F for incomplete interaction to the horizontal force F' for complete interaction is:

---

[4] The physical significance of the expression $\overline{EAz}/\overline{EI}$ may be demonstrated as follows: By differentiating Eq. (14) with respect to x the following expression is obtained:

$$\frac{dF'}{dx} = \frac{\overline{EAz}}{\overline{EI}} \frac{dM}{dx}$$

but dF'/dx is the horizontal shear q'_c at the junction of the slab and the I-beam, and dM/dx is the vertical shear V. Thus $\overline{EAz}/\overline{EI} = q'_c/V$ is the ratio of horizontal unit shear q'_c to the vertical shear V.

for $x < u$

$$\frac{F_L}{F'} = 1 - \frac{\sqrt{C}}{\pi} \frac{1}{\left(1 - \frac{u}{L}\right)\frac{x}{L}} \frac{\sinh\left[\frac{\pi}{\sqrt{C}}\left(1 - \frac{u}{L}\right)\right]}{\sinh\frac{\pi}{\sqrt{C}}} \sinh\left(\frac{\pi}{\sqrt{C}}\frac{x}{L}\right) \quad (15a)$$

and for $x > u$

$$\frac{F_R}{F'} = 1 - \frac{\sqrt{C}}{\pi} \frac{1}{\frac{u}{L}\left(1 - \frac{x}{L}\right)} \frac{\sinh\left(\frac{\pi}{\sqrt{C}}\frac{u}{L}\right)}{\sinh\frac{\pi}{\sqrt{C}}} \sinh\left[\frac{\pi}{\sqrt{C}}\left(1 - \frac{x}{L}\right)\right] \quad (15b)$$

The ratio F/F' for any section depends only on the coefficient C and on the location of the section and load. It is equal to unity for complete interaction and to zero for no interaction. Thus the ratio F/F' furnishes a convenient measure of the degree of interaction.

A graphical solution of Eq. (15a, b) is given in Fig. 49. In this figure the ratios F/F' are plotted against $1/C$-values for load acting at midspan and for three different values of x. It can be seen from these curves that for $1/C$-values greater than about 10 the ratio F/F' does not vary much and also that the decrease of interaction is larger at the location under the load than at a section located at some distance from the load.
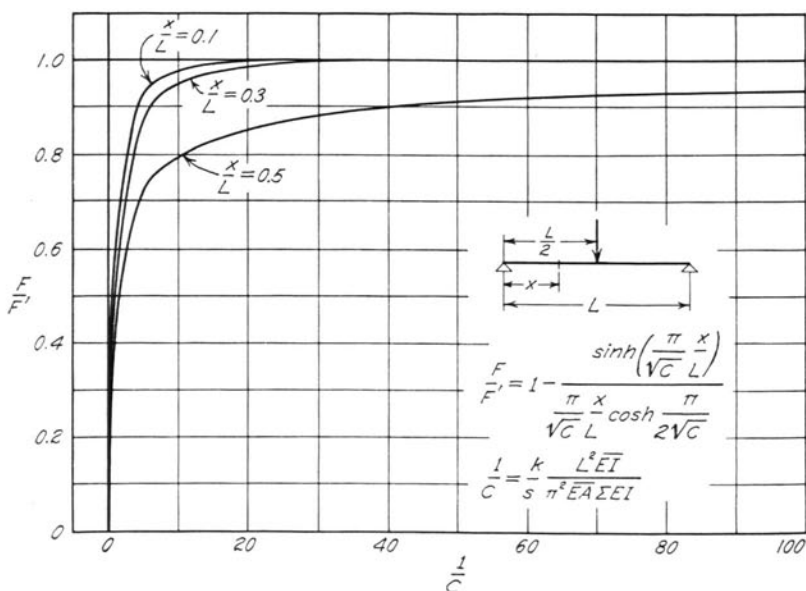
Fig. 49. F/F' versus $1/C$ Curves

The manner in which F/F' varies along the length of the beam is better shown in Figs. 50 and 51. The curves in these figures bring out the important fact that the reduction in the interaction is a somewhat localized effect. The curves for $C = 0.01$ and 0.05 are of primary interest as they represent reasonable limits for the full-size concrete and steel T-beams. For $C = 0.01$ the interaction is appreciably reduced only for a distance of less than one-tenth the span on each side of the load: for $C = 0.05$ the interaction is practically perfect for more than half the length of the beam.
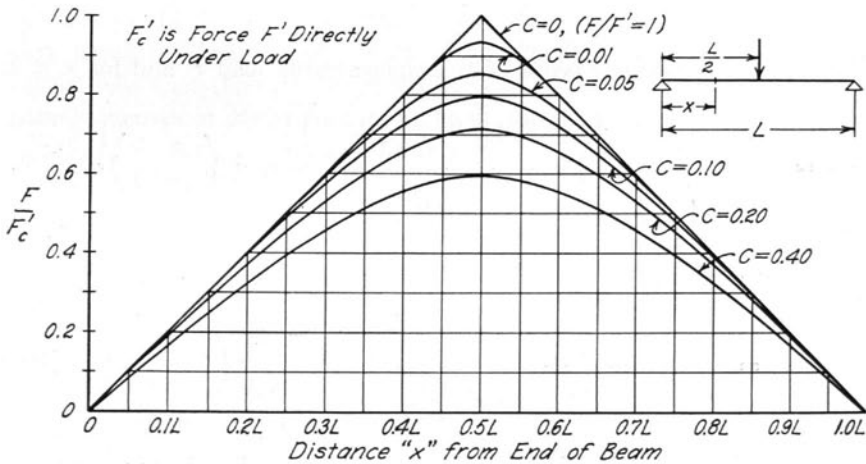
Fig. 50. *Variation of F/F_c' Along Length of Beam for Various Values of C, Load at Midspan*
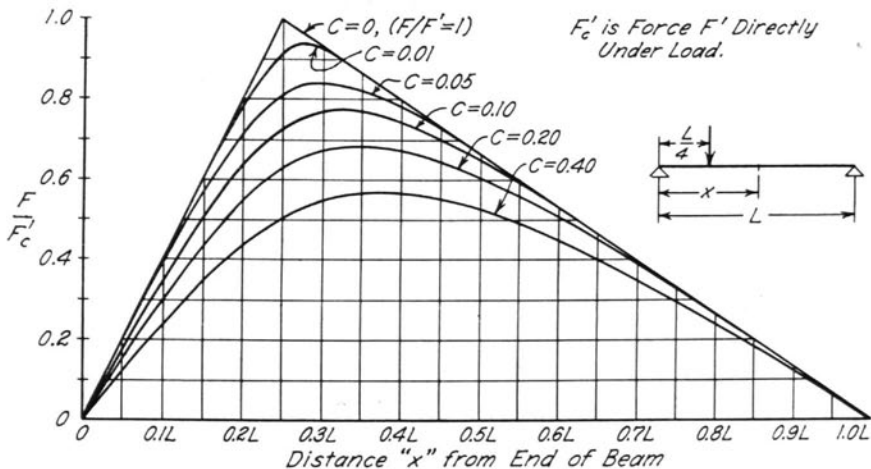
Fig. 51. *Variation of F/F_c' Along Length of Beam for Various Values of C, Load at Quarter-point*

This is true for the load at the quarter-point as well as for the load at midspan, even though for the load at the quarter-point the degree of interaction at the load point is somewhat less than the corresponding value for the load at midspan.

50. Load on Shear Connectors and Slip

The load on any connector may readily be obtained from Eq. (6) and (12):

$$Q = q_c s = \frac{dF}{dx} s$$

For a simply-supported beam with a concentrated load P and for $x < u$

$$q_{cL} = \frac{\overline{EA}z}{\overline{EI}} P \left\{ \left(1 - \frac{u}{L}\right) - \frac{\sinh\left[\frac{\pi}{\sqrt{C}}\left(1 - \frac{u}{L}\right)\right]}{\sinh\frac{\pi}{\sqrt{C}}} \cosh\left(\frac{\pi}{\sqrt{C}}\frac{x}{L}\right) \right\} \quad (16a)$$

and for $x > u$

$$q_{cR} = \frac{\overline{EA}z}{\overline{EI}} P \left\{ -\frac{u}{L} + \frac{\sinh\left(\frac{\pi}{\sqrt{C}}\frac{u}{L}\right)}{\sinh\frac{\pi}{\sqrt{C}}} \cosh\left[\frac{\pi}{\sqrt{C}}\left(1 - \frac{x}{L}\right)\right] \right\} \quad (16b)$$

The horizontal unit shear for complete interaction is given by the equation

$$q_c' = V \frac{\overline{EA}z}{\overline{EI}}$$

Equations (16) may then be written in the form of ratios. For $x < u$

$$\frac{q_{cL}}{q_c'} = 1 - \frac{1}{\left(1 - \frac{u}{L}\right)} \frac{\text{inh}\left[\frac{\pi}{\sqrt{C}}\left(1 - \frac{u}{L}\right)\right]}{\sinh\frac{\pi}{\sqrt{C}}} \cosh\left(\frac{\pi}{\sqrt{C}}\frac{x}{L}\right) \quad (17a)$$

and for $x > u$

$$\frac{q_{cR}}{q_c'} = 1 - \frac{L}{u} \frac{\sinh\left(\frac{\pi}{\sqrt{C}}\frac{u}{L}\right)}{\sinh\frac{\pi}{\sqrt{C}}} \cosh\left[\frac{\pi}{\sqrt{C}}\left(1 - \frac{x}{L}\right)\right] \quad (17b)$$

Slip at any point may be expressed with the aid of Eq. (3) and (16). For $x < u$

$$\gamma_L = \frac{s}{k} q_{cL} \tag{18a}$$

and for $x > u$

$$\gamma_R = \frac{s}{k} q_{cR} \tag{18b}$$

Equations (16), (17), and (18) show that the load q_c transmitted from the slab to the I-beam, and the slip γ between the slab and the I-beam vary along the beam. The curves in Fig. 29 illustrate this variation. It can be seen that the increase in slip is rapid at locations close to the load point, whereas at locations remote from the load the slip is practically constant. Similarly, connectors located close to the point of load application are loaded less than the more remote connectors.

51. Strains

Strains in the I-beam may be determined for any degree of interaction from the equation

$$\epsilon_b = \frac{F}{E_b A_b} + \frac{M_b y_b}{E_b I_b} \tag{19a}$$

and in the slab from the equation

$$\epsilon_s = -\frac{F}{E_s A_s} + \frac{M_s y_s}{E_s I_s} \tag{19b}$$

where y_b and y_s are the distances from the centroid of the I-beam or of the slab to the point at which the strain is desired. In both cases y is positive when measured downward. The force F in these equations may be computed from Eq. (12) or (15), and the moments M_b and M_s may be obtained from Eq. (10) as follows:

$$M_b = \frac{E_b I_b}{\Sigma EI} (M - Fz) \tag{20a}$$

$$M_s = \frac{E_s I_s}{\Sigma EI} (M - Fz) \tag{20b}$$

Thus the equations for strains may be written in the form

$$\epsilon_b = \left[s_b - \frac{F}{F'} \frac{\overline{EA}z}{\overline{EI}} \left(s_b z - \frac{1}{E_b A_b} \right) \right] M \tag{21a}$$

$$\epsilon_s = \left[s_s - \frac{F}{F'} \frac{\overline{EA}z}{\overline{EI}} \left(s_s z + \frac{1}{E_s A_s} \right) \right] M \tag{21b}$$
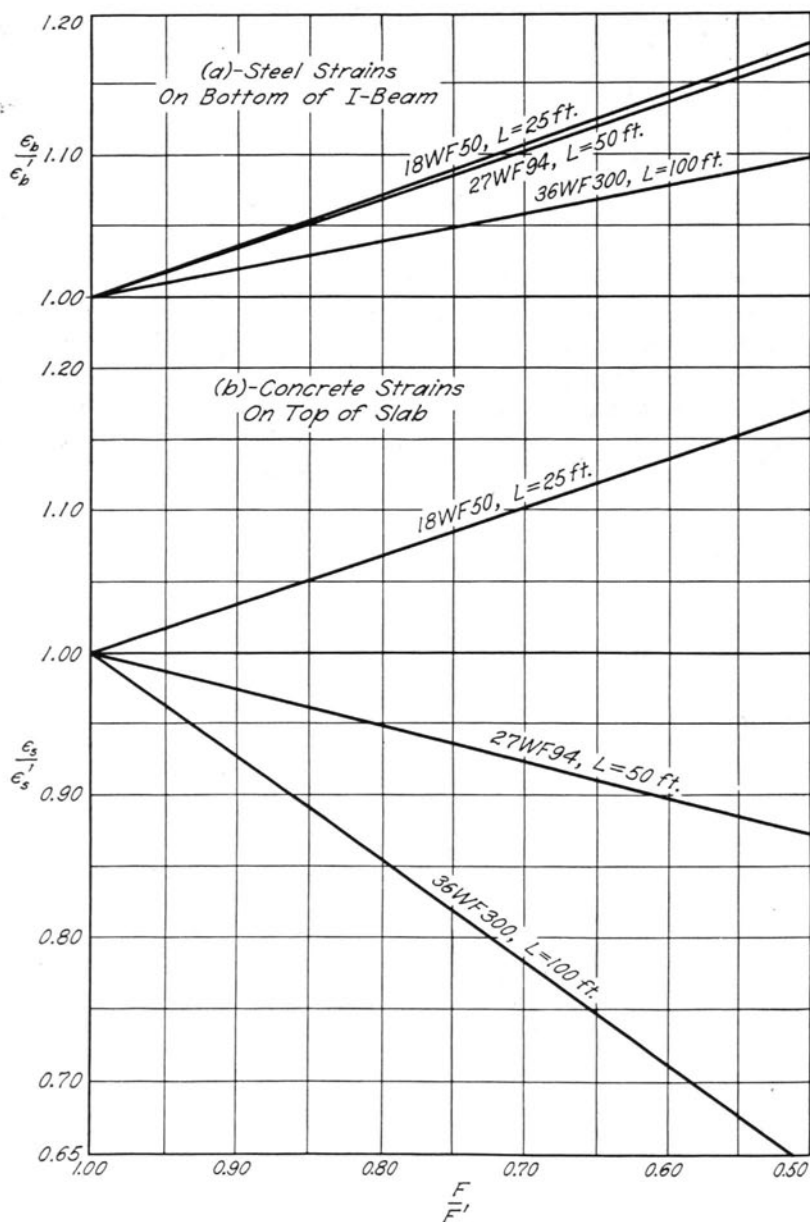
Fig. 52. Variation of Strain with Degree of Interaction F/F'

where

$$s_b = \frac{y_b}{\Sigma EI} \tag{22a}$$

$$s_s = \frac{y_s}{\Sigma EI} \tag{22b}$$

The strains for complete interaction ϵ_b' and ϵ_s' are obtained from Eq. (21) by substituting $F/F' = 1$. The ratios ϵ/ϵ' may then be expressed as follows:

$$\frac{\epsilon_b}{\epsilon_b'} = \frac{\overline{EI}s_b}{\bar{y}} + \frac{F}{F'} \left(1 - \frac{\overline{EI}s_b}{\bar{y}} \right) \tag{23a}$$

$$\frac{\epsilon_s}{\epsilon_s'} = \frac{\overline{EI}s_s}{\bar{y}} + \frac{F}{F'} \left(1 - \frac{\overline{EI}s_s}{\bar{y}} \right) \tag{23b}$$

The symbol $\bar{y}$ designates the distance of the point considered from the neutral axis of the composite section. It may be determined directly from the equation

$$\bar{y} = y_b + \frac{\overline{EA}z}{E_b A_b} = y_s - \frac{\overline{EA}z}{E_s A_s} \tag{24}$$

The distance $\bar{y}$ is positive when measured downward.

Equations (21) show that strains depend on the moment M, the properties of the T-beam section, and the degree of interaction F/F' at the particular section at which strains are desired. F/F' depends on the modulus of the connectors k, on the spacing of the connectors s, and on the properties of the T-beam section; all these are contained in the coefficient C given by Eq. (13).

For a given T-beam the change in strain caused by a decrease in the degree of interaction is a linear function of the ratio F/F'. This is illustrated in Fig. 52, in which the ratio ϵ/ϵ' is plotted against F/F' for three different beams. All three beams were designed as simple-span structures for the following span lengths: 100, 50, and 25 ft. They were designed with a concrete slab 6 ft wide and 6 in. thick and with a modular ratio $n = 10$. One H-20-44 wheel load at midspan with 30-percent impact required the following beam sizes: 36 WF 300, 27 WF 94, and 18 WF 50 for the 100-, 50-, and 25-ft spans respectively.

The curves in Fig. 52a show changes in the governing bottom-flange strains due to the presence of incomplete interaction. The position of each line in this figure depends only on the properties of the T-beam and on the distance of the bottom flange from the neutral axis. For the bottom

flange strains at midspan, $F/F' = 0.90$ is a reasonable value for a full-size structure. The corresponding increase of the steel strains is less than 4 percent. A slightly greater effect can be noticed for strains and loading at the quarter-point, since in this case the degree of interaction at the load point is lower. However, loading at the quarter-point usually does not govern.

An interesting effect of the section properties on strain at the top of the slab is brought out in Fig. 52b. In long beams with relatively light slabs the presence of slip causes a decrease in strain, while in short beams with relatively heavy slabs the effect of slip is just the opposite. An explanation of this phenomenon may be found by inspection of Eq. (19b). Since the distance between the extreme fibers of the slab and its centroidal axis is a negative value, both the direct force F and the moment M_s cause compressive stresses on the top of the slab when a downward load is applied to the beam. It must be remembered, however, that the moment M_s is composed of two parts: (1) the moment which would exist for the case of no interaction, and (2) the moment $\dfrac{E_s I_s}{\Sigma EI} Fz$ due to the force F. The second part of the moment M_s is always smaller than the first part and opposite in sign; in other words, the force F causes tensile flexural stresses in the upper fiber of the slab. Thus the net effect of the presence of incomplete interaction depends on the relative magnitudes of the two separate effects of the force F, the flexural and the direct stresses. Obviously, in the case of a short beam with heavy slab the effect of additional bending offsets the effect of the decrease in direct stress.

52. Flexural Deflections

The expression for the curvature of a composite T-beam may be obtained from Eq. (10) as

$$\frac{d^2y}{dx^2} = -\frac{M}{\Sigma EI} + \frac{Fz}{\Sigma EI} \tag{25a}$$

After substituting for F from Eq. (11a) and rearranging, Eq. (25a) will have the form

$$\frac{d^2y}{dx^2} = -\frac{M}{\overline{EI}} + \frac{s}{k}\frac{\overline{EA}z}{\overline{EI}}\frac{d^2F}{dx^2} \tag{25b}$$

The deflection due to flexural deformation may be evaluated by integrating Eq. (25b) twice after proper end conditions have been considered. These end conditions are:

$$\text{at } x = 0 \qquad y = 0,\ y' = 0,\ \text{and } F = 0$$
$$\text{at } x = \text{L} \qquad y = 0,\ y' = 0,\ \text{and } F = 0$$

As the result of integrating twice the term $-M/\overline{EI}$ is the flexural deflection y' of a composite beam with complete interaction, the solution of Eq. (25b) is

$$y = y' + \frac{s}{k} \frac{\overline{EA}z}{\overline{EI}} F \tag{26a}$$

which may be written also in the form

$$y = y' + \frac{ML^2}{\overline{EI}} \frac{C}{\pi^2} \frac{\overline{EA}z^2}{\Sigma EI} \frac{F}{F'} \tag{26b}$$

Equations (26a, b) are general expressions for flexural deflections of a composite beam with incomplete interaction and apply to any type of loading. If the beam is loaded with a concentrated load P, the corresponding expressions for flexural deflections can easily be derived by substituting proper values of y', M, and F. The ratio y/y' for this type of loading is for $x < u$

$$\frac{y_L}{y'} = 1 + \frac{\overline{EA}z^2}{\frac{1}{6}\left[2\frac{u}{L} - \left(\frac{u}{L}\right)^2 - \left(\frac{x}{L}\right)^2\right]\Sigma EI} \frac{C}{\pi^2} \frac{F_L}{F'} \tag{27a}$$

and for $x > u$

$$\frac{y_R}{y'} = 1 + \frac{\overline{EA}z^2}{\frac{1}{6}\left[2\frac{x}{L} - \left(\frac{u}{L}\right)^2 - \left(\frac{x}{L}\right)^2\right]\Sigma EI} \frac{C}{\pi^2} \frac{F_R}{F'} \tag{27b}$$

The ratios y/y' are plotted in Fig. 53 as functions of C for the beams described in the preceding section. Fig. 53a shows the increase in deflection at midspan when the beam is loaded at midspan. The increase in deflection at the quarter-point is shown in Fig. 53b. For $C = 0.01$ the increase in the center deflection due to incomplete interaction is about 2 percent; for $C = 0.02$ it is less than 4 percent. These values are comparable to the corresponding increase in strains. As the lack of interaction increases, however, the increase in deflections is more pronounced than that of strains. For example, for $C = 0.05$ the maximum deflection of the shortest beam is 9 percent larger than for $C = 0$, while the increase in strain is only 5 percent. In addition to the larger effect of slip, the deflection of a beam is an integrated quantity in which minor variations are smoothed out. A comparison of the computed and measured deflections is, therefore, more reliable than the comparison of computed and measured strains.
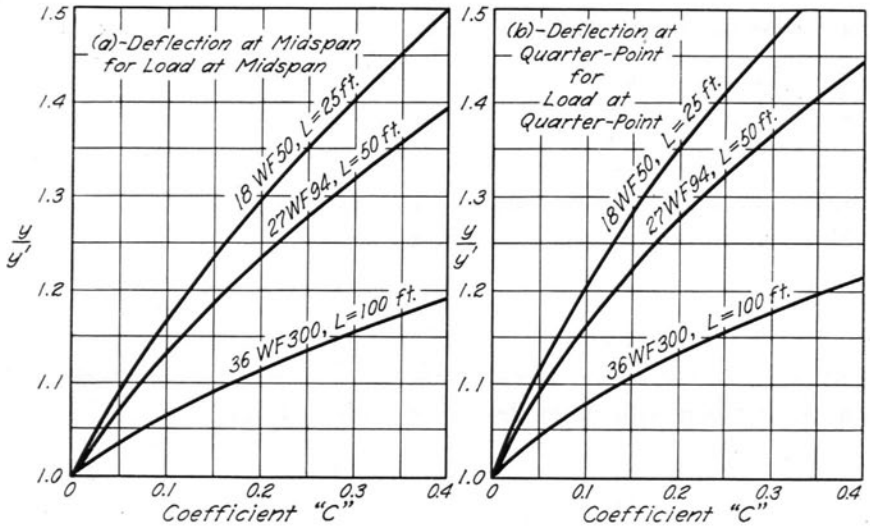
Fig. 53. Variation of Deflection with Various Values of Coefficient C

53. Shearing Deflections

Concrete and steel composite T-beams have rather heavy cross-sections; hence in some cases it may be desirable to correct the deflections for the shear distortions. An approximate solution for this correction may be derived on the basis of equation

$$\tau = \frac{d\delta}{dx} \tag{28}$$

Here τ is the angle of the shear distortion and δ is the deflection due to shear. Assuming that along some axis of the beam shear causes only distortion without rotation, the shearing deflection may be obtained by integrating Eq. (28):

$$\delta = \int_0^x \tau dx = \int_0^x \frac{v}{G_b} dx \tag{29}$$

G_b is the shearing modulus of the beam material and v is the shearing stress. The intensity of the shearing stress in the flanges of the I-beam and in the slab is negligible when compared with that in the web of the I-beam. It will be assumed, therefore, that all the distortion due to shear takes place in the web of the I-beam and also that the intensity of the shearing stress remains constant throughout the thickness of the web. Thus

$$v = \frac{q}{t} \tag{30}$$

where q is the horizontal shear per unit length of the beam and t is the thickness of the web.

An expression for the horizontal shear may be derived from statics. If A is the area above (or under) the section at which horizontal shear is computed, and K is the first moment of the area A with respect to the centroidal axis of the I-beam, then the unit horizontal shear is

$$q = \left(\frac{A}{A_b} - \frac{E_b z}{\Sigma EI} K\right)\frac{dF}{dx} + \frac{E_b}{\Sigma EI} K \frac{dM}{dx} \tag{31}$$

After substituting Eq. (31) into Eq. (30) and further into Eq. (29), the integration of the latter equation may be performed; the result gives the shear deflection as

$$\delta = \frac{1}{tG_b}\left[\left(\frac{A}{A_b} - \frac{E_b z}{\Sigma EI} K\right)F + \frac{E_b}{\Sigma EI} KM\right] \tag{32a}$$

which may be written also as follows:

$$\delta = \frac{M}{tG_b}\left[\left(\frac{A}{A_b} - \frac{E_b z}{\Sigma EI} K\right)\frac{\overline{EA}z}{EI}\frac{F}{F'} + \frac{E_b}{\Sigma EI} K\right] \tag{32b}$$

The shear deflections for the limiting cases of beams with complete and no interaction may be obtained readily from Eq. (32b) by substituting the proper values of F/F', or they may be obtained directly. For complete interaction

$$\delta' = \frac{M}{tG_b}\left[\left(\frac{A}{A_b} - \frac{E_b z}{\Sigma EI} K\right)\frac{\overline{EA}z}{EI} + \frac{E_b}{\Sigma EI} K\right] = \frac{vM}{VG_b} \tag{33}$$

where V is the vertical shear. For no interaction

$$\delta_o = \frac{M}{tG_b}\frac{E_b K}{\Sigma EI} = \frac{vM}{VG_b}\frac{E_b I_b}{\Sigma EI} \tag{34}$$

Thus the shearing deflection for a beam with incomplete interaction may be expressed as

$$\delta = \delta_o - (\delta_o - \delta')\frac{F}{F'} \tag{35}$$

In order to evaluate the shearing deflection δ' for complete interaction and δ_o for no interaction, the ratio v/V must be known for both cases. For a steel I-beam the variation of v/V from the top to the bottom of the web is small; it is even smaller for a T-beam. It seems satisfactory, therefore, to compute δ' and δ_o on the basis of average values of v/V.

The difference between the shear deflections for the limiting cases of complete and no interaction is seldom more than 1 percent of the total deflection. For T-beams with a satisfactory shear connection the value of the ratio F/F' is usually close to one. Consequently in almost all cases it will be sufficiently accurate and considerably more convenient to ignore the effect of imperfect interaction, and to compute the deflection due to shear on the assumption of complete interaction.

54. Methods of Determining Connector Modulus

All equations derived in the previous sections contain the factor C which in turn depends on the modulus k and spacing s of the shear connectors. At present there is no rational way of determining the modulus k. There are, however, two experimental methods available.

The first and simpler method is based directly on Eq. (2) and the results of push-out tests. Values of the load Q on the shear connector and the corresponding slip γ in the equation $k = Q/\gamma$ are taken directly from the tests of push-out specimens.

The second method is based on the slip data obtained in the tests of composite beams and on Eq. (3) and Eq. (16) or (17). This method can be used, however, only for interpretation of the tests of composite beams.

For any particular section of a composite beam and for a particular location of the concentrated load, Eqs. (17) express the ratio q_c/q_c' as a function of C:

$$q_c/q_c' = f(C) \tag{17a, b}$$

The ratio q_c/q_c' may be expressed also from Eq. (3) and (13) as follows:

$$\frac{q_c}{q_c'} = \frac{\pi^2 \overline{EA} \ \Sigma EI}{CL^2 \overline{EI}} \frac{\gamma}{q_c'} \tag{36}$$

The only unknowns in Eq. (17) and (36) are q_c/q_c' and C, as the slip γ is known from the test. Thus C can be found by equating Eq. (17) and (36). The solution may be analytical or graphical.

The easiest analytical solution is by successive approximations. For an arbitrarily chosen value of q_c/q_c', C is determined first from Eq. (17). Then Eq. (36) is solved for q_c/q_c' corresponding to the C found above. In the second cycle the operation is repeated with the new value of q_c/q_c'. This process is repeated until the values q_c/q_c' put into Eq. (17) and computed from Eq. (36) are the same. The corresponding C is the correct solution. A good first choice is $q_c/q_c' = 1$, corresponding to a beam with complete interaction. The ratio q_c/q_c' varies from 0 to 1.[5]

---

[5] A similar solution can be worked out for the value of q_c instead of for q_c/q_c' by the use of Eq. (16) instead of (17). A disadvantage of this solution is the large range of possible values for q_c.

The graphical solution consists of plotting q_c/q_c' against $1/C$. In such a graph Eq. (36) is represented by a straight line and Eq. (17) by a curve. The point of intersection of the two lines determines the correct values of both C and q_c/q_c'.

After the value C has been determined the shear connector modulus k may be evaluated from Eq. (13).

Since the foregoing theory for composite beams with incomplete interaction is based on several assumptions which only approximate the actual conditions and since the measured values of slip γ will also introduce some degree of inaccuracy, values of C computed for different locations along the beam will not be exactly the same. An average value of C will give satisfactory results, although in some cases it may be desirable to omit from the average the values of C computed for the sections located close to the point of load application.

This page is intentionally blank.

LIST OF PUBLICATIONS OF THE
CONCRETE SLAB INVESTIGATION.

Bulletins

303. Solutions for Certain Rectangular Slabs Continuous over Flexible Supports, by V. P. Jensen. 1938. *None available.*

304. A Distribution Procedure for the Analysis of Slabs Continuous over Flexible Beams, by N. M. Newmark. 1938. *Sixty cents.*

313. Tests of Plaster-Model Slabs Subjected to Concentrated Loads, by N. M. Newmark and H. A. Lepper. 1939. *Twenty-five cents.*

314. Tests of Reinforced Concrete Slabs Subjected to Concentrated Loads, by F. E. Richart and R. W. Kluge. 1939. *Forty cents.*

315. Moments in Simple Span Bridge Slabs with Stiffened Edges, by V. P. Jensen. 1939. *Sixty cents.*

332. Analyses of Skew Slabs, by V. P. Jensen. 1941. *Sixty cents.*

336. Moments in I-Beam Bridges, by N. M. Newmark and C. P. Siess. 1942. *Seventy-five cents.*

345. Ultimate Strength of Reinforced Concrete Beams as Related to the Plasticity Ratio of Concrete, by V. P. Jensen. 1943. *Thirty cents.*

346. Highway Slab-Bridges with Curbs; Laboratory Tests and Proposed Design Method, by V. P. Jensen, R. W. Kluge, and C. B. Williams, Jr. 1943. *Forty-five cents.*

363. Studies of Slab and Beam Highway Bridges: Part I—Tests of Simple-Span Right I-Beam Bridges, by N. M. Newmark, C. P. Siess, and R. R. Penman. 1946. *Sixty-five cents.*

369. Studies of Highway Skew Slab-Bridges with Curbs: Part I—Results of Analyses, by V. P. Jensen and J. W. Allen. 1947. *Seventy-five cents.*

375. Studies of Slab and Beam Highway Bridges: Part II—Tests of Simple-Span Skew I-Beam Bridges, by N. M. Newmark, C. P. Siess, and W. M. Peckham. 1948. *Fifty cents.*

385. Moments in Two-Way Concrete Floor Slabs, by C. P. Siess and N. M. Newmark. 1950. *Sixty cents.*

386. Studies of Highway Skew Slab-Bridges with Curbs—Part II: Laboratory Research, by M. L. Gossard, C. P. Siess, N. M. Newmark, and L. E. Goodman. 1950. *Forty-five cents.*

Reprints

45. Highway Bridge Floors, by F. E. Richart, N. M. Newmark, and C. P. Siess. 1949. *None available.*

This page is intentionally blank.